Design Guidelines of Low-Density Parity-Check Codes for Magnetic Recording Systems

Yi Fang, *Member, IEEE*, Guojun Han, *Senior Member, IEEE*, Guofa Cai, *Member, IEEE*, Francis C. M. Lau, *Senior Member, IEEE*, Pingping Chen, *Member, IEEE*, and Yong Liang Guan, *Senior Member, IEEE*

***Abstract*—As one of the most classical data-storage systems, magnetic recording (MR) systems have attracted a significant amount of research attention in the past several decades due to the advantages of low cost and high storage density. Along with the continual increase of areal density of modern MR devices, more severe inter-symbol interference (ISI) and noise appear and thus reliable storage becomes more difficult. To address this challenging problem, turbo detections and error-correction codes (ECCs) have been applied to MR systems so as to significantly improve the overall data-storage reliability. Among all the existing ECCs, low-density parity-check (LDPC) codes are of particular interest because they can offer excellent error performance with relatively low encoding and decoding complexity. This paper presents a comprehensive survey of the latest research advancements in LDPC-code design for MR systems from the perspectives of code construction, decoder design, as well as asymptotic performance-evaluation methodology. More specifically, we summarize the design guidelines of LDPC encoder and decoder over both one-dimensional (OD) ISI and two-dimensional (TD) ISI channels, which are commonly used to characterize MR systems with different areal densities. We also concisely portray the research progress in the design of some LDPC-code variants, such as protograph codes, repeat-accumulate codes, spatially coupled codes, and their non-binary counterparts over the aforementioned ISI channels. In particular, we restrict our attention to the reading process and ignore the written-in errors in MR systems unless otherwise stated. Hopefully, this survey will inspire more research activities in the area of LDPC-coded MR systems.**

***Index Terms*—Asymptotic performance, asymptotic weight distribution (AWD), extrinsic information transfer (EXIT), density evolution (DE), inter-symbol interference (ISI), low-density parity-check (LDPC) codes, magnetic recording (MR), turbo detection.**

Manuscript received July 17, 2017; revised October 27, 2017 and December 6, 2017; accepted January 21, 2018. Date of publication January 25, 2018; date of current version May 22, 2018. This work was supported in part by the NSF of China under Grant 61771149, Grant 61471131, Grant 61501126, and Grant 61701121, in part by the Hong Kong Scholars Program under Grant XJ2016027, in part by the Open Research Fund of National Mobile Communications Research Laboratory, Southeast University, under Grant 2018D02, in part by the NSF of Guangdong Province under Grant 2016A030310337, in part by the Science and Technology Program of Guangzhou under Grant 201607010155, in part by the Guangdong Province Universities and Colleges Pearl River Scholar Funded Scheme under Grant 2017-ZJ022, in part by the Graduate Education & Innovation Project of Guangdong Province under Grant 2016QTLXXM_28, and Grant 2018XSLT13, in part by the Fujian 2015 Joint Industrial Research under Grant 2015H6014, in part by the Fujian Outstanding Youth Talent Program, and in part by the Guangdong Innovative Research Team Program under Grant 2014ZT05G157. *(Corresponding author: Guofa Cai.)*

Y. Fang is with the School of Information Engineering, Guangdong University of Technology, Guangzhou 510006, China, and also with the Department of Electronic and Information Engineering, Hong Kong Polytechnic University, Hong Kong (e-mail: fangyi@gdut.edu.cn).

G. Han is with the School of Information Engineering, Guangdong University of Technology, Guangzhou 510006, China (e-mail: gjhan@gdut.edu.cn).

G. Cai is with the School of Information Engineering, Guangdong University of Technology, Guangzhou 510006, China, and also with the National Mobile Communications Research Laboratory, Southeast University, Nanjing 210096, China (e-mail: caiguofa2006@126.com).

F. C. M. Lau is with the Department of Electronic and Information Engineering, Hong Kong Polytechnic University, Hong Kong (e-mail: encmlau@polyu.edu.hk).

P. Chen is with the Department of Electronic Information, Fuzhou University, Fuzhou 350116, China (e-mail: ppchen.xm@gmail.com).

Y. L. Guan is with the School of Electrical and Electronic Engineering, Nanyang Technological University, Singapore 639798 (e-mail: eylguan@ntu.edu.sg).

Digital Object Identifier 10.1109/COMST.2018.2797875

I. Introduction

A. Overview of LDPC-Coded MR Systems

LOW-DENSITY parity-check (LDPC) codes were first proposed by Gallager in his doctoral dissertation [1]. This type of codes has appeared to be one of the most widely used error-correction codes (ECCs) in the digital communication and data storage systems. However, Gallager's research work has been largely ignored for more than thirty years because of the high computational complexity for implementing LDPC codes. In 1993, an important paradigm shift in the evolution from algebraic codes to random codes has emerged — the invention of the capacity approaching *turbo codes* [2]. Turbo codes have been proved to perform very close to Shannon capacity over additive white Gaussian noise (AWGN) channels under iterative decoding algorithms.[1] In parallel with the phenomenal success of turbo codes, LDPC codes, which can exhibit near-capacity error performance under iterative decoding as well, have been rediscovered by Mackay [3]. Compared with turbo codes, LDPC codes not only possess better error performance (e.g., lower error floors), but also require lower computational complexity [4]–[8]. Thereafter, such type of codes has played a significant role in modern communication systems and has thus attracted more and more attention in both academia and industry [9]–[22]. During the long-term renaissance of LDPC codes, one milestone work is the exploitation of "Tanner graph" [23]. In that work, Tanner has conceived a bipartite-graph representation for LDPC codes that makes their design and analysis much easier. Nowadays,

[1] "Shannon capacity" and "channel capacity" may be used interchangeably in this paper.

LDPC codes have been extensively adopted in a variety of communication systems, such as deep-space communication systems [24], [25], wireless communication systems [26], optical communication systems [27], and underwater acoustic communication systems [28].

Inspired by their appealing characteristics, LDPC codes have been further applied to enhance the reliability of data storage systems, such as magnetic recording (MR) systems and flash memory systems [29]–[33]. Data storage systems and digital communication systems are very similar due to the fact that the original (written/transmitted) information should be extracted from the readback/received signal in both systems. To be specific, in an MR system, the write head, magnetic medium, and read head are respectively analogous to the transmitter, channel, and receiver in a digital communication system [34]. In addition to noise, intersymbol interference (ISI) and inter-track interference (ITI) are two other important factors that deteriorate the reliability of stored data over MR channels. From the storage-density prospective, the development of MR devices has experienced two stages, during which two classical types of MR systems (one-dimensional MR (ODMR) system and two-dimensional MR (TDMR) system) have been proposed, respectively. As compared to the ODMR systems, the TDMR systems benefit from much higher storage density, but suffer from more severe ISI (i.e., TD-ISI) and lower reliability [35]. According to [36] and [37], the promising TDMR techniques, e.g., bit-patterned media recording (BPMR) and heat-assisted (HA) MR, can dramatically increase the data-storage (i.e., areal) density far beyond $1\,\mathrm{Tb/in^2}$. Particularly, the HAMR systems, whose areal density may achieve $10\,\mathrm{Tb/in^2}$, is likely to be commercially available after 2018 [38]. Moreover, the aforementioned TDMR techniques can possibly achieve $20\,\mathrm{Tb/in^2}$ in the future because the areal density is expected to continue increasing by 10% per year during the next decade. The high-density and low-cost properties make such MR techniques a preferred choice for large-capacity storage applications.[2]

With an aim to alleviating the negative effect caused by ISI, various techniques have been developed. Among all the ISI-combating techniques, of particular interest are the turbo detection (i.e., turbo equalization) [40] and precoding [41]. After the advent of turbo codes, turbo detection has been extensively exploited to retrieve the original information from the "corrupted" received (or readback) signal of MR systems [42], [43]. Besides, it has been proven that turbo detection is very effective in improving the performance of digital communication and data storage systems that are subject to ISI [37], [44]–[46]. The basic principle of turbo detection is to treat the ISI channel and ECC, respectively, as the inner code and the outer code of a serial concatenated coding scheme. Thus, a turbo-like iterative decoding process can be performed to equalize the ISI channel and to decode the original information. In turbo detection, an inner soft-input-soft-output (SISO) detector and an outer SISO decoder are utilized and their extrinsic "soft" information is exchanged iteratively [41], [42]. Unlike the hard information, the soft information contains the maximum amount of knowledge regarding the channel characteristics and is of great importance to achieve noticeable gain in MR channels. The Bahl-Cocke-Jelinek-Raviv (BCJR) algorithm [47] and soft-output Viterbi algorithm (SOVA) [48], which take ISI into consideration, are two notable SISO detection techniques for MR channels.

Initially, most related works studying turbo detection have directly adopted convolutional codes as the outer code (channel code). However, such type of codes is not capable of achieving capacity-approaching performance and has subsequently been replaced by turbo codes [40], [49]. In MR systems, high-rate codes ($R \geq 4/5$) are preferable because they are more promising in pursuing the ultimate limit of areal density [34]. During the past fifteen years, LDPC codes have become a competitive scheme for the outer code because of their powerful error-correction capability and low decoding complexity [50]–[60]. Different from AWGN and ergodic fading channels which are memoryless, MR channels belong to the "channel with memory" category. The capacity of channels with memory is extremely difficult to derive and it is still a challenging problem today. As a remedy, a new performance metric, namely *symmetric information rate (SIR)*, has been proposed to characterize the fundamental lower-limit of the achievable information rate for reliable storage [61]–[67]. Owing to the inherent memory property of ODMR and TDMR channels, LDPC codes that have capacity-approaching performance in AWGN and ergodic fading channels do not perform that well in such scenarios [12], [34], [68]. Accordingly, a great deal of research effort has been dedicated to modifying the asymptotical analysis tools, e.g., density evolution (DE) [57], [69], [70], extrinsic information transfer (EXIT) function [71]–[73], and asymptotic weight distribution (AWD) [73], so as to facilitate the design of LDPC codes in MR scenarios. In [55] and [57], several capacity-approaching LDPC codes have been constructed in the context of OD-ISI and TD-ISI, respectively.[3] Furthermore, the detection and decoding algorithms for LDPC-coded MR systems have been carefully discussed in order to either improve the performance or reduce the complexity [58], [63], [72], [74]–[80]. Especially, various joint designs of iterative decoder in conjunction with channel detector have been proposed and studied in [74], [77], and [78].

Nevertheless, most capacity-approaching LDPC codes suffer from quadratic encoding complexity because of their irregular structures. This drawback severely limits their application in practical data-storage devices. To clear this obstacle, a type of structured LDPC codes, quasi-cyclic LDPC (QC-LDPC) codes, has been investigated and optimized in MR systems [81]–[84]. Meanwhile, the protograph LDPC codes

[2]Although solid-state drives have been widely exploited as a primary data-storage method in recent years because of the fast read/write speed and low power consumption [39], they suffer from limited number of program/erase cycles and high cost. The aforementioned disadvantages limit the applications of SSD techniques in certain scenarios, especially for large-capacity storage scenarios (e.g., video storage).

[3]Here, the capacity, also known as *independent and identically distributed (i.i.d) capacity*, establishes the fundamental lower limit on the decoding threshold of any code-design scheme in MR channels [70]. This performance metric is specified by the SIR and will be elaborated in Section II-B3.

that not only can achieve very desirable performance but also can realize linear encoding and fast decoding have emerged as a promising solution for modern digital communication systems [21], [68], [85]–[90]. Inspired by the above superiority, many researchers have endeavored to analyze and design good protograph codes so as to approach the capacity of MR channels [73], [91]–[96]. For example, Van Nguyen *et al.* [94] have proposed a family of rate-compatible (RC) protograph codes that possesses decoding thresholds very close to the capacity and minimum distances growing linearly with the codeword length (i.e., the linear-minimum-distance property) over OD-ISI channels. As a further advancement, the spatially-coupled (SC) LDPC codes, which are formulated by coupling a series of identical LDPC codes together into a single coupled chain [97], [98], have also been investigated and optimized in MR scenarios [99], [100]. It has been pointed out in [101] that SC codes are able to exhibit both the capacity-approaching iterative decoding threshold and the linear-minimum-distance property, which is extremely difficult to be realized in other LDPC-based codes.[4] In addition, the LDPC codes together with their variants can be easily extended to the non-binary domain, forming the non-binary LDPC codes [102], [103], non-binary protograph codes [104], and non-binary SC codes [105]. As is well known, the non-binary LDPC-based codes are superior to their binary counterparts in certain cases, such as short- and moderate-codeword-length cases [102]. Due to such attractive benefits, a myriad of researchers have tried to explore the feasibility of non-binary LDPC-based codes in MR systems as well as to devise their corresponding encoding and decoding algorithms [31], [32], [36], [106]–[110].

In parallel with the advances in turbo detection and channel coding, precoding techniques can be incorporated into MR systems for the sake of pre-canceling (at least partially) the ISI. Actually, the effect of precoding on the convergence process of turbo detector has been deeply discussed in [42]. Aiming at perfectly matching the characteristics of a given MR channel, more research attention has been focused on the joint design of precoders and channel codes (e.g., LDPC codes) [41], [111], [112]. It has been demonstrated that coupling the precoder and ECC can offer a gain of about 6 dB with respect to the uncoded MR channels [42]. All in all, it is possible to realize reliable data storage even in ultra-high-density (UHD) MR systems if the benefits of LDPC codes, precoders, and turbo detectors can be substantially exploited.

B. Contributions and Motivations

In this paper, we provide a comprehensive survey of the state-of-the-art design and analysis methodologies of LDPC codes over ODMR and TDMR channels, as well as their detection and decoding algorithms. More specifically, we start our discourse by introducing the typical architecture and fundamental principles of LDPC-coded MR systems, the relevant channel models and ISI-cancelation techniques. Afterwards, we briefly review the concepts of LDPC codes and their variants that are particularly suitable for MR applications. We then proceed to outline the prevailing theoretical-analysis tools that are very useful for both performance evaluation and code design in the context of MR channels. Based on the fundamental knowledge, we further summarize the current research achievements in the design of LDPC codes and their classical variants. Finally, we highlight the pivotal open research problems for the future development of LDPC-coded MR systems. Since our target is to offer a specific overview of LDPC-coded MR systems rather than an extremely wide coverage of all channel-coded MR systems, certain topics may not be included in this paper.

Although the list of references in this treatise may be not exhaustive, the articles cited are carefully selected and thus can serve as a good starting point for further reading. Actually, there exist several tutorial-like coverages related to LDPC-coded MR systems [29], [34], [113], which have quite different focuses. For example, Song and Kumar [29] have discussed the feasibility of using LDPC codes in MR systems and ways to reduce their hardware implementation complexity. Dholakia *et al.* [34] have illustrated that the capacity-approaching codes in AWGN channels can be applied to MR channels after appropriate re-designing. Moreover, Vasic and Kurtas [113] have provided the first comprehensive review of the attainable coding and signal processing techniques for MR channels. However, the above-mentioned papers have mainly limited their attention to ODMR channels and the available advancements before 2004. During the following decade, a flurry of research works on LDPC-coded MR systems have been carried out, and consequently significant research progresses have been achieved. Against this background, it is indispensable a new and thorough overview of the important milestones in LDPC-coded MR systems be presented. To this end, most of the related works surveyed in this paper were published in the past thirteen years. Yet, we also include a few earlier works that have vital impacts on this research topic. Moreover, this is the first survey that touches upon the research progress regarding the variants of LDPC codes for MR applications. We believe that this treatise can be considered as a useful reading for potential researchers.

C. Roadmap of This Survey

This paper is structured as in Fig. 1. As can be seen, Section II introduces the system model of LDPC-coded MR frameworks as well as their channel models and crucial anti-ISI techniques. This section also offers a historical overview of LDPC-coded MR systems. Section III outlines the basic concepts of LDPC codes and their relevant variants, emphasizing the representation methods, code constructions, and decoding algorithms. Section IV details three types of theoretical methodologies that can noticeably facilitate the design and analyses of LDPC-based codes in MR scenarios. Section V summarizes the design paradigms of LDPC codes and their decoding algorithms over two different types of MR channels, i.e., ODMR and TDMR channels. Section VI concisely portrays the design guidelines of several attractive variants of

[4]To simplify the exposition, we refer to the LDPC codes and all their variants as the LDPC-based codes in the remainder of this paper.

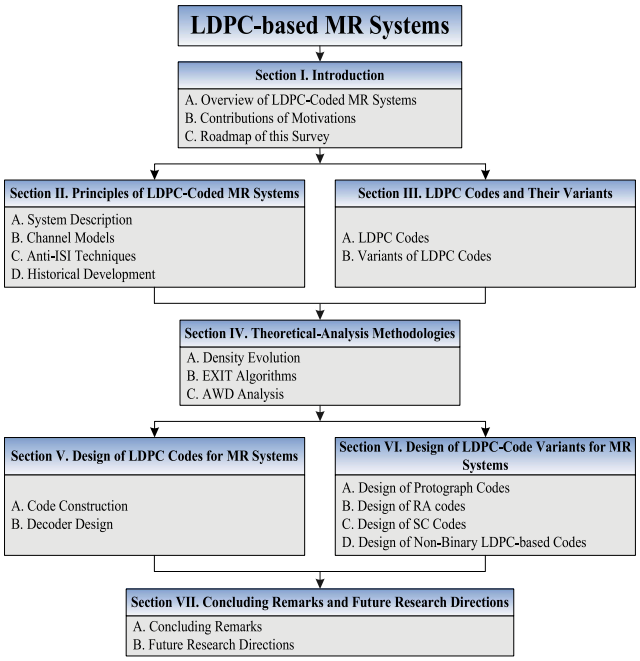

Fig. 1. Structure of this paper.

LDPC codes for use in MR systems. Finally, Section VII concludes this paper and conceives some future research directions. To facilitate the reading of this paper, the list of abbreviations used in this survey is shown in Table I.

TABLE I
LIST OF ABBREVIATIONS USED IN THIS SURVEY

AR3A	accumulate-repeat-3-accumulate
AR4JA	accumulate-repeat-by-4-jagged-accumulate
AS/BAS	absorbing set/balanced AS
AWGN	additive white Gaussian noise
AWD	asymptotic weight distribution
BCH	Bose-Chaudhuri-Hocquenghem
BCJR	Bahl-Cocke-Jelinek-Raviv
BER/WER	bit-error-rate/word error rate
BP	belief propagation
BPMR	bit-patterned media recording
CIR	channel impulse-response
CSI	channel state information
CW-3	column-weight-3
DE	density evolution
ECC	error-correction code
EMD/ACE	extrinsic message degree/approximate cycle EMD
EXIT/PEXIT	extrinsic information transfer/protograph EXIT
FFT	fast-Fourier-transform
FL/IL	finite-length/infinite-length
FPGA	field-programmable gate array
GA	Gaussian approximation
GF	Galois field
i.i.d.	independent and identically distributed
IRCSDF	iterative row-column soft decision feedback algorithm
ISI/ITI	inter-symbol interference/inter-track interference
LDPC	low-density parity-check
LLR	log-likelihood-ratio
MAP/ML	maximum a posteriori/maximum likelihood
MI	mutual information
MP	message-passing
MR/HAMR	magnetic recording/heated-assisted MR
OD/TD	one-dimensional/two-dimensional
PDF	probability density function
PEG	progressive-edge-growth
PPM	pulse-position modulation
PR4/EPR4	class-4 PR/extended PR4
PR	partial response
QC	quasi-cyclic
qPSK	q-ary phase-shift-keying
QPSK	quadrature phase shift keying
QSP	q-ary sum-product
RA/IRA	repeat-accumulate/irregular RA
RC/RCOP	rate-compatible/RC optimized protograph
SC	spatially coupled
SIR	symmetric information rate
SISO	soft-input soft-output
SNR	signal-to-noise-ratio
SOVA	soft-output Viterbi algorithm
TMDR	typical minimum distance ratio
SPC/TP	single-parity-check-based turbo product
UHD	ultra-high-density
VN/CN	variable node/check node

II. PRINCIPLES OF LDPC-CODED MR SYSTEMS

As a type of ECCs, LDPC codes, which were invented by Gallager [1], dominate the development of coding theory in modern MR systems because of their capacity-approaching performance [113]–[116]. In this section, the system architecture of a typical LDPC-coded MR system is first presented. In the sequel, the prevailing channel models and anti-ISI techniques for MR-system research are introduced. Finally, the major contributions achieved on the study of LDPC-based codes over MR channels in the past two decades are summarized.

A. System Description

Fig. 2 depicts the block diagram of a typical MR system utilizing an LDPC-based code. At the beginning, a sequence of i.i.d. information bits $\mathbf{s} = \{s_1, s_2, \ldots, s_K\}$ is generated, where $s_j \in \{0, 1\}$.[5] The information sequence is then encoded into an LDPC-based codeword $\mathbf{v} = \{v_1, v_2, \ldots, v_N\}$, where $v_j \in \{0, 1\}$. As can be observed, the lengths of the information sequence and LDPC codeword are K and N, respectively, and thus the code rate becomes $R_c = K/N$. The coded bits will be modulated to $\mathbf{x} = \{x_1, x_2, \ldots, x_N\}$, where $x_j = (-1)^{v_j}$. Afterwards, the bipolar sequence is transmitted through an MR channel, which can be modeled by an ISI channel plus AWGN. At the receiver terminal, the "corrupted" signal output from the channel will be passed into a turbo-like decoder for the sake of retrieving the original information. In the following, we will elaborate a little further on the component modules of such a system.

1) LDPC-Based Encoder: In the system, the channel coding module is implemented by an LDPC-based code, such as LDPC/QC-LDPC code, protograph code, SC code, and their non-binary counterparts. With appropriate designs, all these codes can achieve capacity-approaching error performance over MR channels. Aiming at increasing the code rate and boost the throughput, punctured bits (i.e., punctured variable nodes (VNs)) can be involved in the LDPC-based codes [91]. Such codes are referred to as *punctured LDPC-based codes*. Puncturing is the process of removing some coded bits from

[5]Unless otherwise specified, we assume that a binary LDPC-based code is utilized in this paper.

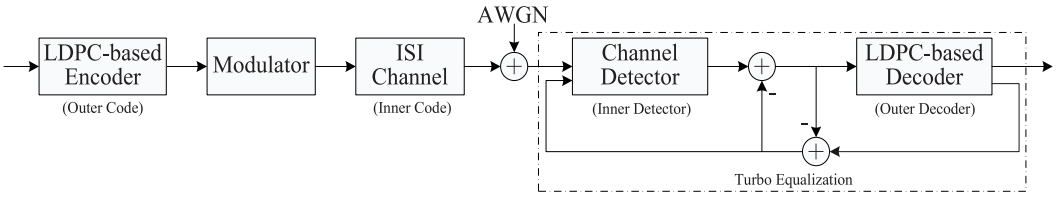

Fig. 2. Block diagram of a typical MR system utilizing an LDPC-based code.

the codeword prior to transmission. This technique was first exploited to increase the code rate at the price of sacrificing some error performance [117], [118]. However, it has been pointed out in [68], [84], [91], and [107] that the convergence performance and the error performance of some protograph codes can also be enhanced if the punctured bits are properly selected. In Fig. 2, the puncturing module is ignored because it can be incorporated into the encoder.

2) Modulator: In MR systems, the modulation is realized by a binary antipodal signaling scheme, i.e., $\{0, 1\} \rightarrow \{+1, -1\}$ [37], [50]. Therefore, for non-binary LDPC-coded MR systems, one should employ a symbol-to-bit converter to convert a q-ary symbol to $\log_2 q$ binary bits before performing modulation [31], [48], [60], [115].

3) MR Channels: There are two major types of MR systems in the data-storage community, i.e., ODMR system [31] and TDMR system [37]. Taking into account the complexity and accuracy, both ODMR and TDMR systems can be described by different types of channel models [35], [119]–[130]. Among these channel models, the discrete-time baseband channel model, in which the MR channel is described by an ISI channel with AWGN (see Fig. 2), is the most popular one [54]–[56], [64], [73], [125]–[127]. Hence, this type of channel model has been widely adopted in the relevant research of both MR systems. Although the ISI channel is an ideal model, it still offers a nice way to develop the related analysis and design methodologies [61], [72], [74], [130]. Moreover, the attained results in the context of ISI channels are of great importance because they can serve as a good benchmark to devise realistic channel-coded MR systems with robust ISI immunity and powerful error-correction capability. Owing to the aforementioned issues, we are primarily interested in the design and analysis of LDPC-based codes over OD-ISI and TD-ISI channels in this paper. It should be noted that the precoding operation can be embedded in the ISI-channel module and thus is ignored in our system model.

4) Turbo Detection: In order to retrieve the original information, the channel output is fed into a turbo-like iterative receiver for further processing. The idea of turbo detection has come from the iterative decoding algorithm of turbo codes [34], [40], [131]. In such an efficient decoding framework, two SISO decoders, namely the *inner detector* and *outer decoder*, are involved. By allowing the inner detector (channel detector) and outer decoder (LDPC-based decoder) to exchange soft extrinsic information iteratively, the ISI of MR channels can be substantially overcome and the original information can be recovered with a high accuracy. We will further elaborate the turbo detection in Section II-C.

B. Channel Models

As discussed in Section II-A3, the discrete-time baseband channels that include finite-state ISI and AWGN are very common channel models used in MR-system research [29], [61], [64], [73], [132].[6] In such channels, the memory length is utilized to manifest how severe the ISI is. To facilitate the design and analysis of MR systems, the ISI channel model does not consider imperfect channel shaping, colored noise, and media noise (e.g., jitter noise) [53], [119]–[124]. Despite its extreme simplification, this type of channels serves as a useful model in developing coding design criterion for MR systems. The resultant code-construction methodologies may turn out to be useful in more general channel models.

To provide a more accurate characterization of ODMR systems, some other channel models, e.g., equalized Lorentzian model, have been proposed in recent years [119], [122], [128]. However, the models proposed for ODMR systems are not applicable to TDMR systems because of different storage mechanisms and noise sources. For this reason, researchers have developed a variety of new models tailored for TDMR configurations [123], [124], [129].

In particular, the performance of MR systems is also dependent on media noise in addition to ISI and AWGN [120], [133], [134]. Different MR technologies, e.g., ODMR [120], TDMR [123], BPMR [59], HAMR [133], and microwave-assisted MR [134], have different read/write mechanisms and manufacturing processes, which may lead to different forms of media noise. To capture the properties of such type of noise, a number of channel models have been developed during the past decade. Specifically, the microtrack model can be used to describe the ODMR channels with media noise [120]–[122], [135], while the Voronoi model and TD microcell model can be used to describe the TDMR channels with media noise [50], [136]–[138].

Nevertheless, conventional ECCs (e.g., LDPC codes) are no longer effective in overcoming insertion and deletion errors caused by media noise [116], [120], [136]. These insertion and deletion errors must be corrected by some special ECCs, such as *watermark codes* [139] and *marker codes* [116]. Furthermore, it has been pointed out by a myriad of research articles [50], [120]–[122], [137], [138], [140], [141] that media noise can be estimated and compensated (or partially compensated) by appropriate detection algorithms. For example, the pattern-dependent noise-predictive detection

[6]Precisely speaking, one should apply an equalization filter to shape the physical ODMR/TDMR channel to an OD-ISI/TD-ISI channel [31], [34], [113].

algorithms [120], [141] and improved multitrack detection algorithms [50], [137], [138], [140] can efficiently eliminate some media noise in MR systems at the expense of increasing implementation complexity. Although mitigating the negative effect of media noise is an important topic and may require further study, it is outside the scope of this treatise. More comprehensive treatments on this topic can be readily found in the literature.

In fact, most of the aforementioned channels are particularly used to describe the reading process of MR systems while assuming a perfect writing process. In other words, such channel models only characterize the ISI and noise that affect the readback signal. However, due to random island position jitter, variations of magnetic switching field among magnetic grains, and accumulative frequency shift caused by the spindle speed variation and other mechanical vibration, it is difficult to realize near-perfect synchronization in the write head, which may result in written-in errors. To deal with this problem, some researchers have investigated the effect of such imperfection and have conceived some write channel models to describe the writing process [142], [143]. Furthermore, Han *et al.* [116] have introduced an embedded-marker-code-based scheme to correct the written-in errors. It has also been shown that the scheme can dramatically improve the storage efficiency of TDMR systems. In this survey paper, we are primarily interested in the read channels and thus do not consider the written-in errors in MR systems. Interested readers can find more details of these write channel models in the above articles and the references therein.

In the following, we will present the discrete-time baseband channel models for both ODMR and TDMR systems which are adopted in this treatise.

1) OD-ISI Channel: The OD-ISI channel can be commonly modeled by a partial response (PR) channel with AWGN. Specifically, the impulse response of a PR channel is $H(D) = (1-D)(1+D)^{\kappa-1} = \sum_{\tau=0}^{\kappa} h_\tau D^\tau$, where D is the unit-delay operator corresponding to the symbol interval, $\kappa \in \mathbb{N}^+$ is the length of channel memory, h_τ is the channel coefficient of the τ-th tap. Therefore, the OD-ISI channel model can be written as

$$y_j = \sum_{\tau=0}^{\kappa} h_\tau x_{j-\tau} + n_j, \tag{1}$$

where $x_{j-\tau}$ and y_j are the (binary) channel input and output, respectively, $n_j \sim \mathcal{N}(0, \sigma_n^2)$ is the AWGN with zero mean and variance $\sigma_n^2 = N_0/2$, and N_0 is the noise power-spectral density. In actual implementation, different types of OD-ISI channels can be formulated by varying the memory length κ. For instance, three typical OD-ISI channels are listed in Table II. Referring to this table, a larger value of κ allows higher storage density, but results in more severe ISI simultaneously.

2) TD-ISI Channel: In TDMR systems, the readback signal suffers from not only the ISI in the down-track direction but also the ITI in the cross-track direction. Therefore the $\kappa_\mu \times \kappa_\tau$ impulse-response matrix for a discrete-time TD-ISI channel is given by

TABLE II
LIST OF THREE TYPICAL OD-ISI CHANNELS

Memory Length	Channel Type	$H(D)$
$\kappa = 1$	Dicode	$1 - D$
$\kappa = 2$	Class-4 PR (PR4)	$1 - D^2$
$\kappa = 3$	Extended PR4 (EPR4)	$1 + D - D^2 - D^3$

$$\mathbf{\Lambda} = \begin{pmatrix} h_{1,1} & h_{1,2} & \cdots & h_{1,\kappa_\tau} \\ h_{2,1} & h_{2,2} & \cdots & h_{2,\kappa_\tau} \\ \vdots & \vdots & \ddots & \vdots \\ h_{\kappa_\mu,1} & h_{\kappa_\mu,2} & \cdots & h_{\kappa_\mu,\kappa_\tau} \end{pmatrix}, \tag{2}$$

where κ_μ and κ_τ are the numbers of magnetic islands that the read head sense in the cross-track and down-track directions, respectively, $h_{\mu,\tau}$ is the (μ,τ)-th element of the channel-impulse-response (CIR) matrix. In fact, the interference coming from the two adjacent tracks of each main track dominates the ITI while the interference due to the nonadjacent tracks is extremely small and can be ignored [78]. In this sense, (2) can be simplified to a matrix with three rows (i.e., $\kappa_\mu = 3$). Due to the aforementioned reason, a large set of research works related to TDMR systems have assumed a 3×3 CIR matrix [36], [58]–[60], [69], [73], [77]–[80]. As an example, the CIR matrix for TDMR systems with a recording density of 4 Tb/in^2 can be expressed by [79]

$$\mathbf{\Lambda}_{4\mathrm{T}} = \begin{pmatrix} 0.0368 & 0.1435 & 0.0368 \\ 0.2299 & 0.8966 & 0.2299 \\ 0.0368 & 0.1435 & 0.0368 \end{pmatrix}. \tag{3}$$

Assume that a bipolar sequence $\{x_{j'} \in \{+1,-1\} \mid 1 \le j' \le N\}$ is distributed on a TD array of size $L_m \times L_n$, forming $\{x_{l,j} \in \{+1,-1\} \mid 1 \le l \le L_m, 1 \le j \le L_n\}$, where $N = L_m \times L_n$, L_m and L_n are the numbers of rows and columns of the TD array, respectively. Then, $x_{j'} \to x_{l,j}$ represents the mapping rule from the original OD sequence to a TD array. For ease of analysis and exposition, we also assume that the TD array is surrounded by "-1s", i.e., $x_{l,j} = -1$ if $(l,j) \notin \{1 \le l \le L_m, 1 \le j \le L_n\}$, as in [55], [69], and [78]. In general, the input-output relationship for the discrete-time 2D-ISI channel can be described as

$$y_{l,j} = \sum_{\mu=1}^{\kappa_\mu} \sum_{\tau=1}^{\kappa_\tau} h_{\mu,\tau} x_{l-\mu,j-\tau} + n_{l,j}, \tag{4}$$

where $y_{l,j}$ is the readback signal corresponding to the magnetic data bit in the l-th row and j-th column of the TD array, $n_{l,j} \sim \mathcal{N}(0, \sigma_n^2)$ is the AWGN with zero mean and variance $\sigma_n^2 = N_0/2$.

3) SIR for ISI Channels: Although a significant amount of research effort has been devoted to investigating the capacity of OD/TD-ISI channels, it remains as an open problem nowadays. In other words, it is rather difficult to derive the maximum mutual information (MI) between the input and output of an OD/TD-ISI channel because all the input distributions should be enumerated. Alternatively, the SIR, i.e., the MI based on the i.i.d. equiprobable input assumption, can

be utilized to establish a lower bound on the channel capacity [144]. In MR channels, SIR is considered as the maximum achievable rate that can realize reliable communication for a given E_b/N_0. Moreover, the E_b/N_0 corresponding to a given SIR is referred to as *i.i.d. capacity signal-to-noise-ratio (SNR) limit* [61], [62], [70], [145].[7] In the past two decades, many researchers have tried to develop effective algorithms to calculate the SIR of MR systems [64]–[67], [70], [126], [145]. To be specific, the SIR of OD-ISI channels has first been investigated in [61], [70], and [145], which has been subsequently generalized to SIR of TD-ISI channels [64]–[67], [126]. In accordance with [61], [64], [145], Monte-Carlo techniques can be exploited to estimate the SIRs with reasonable accuracy. Here, we skip the calculation procedure of SIR but refer the interested readers to the aforementioned literature for more details since it includes a large set of mathematical derivations.

C. Anti-ISI Techniques

In Section II-A, we briefly introduced the component modules involved in an LDPC-coded MR system. In what follows, we will spend particular attention on two prevailing anti-ISI techniques, i.e., precoding and turbo detection, for such scenarios.

1) Precoding: It has been demonstrated by a vast number of references that introducing ECC and precoding is able to achieve a gain of $4 \sim 5$ dB over uncoded MR systems. Precoding is a preprocessing technique for the transmitted signals before they are passed through MR channels. In particular, the main idea of precoding is to design an appropriate code (e.g., a rate-1 convolutional code) based on the type of ISI channel so as to alleviate the corresponding interference and accelerate the convergence of the decoding process. By incorporating a precoding scheme, the resultant ISI channel is referred to as a *precoded ISI channel* [41]. In this case, the precoded ISI channel can also be considered as the inner code.

At the beginning, most research on precoding schemes has separated their designs from the ECCs. For instance, Ryan [146] has only considered the channel characteristics rather than the code structures when optimizing the precoder. Inspired by the idea of turbo detection and iterative decoding, more and more research activities have moved on to investigating the interaction between the precoder and ECC [41], [54], [112]. In such scenarios, the precoded ISI channel and ECC can be treated, respectively, as the inner code and outer code of a serial concatenated coding scheme. This framework has turned out to be a soft-information iterative paradigm, which is of great usefulness to facilitate turbo detection and to enhance the error performance of MR systems.

As indicated in [42] and [53], the effect of the precoder on the performance of channel-coded MR systems is dependent on the constraint length of ECC. Specifically, short-constraint-length codes (e.g., convolutional codes and serial concatenated codes) can achieve a remarkable performance gain by concatenating a precoder while long-constraint-length codes (e.g., LDPC codes and parallel concatenated codes) cannot. In fact, long-constraint-length codes always provide good distance spectrum, and thus the precoder provides no effective spectrum thinning. For this reason, there is no need to design a precoder for LDPC-coded MR systems.

2) Turbo Detection: Distinguished from conventional decoders, the turbo decoder (i.e., turbo detector) possesses two distinguished advantages: (i) the extrinsic soft information output from the inner detector/outer decoder can extract maximal amount of channel state information (CSI) knowledge; and (ii) the iterative processing can efficiently execute soft-decision decoding with acceptable complexity. Benefiting from these advantages, the turbo-equalization technique significantly accelerates the convergence speed of iterative decoding processes. In the past two decades, a great deal of research effort has been devoted to investigating and developing effective turbo-equalization techniques over both OD-ISI [40]–[43], [48], [131], [147], [148] and TD-ISI channels [37], [50].

To implement the inner detector, two notable algorithms, namely the BCJR algorithm [47] and SOVA [149], have been used. As compared with the suboptimal SOVA, the BCJR algorithm is a type of maximum a posteriori (MAP) decoding algorithm and can accomplish more desirable performance [36], [150]–[152]. In order to get the minimum error rate, the BCJR algorithm has been extensively adopted as the channel detector [31], [32], [53]–[60], [153], [154]. Since the computational complexity of BCJR algorithm increases exponentially with the channel memory length, some low-complexity variants have been proposed [79], [114], [155]–[157]. In this paper, we also assume that the BCJR detector is adopted in the LDPC-coded MR systems unless otherwise stated, as in most other related references.

In contrast to the inner detector, the log-likelihood-ratio (LLR)-based belief-propagation (log-BP) decoding algorithm, which achieves identical performance and much lower complexity with respect to the conventional probability-based BP algorithm [10], [150], is exploited in this paper. Besides, some other reduced-complexity decoding algorithms, such as the min-sum decoding algorithm, have been conceived in [158]. It should be noted that we do not consider interleaving in our system because there is already an embedded random interleaver within the LDPC-based codes.

Interested readers are referred to the above-mentioned publications for more comprehensive knowledge of the turbo detection as well as its component inner detector and outer decoder.

D. Historical Development

In the past two decades, LDPC codes have received a significant amount of attention in MR community and hence they represent a dominant research direction for channel-coded MR systems. As a consequence, taking into consideration the characteristics of MR channels, many contributions related to the design and analysis of LDPC codes as well as their promising variants have been shown [28], [29], [31], [32], [48], [53]–[60], [68]–[71], [73], [81]–[83], [113], [116], [143], [159]. In parallel with the code design and performance analysis advancements, the decoding algorithms of LDPC

[7]For simplicity, we will use "capacity (or capacity limit)" to represent "i.i.d. capacity SNR limit" from this point onwards.

codes have been carefully studied and extensively discussed over MR systems so as to enhance the performance or reduce the complexity of the overall systems [30], [40], [51], [63], [72], [74]–[80], [108], [109], [114], [115], [127], [128], [153], [160], [161], In Table III, we summarize the major contributions in the field of LDPC-coded MR systems.

III. LDPC Codes and Their Variants

In this section, we will introduce the encoding and decoding principles of LDPC codes and their sophisticated variants which are particularly suitable for use in MR systems. We restrict ourselves to the concepts and fundamental basis of such type of codes here but leave the detailed design methodologies to Sections V and VI.

A. LDPC Codes

1) Representation Methods: An LDPC code C can be represented by an $M \times N$ sparse parity-check matrix $\mathbf{H} = (h_{i,j})$ that has a low density of "ones" [1], where $h_{i,j}$ is the element in the i-th row and j-th column of $\mathbf{H}$, $K = N - M$ is the length of information bits, N is the length of codeword, and $R = K/N$ is the code rate. Moreover, the j-th column and i-th row in $\mathbf{H}$ correspond to the j-th VN v_j and i-th CN c_i in C, respectively. Consequently, N is the number of VNs while M is the number of CNs. In $\mathbf{H}$, the weights of the j-th column and the i-th row (i.e., denoted by w_{v_j} and w_{c_i}) are defined as the numbers of "ones" in the corresponding column and row, respectively. Furthermore, w_{v_j} and w_{c_i} are also known as the degrees of the j-th VN and i-th CN (i.e., denoted by d_{v_j} and d_{c_i}), respectively. Supposing that $\mathbf{C}_\mu = (v_1, v_2, \ldots, v_N)$ is a valid codeword in C, it should follow $\mathbf{C}_\mu \mathbf{H}^{\mathrm{T}} = \mathbf{0}$, where $v_j \in \{0, 1\}$ and the superscript "T" denotes the transpose operation. This property is called the *checksum constraint*. A *regular* LDPC code is an LDPC code whose VN degree and CN degree are both constant (i.e., the row weight and column weight of $\mathbf{H}$ are both constant); otherwise the code is called an *irregular* LDPC code.

In addition to being represented by the parity-check matrix, an LDPC code C can be represented by a bipartite graph $\mathcal{G}$, also called the *Tanner graph* [23]. A Tanner graph is composed of a set of VNs, CNs, and their associated edges. Given the parity-check matrix of an LDPC code, its corresponding Tanner graph can be generated as follows: the j-th VN is connected to the i-th CN if and only if $h_{i,j}$ in the parity-check matrix $\mathbf{H}$ equals 1. According to the aforementioned construction rule, there are totally N VNs, M CNs, as well as $|\mathbf{H}|$ edges in a Tanner graph, where each VN corresponds to a coded bit and each CN corresponds to a checksum constraint. In the Tanner graph, a *cycle* is defined as a closed path starting and ending with the same node, but passing through different intermediate nodes. The cycle length is equal to the number of edges in a cycle, and a cycle of length l is referred to as an l-cycle. In particular, the length of the shortest cycle in a Tanner graph is called its *girth*. More importantly, the BP iterative decoding route of an LDPC code can be specified by the Tanner graph, in which each node (i.e., VN/CN) represents an SISO decoder [18], [158].

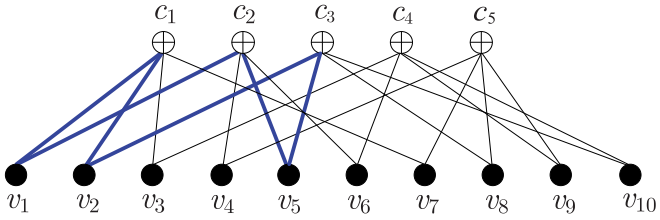

Fig. 3. Tanner graph of a $(2, 4)$-regular LDPC code. The parameters used are $N = 10, K = 5, d_v = 2,$ and $d_c = 4$.

Example 1: Consider a regular LDPC code corresponding to the following parity-check matrix

$$\mathbf{H} = \begin{pmatrix} 1 & 1 & 1 & 0 & 0 & 0 & 1 & 0 & 0 & 0 \\ 1 & 0 & 0 & 1 & 1 & 1 & 0 & 0 & 0 & 0 \\ 0 & 1 & 0 & 0 & 1 & 0 & 0 & 1 & 0 & 1 \\ 0 & 0 & 1 & 0 & 0 & 1 & 0 & 0 & 1 & 1 \\ 0 & 0 & 0 & 1 & 0 & 0 & 1 & 1 & 1 & 0 \end{pmatrix}, \quad (5)$$

where the codeword length and information length of the LDPC code equal $N = 10$ and $K = 5$, respectively. Moreover, the degree of VN is $d_{v_1} = d_{v_2} = \cdots = d_{v_{10}} = d_v = 2$ and the degree of CN is $d_{c_1} = d_{c_2} = \cdots = d_{c_5} = d_c = 4$. Based on the parity-check matrix, we can immediately obtain its corresponding Tanner graph, as depicted in Fig. 3. In this figure, the black circles and circles with a plus sign denote the VNs and CNs, respectively. As can be observed, this LDPC code includes a 6-cycle, which is highlighted by the blue-bold edges and their associated nodes.

More generally, an LDPC ensemble can be specified by a degree-distribution pair, i.e., $(\lambda(x), \rho(x))$, where $\lambda(x) = \sum_{d_{v_j}=2}^{d_{v,\max}} \lambda_{d_{v_j}} x^{d_{v_j}-1}$ and $\rho(x) = \sum_{d_{c_i}=2}^{d_{c,\max}} \lambda_{d_{c_i}} x^{d_{c_i}-1}$; $d_{v_j} \geq 2$ and $d_{c_i} \geq 2$ are the degrees of VNs and CNs, respectively; $d_{v,\max}$ and $d_{c,\max}$ are the maximum VN degree and CN degree, respectively; $\lambda_{d_{v_j}}$ and $\lambda_{d_{c_i}}$ are the fractions of edges connected to degree-d_{v_j} VNs and degree-d_{c_i} CNs, respectively. Given a fixed degree-distribution pair of an LDPC code ensemble, codewords of arbitrary lengths that belong to such an ensemble can be easily generated [5], [158]. For example, the LDPC code with the parity-check matrix (5) can be generated by the degree-distribution pair (x, x^3).

2) Code Construction: Based on a given degree-distribution pair, both the progressive-edge-growth (PEG) and approximate cycle extrinsic-message-degree (ACE) algorithms can be utilized to generate its corresponding parity-check matrix $\mathbf{H}$ (or Tanner graph $\mathcal{G}$) [14], [15], [158]. In this paper, we only focus on the PEG-based permutation rules. In practice, $\mathbf{H}$ is always in a non-systematic form and thus needs to be further processed in order to complete the generation of an LDPC code [164]. To be specific, $\mathbf{H}$ must be first transformed into $\mathbf{H}_{\mathrm{s}} = [\mathbf{I}_M \,|\, \mathbf{P}]$ through Gaussian elimination, where $\mathbf{I}_M$ is the $M \times M$ identity matrix and $\mathbf{P}$ is a $M \times K$ sub-matrix. The systematic generator matrix is then expressed by $\mathbf{G}_{\mathrm{s}} = [\mathbf{P}^{\mathrm{T}} \,|\, \mathbf{I}_K]$, where $\mathbf{I}_K$ is the $K \times K$ identity matrix. This generator matrix can be used to construct a systematic LDPC code $C_{\mathrm{s}} = (\mathcal{V}_{\mathrm{p}}; \mathcal{V}_{\mathrm{i}})$, where $\mathcal{V}_{\mathrm{p}}$ and $\mathcal{V}_{\mathrm{i}}$ are the parity bits and information bits, respectively. After constructing C_{s}, the original LDPC code C can be obtained by switching back the

TABLE III
MAJOR CONTRIBUTIONS ON STUDYING LDPC-CODED MR SYSTEMS

Year	Author(s)	Contribution
1995	Douillard *et al.* [131]	Invented a joint iterative equalizing and decoding technique for MR channels, referred to as turbo detection, which offers an efficient way to alleviate ISI and resist noise.
1999	Fan *et al.* [162]	Explored the feasibility of LDPC codes in MR systems.
2000	Song *et al.* [163]	Proposed a serially concatenated coding scheme exploiting the LDPC code as the outer code and the MR channel as the inner code, which can achieve a gain of $5.9\,\mathrm{dB}$ over the uncoded one in an EPR4 channel.
2001	Narayanan [42]	Discussed the effect of precoding on the convergence of turbo detector over OD-ISI channels, which illustrates that LDPC codes without precoding often outperform their precoded counterparts.
2001	Pfister *et al.* [61]	Introduced two simple Monte-Carlo methods to estimate the SIR of OD-ISI channels.
2002	Kurkoski *et al.* [30]	Presented a novel joint message-passing (MP) decoder for LDPC-coded ODMR systems, which not only achieves comparable performance but also benefits from a lower delay with respect to the conventional BCJR-BP decoder.
2002	Li *et al.* [53]	Compared the performance of single-parity-check-based turbo product (SPC/TP) codes and LDPC codes over OD-ISI channels and illustrated that the precoded SPC/TP codes perform similarly to the LDPC codes.
2003	Kavcic *et al.* [70]	Conducted a comprehensive study on the performance of LDPC codes over OD-ISI channels, including analyzing the channel SIR and developing the DE algorithm.
2003	Varnica *et al.* [57]	Optimized the degree-distribution pair of LDPC codes in order to approach the capacity of OD-ISI channels.
2003	Song *et al.* [108]	Applied non-binary LDPC codes to ODMR systems and proposed a low-complexity decoding algorithm with an aim to mitigating the burst-error impairment.
2004	Song *et al.* [29]	Summarized the principles of turbo detection and discussed the construction methods of structured LDPC codes for ODMR systems.
2005	Franceschini *et al.* [71]	Proposed an EXIT-chart-based design approach for LDPC codes concatenated with a Gray-mapped quadrature phase shift keying (QPSK) modulation over OD-ISI channels.
2005	Soriaga *et al.* [126]	Estimated the SIR of TD-ISI channels by considering the employment of multilevel coding and multistage decoding schemes.
2006	Chen *et al.* [64]	Developed the upper and lower bounds on the SIR of TD-ISI channels, which can provide tight estimates for SIR with relatively low computational complexity.
2007	Zhong *et al.* [82]	Presented the design guidelines for high-rate regular QC-LDPC codes over MR channels and explored their implementation feasibility based on a field-programmable gate array (FPGA) simulation platform.
2008	Tan *et al.* [41]	Proposed a finite-length (FL) EXIT analytical methodology for coded MR systems, which is of great importance to develop FL channel-coding construction schemes in such scenarios.
2008	Karakulak *et al.* [35]	Conceived a classical read channel model for TD-ISI channels, which can be utilized to characterize the feature of patterned media recording with reasonable accuracy.
2008	Shental *et al.* [66]	Invented two simulation-based methods to calculate the SIR of TD-ISI channels from the information theory perspective, and thus offered a better understanding of the theoretical limits of such systems.
2009	Liu *et al.* [58]	Applied non-binary LDPC codes to TD-ISI channels and investigated their decoding algorithm.
2009	Risso [76]	Developed a novel layered decoding algorithm for non-binary LDPC codes over MR channels, which outperforms the conventional BP decoding algorithms in terms of convergence speed and error performance.
2010	Han *et al.* [51]	Conceived bit-pinning/trellis-pruning techniques and a generalized LDPC decoder for LDPC-coded MR systems to improve their error-floor performance.
2010	Chang *et al.* [130]	Developed a multi-track detection technique to enhance the robustness against ITI in TDMR systems.
2011	Yang *et al.* [92]	Applied protograph codes to OD-ISI channels and evaluated their error performance.
2012	Fang *et al.* [91]	Proposed a FL protograph EXIT (PEXIT) algorithm and a two-step design methodology for protograph-coded ODMR systems.
2012	Yao *et al.* [78]	Designed a joint iterative detection-and-decoding schemes for TD-ISI channels, which not only can mitigate the TD interference but also can achieve satisfactory error performance with relatively low complexity.
2013	Kong *et al.* [55]	Proposed an EXIT-chart-based design scheme for matching LDPC codes to TDMR channels.
2013	Han *et al.* [60]	Introduced a non-binary LDPC-coded TDMR system in conjunction with an asymmetric iterative multi-track detection algorithm, which can significantly outperform the conventional multi-track detection algorithms.
2014	Han *et al.* [143]	Conceived a new channel model to characterize the written-in errors of TDMR systems and developed a novel synchronization algorithm and a detection algorithm tailored for such a channel model.
2014	Phakphisut et. al. [107]	Analyzed the convergence performance of non-binary protograph codes over OD-ISI channels by exploiting the infinite-length (IL) PEXIT algorithm.
2015	Kong *et al.* [83]	Constructed the QC protograph codes that realize both high performance and low complexity in TDMR systems.
2015	Han *et al.* [109]	Proposed a low-complexity joint detection-and-decoding algorithm for non-binary LDPC-coded TDMR systems, which possesses faster convergence speed than the existing counterparts.
2016	Y. Fang *et al.* [96]	Designed capacity-approaching RC protograph codes for TDMR systems by extending the FL PEXIT algorithm.
2016	Hareedy *et al.* [31]	Provided a comprehensive study on the error-floor performance of regular non-binary LDPC codes together with their optimization guidelines for ODMR systems.
2017	Mehrnoush *et al.* [37]	Proposed two EXIT-chart-based design techniques for irregular repeat-accumulate (IRA)-coded TDMR systems.
2017	Chen *et al.* [73]	Constructed non-binary protograph codes for TDMR systems, which achieve better error performance than the previously proposed binary and non-binary counterparts.
2017	Yao *et al.* [69]	Developed a modified DE algorithm to facilitate the threshold calculation of LDPC codes over TD-ISI channels.
2017	Esfahanizadeh *et al.* [99]	Offered an insightful investigation of FL SC codes in MR scenarios, and designed excellent SC codes that significantly outperform their block counterparts and the conventional SC codes.

coded bits according to the required order in $\mathbf{H}$. Unfortunately, the sub-matrix $\mathbf{P}^{\mathrm{T}}$ in $\mathbf{G}_{\mathrm{s}}$ is usually not sparse and thus leading to relatively high encoding complexity. As a remedy, some efficient encoding algorithms based on $\mathbf{H}$ have been developed in [8] and [158]. Here, we skip the details of such techniques since they are outside the scope of this paper.

Conventional LDPC codes are randomly generated and thus do not possess any constrained structure. In this sense, these LDPC codes may suffer from complicated encoding and decoding. To overcome this drawback, structured LDPC codes like QC-LDPC codes have been proposed. In particular, an $M \times N$ parity-check matrix of a regular QC-LDPC code can

be represented by

$$\mathbf{H} = \begin{pmatrix} \mathbf{H}_{1,1} & \mathbf{H}_{1,2} & \cdots & \mathbf{H}_{1,n_\mathrm{p}} \\ \mathbf{H}_{2,1} & \mathbf{H}_{2,2} & \cdots & \mathbf{H}_{2,n_\mathrm{p}} \\ \vdots & \vdots & \ddots & \vdots \\ \mathbf{H}_{m_\mathrm{p},1} & \mathbf{H}_{m_\mathrm{p},2} & \cdots & \mathbf{H}_{m_\mathrm{p},n_\mathrm{p}} \end{pmatrix},$$

where $\mathbf{H}_{i,j}$ is a $Q \times Q$ circulant permutation matrix,[8] $1 \leq i \leq m_\mathrm{p}$, $1 \leq j \leq n_\mathrm{p}$, $M = Qm_\mathrm{p}$, and $N = Qn_\mathrm{p}$. Irregular QC-LDPC codes can be constructed via setting some of the sub-matrices $\mathbf{H}_{i,j}$ to all-zero matrices. In general, a regular or irregular QC-LDPC code can be represented by an $m_\mathrm{p} \times n_\mathrm{p}$ "base matrix" $\mathbf{B} = (b_{i,j})$ where $b_{i,j} \in \{-1, 0, 1, \ldots, Q-1\}$ [165]. Specifically, $b_{i,j} = -1$ represents an all-zero matrix while $b_{i,j} = 0, 1, \ldots, Q-1$ denotes a circulant permutation matrix formed by cyclically right-shifting the identical matrix $b_{i,j}$ times. In recent years, a variety of efficient algorithms, such as the hill-climbing algorithm [158], the "pre-lifted" algorithm [166], and the circulant-based PEG algorithm [167], have also been conceived to design QC-LDPC codes. Well-designed QC-LDPC codes not only can realize linear encoding (i.e., encoding complexity growing linearly with the codeword length) with the aid of simple shift registers, but also can produce similar error performance as unstructured LDPC codes.

3) Decoding Algorithms: At the receiver terminal of an MR system, a BP decoder is serially concatenated with a BCJR detector to retrieve the original information. To facilitate the description of BP decoding algorithm, we first define several types of LLRs for turbo decoder and LDPC-based BP decoder, respectively, as below.

(i) Turbo decoder:

- $L_\mathrm{ch}(j)$ denotes the channel LLR of v_j;
- $L_\mathrm{A,IO}(j)$ denotes the input *a-priori* LLR of v_j flowing from the outer decoder to the inner detector;
- $L_\mathrm{A,OI}(j)$ denotes the input *a-priori* LLR of v_j flowing from the inner detector to the outer decoder;
- $L_\mathrm{E,IO}(j)$ denotes the output *extrinsic* LLR of v_j passing from the inner detector to the outer decoder;
- $L_\mathrm{E,OI}(j)$ denotes the output *extrinsic* LLR of v_j passing from the outer decoder to the inner detector;
- $L_\mathrm{app,I}(j)$ denotes the *a-posteriori* LLR of v_j output from the inner detector;
- $L_\mathrm{app,O}(j)$ denotes the *a-posteriori* LLR of v_j output from the outer decoder.

(ii) BP decoder:

- $L_\mathrm{Av}(i,j)$ denotes the input *a-priori* LLR flowing from c_i to v_j;
- $L_\mathrm{Ac}(i,j)$ denotes the input *a-priori* LLR flowing from v_j to c_i;
- $L_\mathrm{Ev}(i,j)$ denotes the output *extrinsic* LLR passing from v_j to c_i;
- $L_\mathrm{Ec}(i,j)$ denotes the output *extrinsic* LLR passing from c_i to v_j.

When performing turbo decoding, the output extrinsic LLR of the inner detector becomes the input a-priori LLR of the outer decoder during each iteration, and vice versa, i.e., $L_\mathrm{A,OI}(j) = L_\mathrm{E,IO}(j)$ and $L_\mathrm{A,IO}(j) = L_\mathrm{E,OI}(j)$. This property also holds for the BP decoder, i.e., $L_\mathrm{Ac}(i,j) = L_\mathrm{Ev}(i,j)$ and $L_\mathrm{Av}(i,j) = L_\mathrm{Ec}(i,j)$.

[8] A circulant permutation matrix is an identity matrix or its cyclic-shifted version.

Algorithm 1: Log-BP Decoding Algorithm

(1) **Initialization:** For $j = 1, 2, \ldots, N$, the channel LLR is calculated by $L_\mathrm{ch}(j) = \ln\big[\Pr(x_j = +1|y_j)/\Pr(x_j = -1|y_j)\big]$. Afterwards, the a-posteriori LLR $L_\mathrm{app,I}(j)$ is yielded by passing $L_\mathrm{ch}(j)$ and $L_\mathrm{A,IO}(j)$ into the inner detector (i.e., BCJR detector) [47]. In accordance with the principles of turbo decoding, one can immediately obtain the initial a-priori LLR of the BP decoder by $L_\mathrm{A,OI}(j) = L_\mathrm{E,IO}(j) = L_\mathrm{app,I}(j) - L_\mathrm{A,IO}(j)$.

(2) **Calculating the extrinsic LLR passing from v_j to c_i:** For $i = 1, 2, \ldots, M$, and $j = 1, 2, \ldots, N$, calculate the extrinsic LLR $L_\mathrm{Ev}(i,j)$ by exploiting $L_\mathrm{A,OI}(j)$ and $L_\mathrm{Av}(i,j)$, as

$$L_\mathrm{Ev}(i,j) = L_\mathrm{A,OI}(j) + \sum_{\mu \in \mathcal{C}(j)/i} L_\mathrm{Av}(\mu, j),$$

where $\mathcal{C}(j)$ is the index set of CNs connecting to v_j and $\mathcal{C}(j)/i = \{\mu \in \mathcal{C}(j) \,|\, \mu \neq i\}$.

(3) **Calculating the extrinsic LLR passing from c_i to v_j:** For $i = 1, 2, \ldots, M$, and $j = 1, 2, \ldots, N$, calculate the extrinsic LLR $L_\mathrm{Ec}(i,j)$ by exploiting $L_\mathrm{Ac}(i,j)$, as

$$L_\mathrm{Ec}(i,j) = 2\tanh^{-1}\left(\prod_{\mu \in \mathcal{V}(i)/j} \tanh(L_\mathrm{Ac}(i,\mu)/2)\right),$$

where $\mathcal{V}(i)$ is the index set of VNs connecting to c_i and $\mathcal{V}(i)/j = \{\mu \in \mathcal{V}(i) \,|\, \mu \neq j\}$.

(4) **Finalization:** For $v_j \in \mathcal{V}_\mathrm{i}$, compute the a-posteriori LLR by

$$L_\mathrm{app,O}(j) = L_\mathrm{A,OI}(j) + \sum_{\mu \in \mathcal{C}(j)} L_\mathrm{Av}(\mu, j), \tag{6}$$

where $\mathcal{V}_\mathrm{i}$ denotes the VN set corresponding to the information bits.

Repeat Steps (1) $\sim$ (1) until the original information bits are successfully decoded or the predefined maximum BP iteration number is reached. Subsequently, terminate the algorithm and measure the extrinsic LLR output from the BP decoder as $L_\mathrm{E,OI}(j) = L_\mathrm{app,O}(j) - L_\mathrm{A,OI}(j)$.

Consider an LDPC-coded MR system with turbo decoding. The channel model can be described as $y_j = f_\mathrm{MR}(v_j, v_{j-1}, \ldots, v_{j-\kappa})$, where $f_\mathrm{MR}(\cdot)$ is determined by the channel transfer function and $\kappa \in \mathbb{N}^+$ is the length of channel memory. At the beginning of each turbo iteration, all the a-priori/extrinsic LLRs of BP decoder should be set to zero. Then, the log-BP decoding algorithm is summarized as ***Algorithm 1***.

Remark:

- In a turbo decoder over MR channels, the extrinsic LLR output from the BP decoder (i.e., $L_\mathrm{E,OI}(j)$) will be fed back to the BCJR detector and will become its a-priori

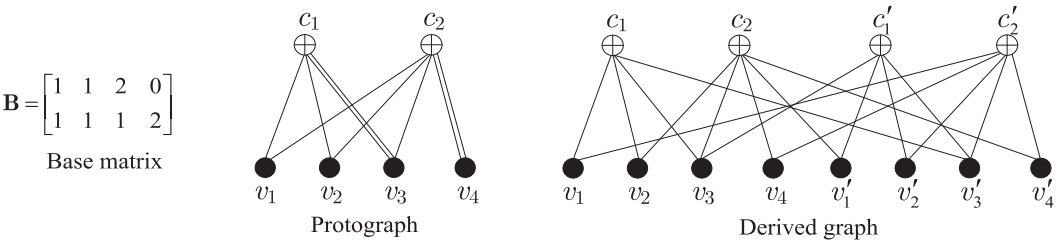

Fig. 4. Base matrix, protograph, and derived graph of a rate-1/2 protograph code. The parameters used are $m_{\mathrm{P}} = 2, n_{\mathrm{P}} = 4, z = 2, M = 4,$ and $N = 8$.

LLR (i.e., $L_{\mathrm{A,IO}}(j)$) during the next turbo iteration. This a-priori LLR will be used to update the extrinsic LLR $L_{\mathrm{E,IO}}(j)$.

- In memoryless channels, the channel detector is no longer required and thus the channel LLR can be directly considered as the initial LLR of the BP decoder.

B. Variants of LDPC Codes

1) Protograph Codes: As a meritorious variant of LDPC codes, protograph codes, which not only inherit the advantages of traditional LDPC codes but also require low encoding complexity, have already been extensively applied in MR systems [68], [73], [83], [91], [95], [96], [107]. Especially, each regular LDPC code has a protograph representation and thus can be constructed via its corresponding protograph [68].

A protograph is a Tanner graph with a relatively small number of nodes and edges. The protograph $\mathcal{G}_{\mathrm{P}} = (\mathcal{V}, \mathcal{C}, \mathcal{E})$ is composed by a set of n_{P} VNs $\mathcal{V}$, a set of m_{P} CNs $\mathcal{C}$, and a set of edges $\mathcal{E}$. Each edge $e_{i,j} \in \mathcal{E}$ connects a VN $v_j \in \mathcal{V}$ to a CN $c_i \in \mathcal{C}$. To simplify the exposition, we refer to a protograph with m_{P} CNs and n_{P} VNs as an $m_{\mathrm{P}} \times n_{\mathrm{P}}$ protograph, where $m_{\mathrm{P}} \times n_{\mathrm{P}}$ denotes the size of the protograph. Besides, a protograph can be specified by an $m_{\mathrm{P}} \times n_{\mathrm{P}}$ base matrix $\mathbf{B} = (b_{i,j})$, in which $b_{i,j}$ is the number of edges connecting v_j to c_i and $R = (n_{\mathrm{P}} - m_{\mathrm{P}})/n_{\mathrm{P}}$ is the code rate. An $M \times N$ expanded protograph that corresponds to the parity-check matrix $\mathbf{H}$ of a protograph code can be constructed by performing a "copy-and-permute" operation on a given protograph, where $M = zm_{\mathrm{P}}$, $N = zn_{\mathrm{P}}$, and z denotes the number of such operations. In particular, the "expanded protograph", "copy-and-permute" and "z" are also called "*derived graph*", "*lifting*" and "*lifting factor*", respectively. Unlike conventional Tanner graph, parallel edges are allowed in a protograph, but they must be thoroughly eliminated during the expansion procedure. As is well known, the expansion from a protograph to a derived graph can be implemented by a modified progressive-edge-growth (PEG) algorithm [87]. As a simple example, Fig. 4 illustrates the base matrix, protograph, and derived graph of a rate-1/2 protograph code, where $m_{\mathrm{P}} = 2, n_{\mathrm{P}} = 4, z = 2, M = 4,$ and $N = 8$.

2) Repeat-Accumulate Codes: RA codes, which have been extensively studied during the past two decades [168], stand out as another valuable variant of LDPC codes. This type of codes has very simple encoding procedure and graph representation, which not only allow linear encoding and fast decoding implementation, but also lead to good error performance.

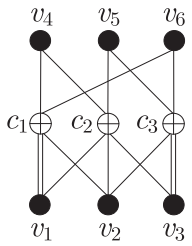

Fig. 5. Protograph of a rate-1/2 regular RA code with $q = 3$.

Typically, an RA code can be generated by performing a "repeat-permute-accumulate" operation on a given sequence of information bits. Supposing that the length of an information sequence $\mathbf{s}$ is K, it should be first repeated q ($q > 1$) times and permuted by an interleaver of size qK. After that, the permuted information sequence is passed through an accumulator to obtain the parity bits. Finally, the information bits and their corresponding parity bits constitute a regular RA code. Moreover, an IRA code can be constructed if the repetition factor q is not constant for different information bits [169]. The code rate of an RA code is specified by both the repetition factor and accumulation rule. As shown in [168], both regular and irregular codes can be represented by simple protographs. For example, the protograph of a rate-1/2 regular RA code with $q = 3$ is shown in Fig. 5, where v_1, v_2, v_3 are the information-bit-related VNs, v_4, v_5, v_6 are the parity-bit-related VNs, and c_1, c_2, c_3 are the CNs.

3) Spatially-Coupled Codes: SC codes belong to a type of LDPC-convolutional-like codes, and they are able to achieve capacity-approaching decoding threshold and linear-minimum-distance property [97], [98], [101].[9] Recently, the performance of SC codes has been carefully studied over ODMR channels [99], [100]. It has been demonstrated that this type of codes can exhibit excellent error performance in MR scenarios after appropriate design.

Broadly speaking, SC codes can be constructed by coupling a series of L_c disjoint LDPC codes together into a single coupled chain, where L_c is defined as the coupling length. SC codes can be viewed as a special type of LDPC convolutional codes because the "spatial coupling" operation is equivalent

[9]Distinguished from LDPC-block codes, the *minimum free distance* is utilized to evaluate the asymptotic error performance of SC codes in the high-SNR region [101]. In this paper, we refer to both the minimum free distance and minimum Hamming distance as minimum distance. Thanks to the convolutional property, the SC code always possesses a larger minimum distance than that of its original LDPC code [170].

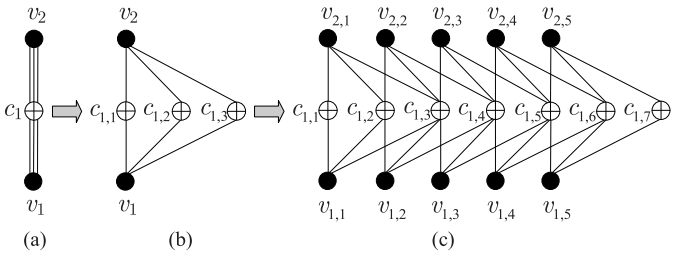

Fig. 6. Structures of a rate-1/2 (3, 6)-protograph code (a), edge-spreading rule (b), and its corresponding terminated SC code (c). The parameters used are $d_v = 3, d_c = 6,\ \omega_c = 2$ and $L_c = 5$.

to introducing memory into LDPC codes. In fact, LDPC convolutional codes are yielded if the coupling length approaches infinity ($L_c \to +\infty$) while SC codes are formulated if the coupling length is a finite positive integer. Interestingly, the decoding threshold of an LDPC code may be improved by exploiting the coupling operation. Also, an SC code can be produced by performing the "coupling" operation on a given protograph [101]. As compared with non-protograph-based SC codes, protograph-based SC codes enable the benefits of simpler representation and being easier to analyze, which make them a more preferable choice for both theoretical research and practical applications.

In the past several years, a variety of techniques have been conceived to realize the "spatial coupling" operation, among which "edge spreading" is a convenient and efficient solution [98], [101]. Consider a $(d_v, d_c = n_{\rm P} d_v)$-regular protograph with $n_{\rm P}$ VNs and single CN (i.e., $m_{\rm P} = 1$), that is, each VN v_j $(j = 1, 2, \ldots, n_{\rm p})$ possesses d_v edges connecting to the CN c_1. Suppose that this protograph is copied L_c times and its replicas are successively placed at the positions $1, 2, \ldots,$ and L_c. Then, one can connect the d_v edges emanating from v_j at position μ $(\mu = 1, 2, \ldots, L_c)$ arbitrarily to the ω_c replicas of c_1 at positions $\mu, \mu+1, \ldots, \mu+\omega_c$, where $0 < \omega_c < L_c$ is the coupling width. By repeatedly performing such a coupling operation on all the $n_{\rm p}$ VNs, the protograph of its corresponding SC code can be generated. This type of SC codes is referred to as *terminated SC codes*. Based on the aforementioned construction method, the code rate of a terminated SC code is $R_{\rm sc} = 1 - ((L_c + \omega_c)m_{\rm P})/(L_c n_{\rm P}) = R - (\omega_c m_{\rm P})/(L_c n_{\rm P}) < R$, where R is the code rate of its original protograph code. As a consequence, the terminated SC code possesses a relatively lower code rate with respect to its original protograph code. For instance, the structures of a rate-1/2 (3, 6)-protograph code, "edge-spreading rule", and its corresponding terminated SC code are shown in Fig. 6, where the coupling width and coupling length are $\omega_c = 2$ and $L_c = 5$, respectively. In this figure, $v_{j,\mu}$ $(\mu = 1, 2, \ldots, L_c)$ and $c_{i,\mu}$ represent the j-th type VN and the i-th type CN at position μ, respectively. As can be easily observed, the (3, 6)-regular SC code suffers from a decrease in code rate, i.e., $R_{\rm SC} = 3/10 < 1/2$. It is because two additional CNs are generated on the rightmost side of the protograph via edge spreading.

From the matrix perspective, the edge spreading for a protograph with coupling width ω_c results in the division of its corresponding base matrix into $\omega_c + 1$ sub-base-matrices, i.e., $\mathbf{B} = \mathbf{B}_{\rm S,1} + \mathbf{B}_{\rm S,2} +, \ldots, \mathbf{B}_{\rm S,\omega_c+1}$, where $\mathbf{B}_{{\rm S},\mu}$ is the μ-th sub-base-matrix of $\mathbf{B}$. It should be noted that all the sub-base-matrices must have the same size as the overall base matrix. According to [170], the division rule of the base matrix can be succinctly represented by a so-called "*cutting vector*" $\Xi = (\varepsilon_1, \varepsilon_2, \ldots, \varepsilon_{m_{\rm P}})$, where $0 \le \varepsilon_\mu \le \varepsilon_{\mu+1} \le n_{\rm P}$ and $\mu = 1, 2, \ldots, m_{\rm P} - 1$. Similarly, one can also apply the edge spreading to the Tanner graph (i.e., the derived graph) of a traditional LDPC codes in order to construct a terminated SC code.[10] The details of the related methodologies can be found in [97], [99], and [171].

In general, terminated SC codes can achieve lower decoding threshold than their LDPC/protograph counterparts at the expense of degrading the code rate. As a remedy, a new type of SC codes, called *tail-biting SC code*, has been proposed. Tail-biting SC codes can outperform their corresponding LDPC codes without decreasing the code rate [98], [101]. The main idea of constructing a tail-biting SC code is to combine the μ-th $(\mu = 1, 2, \ldots, m_{\rm p})$ type CNs at positions $L_c+1, L_c+2, \ldots, L_c+\omega_c$ with the same type CNs at positions $1, 2, \ldots, \omega_c$, respectively, in the protograph of a terminated SC code.[11] Referring to Fig. 6, the tail-biting SC code corresponding to the (3, 6)-regular terminated SC code can be obtained by combining $c_{1,6}, c_{1,7}$ with $c_{1,1}, c_{1,2}$, respectively. As a result, the (3, 6)-regular tail-biting SC code not only has the same code rate and decoding threshold as those in the original protograph code, but also has a larger minimum distance than that of the original protograph code [101], [170].

Remark:

- In the above-mentioned discussions, we have paid most attention to the construction aspect of protograph codes and SC codes because all these codes can be decoded using BP decoding algorithm.
- Although we only give the examples of an LDPC code, a protograph code, as well as an SC code with a code rate $R = 1/2$, LDPC-based codes with higher code rates (e.g., $R \ge 4/5$) can be constructed in similar ways so as to satisfy the requirement of MR applications.

4) Non-Binary LDPC-Based Codes: As a generalization of LDPC codes to the non-binary domain, non-binary LDPC codes over Galois fields GF(q) have shown better error performance over their binary counterparts in certain cases [103]–[106]. In particular, non-binary LDPC codes as well as their variants find their natural applications in MR systems thanks to their strong robustness against burst-error impairment and powerful error-correction capability in short/moderate-codeword-length cases [31], [32], [48], [58], [60], [73]. In contrast to the binary case, the elements of the parity-check matrix $\mathbf{H} = (h_{i,j})$ for a non-binary LDPC code over GF(q) are no longer equal to zero or one, but are

[10]For a terminated SC code generated from a (d_v, d_c)-regular LDPC code, the cutting vector for the original parity-check matrix $\mathbf{H}$ should be defined as $\Xi = (\varepsilon_1, \varepsilon_2, \ldots, \varepsilon_{d_v})$, where $0 \le \varepsilon_\mu \le \varepsilon_{\mu+1} \le d_c$ and $\mu = 1, 2, \ldots, d_v - 1$.

[11]Note also that the number of CN types at each position for a protograph-based SC code should be equal to the number of CNs in the original protograph. On the other hand, the number of CN types at each position for a non-protograph-based SC code should be equal to the number of CN degrees in the original Tanner graph.

selected from the set $\mathcal{D}_q = \{0, 1, \ldots, q-1\}$, i.e., $h_{i,j} \in \mathcal{D}_q$. The Tanner graph of a non-binary LDPC-based code is identical to that of a binary LDPC code except the edge weight, where the VNs and CNs correspond to the coded symbols and their check-sum constraints, respectively. More specifically, the value of the element in the j-th column and i-th row is treated as the weight of the edge connecting the j-th VN to the i-th CN. The performance of a non-binary LDPC-based code is determined by both the structure of Tanner graph and the distribution of edge weight. In fact, all LDPC codes, protograph codes, and SC codes can be easily extended to non-binary scenario [104]–[106]. Since the encoding methods of non-binary LDPC-based codes are quite similar to those of their binary counterparts (with slight difference), we do not provide elaborations on such issues but refer interested readers to the above literature.

In the decoding aspect, fast-Fourier-transform-based q-ary sum-product (FFT-QSP) algorithm is one of the most classical techniques to achieve good performance with acceptable computational complexity [158]. In recent years, some other improved versions of the FFT-QSP algorithm have also been proposed in order to either boost the performance or reduce the complexity. However, with respect to their binary cases, the complicated non-binary decoder remains one challenging problem to be resolved before non-binary LDPC-based codes can be widely adopted in practical applications.

IV. Theoretical-Analysis Methodologies

In the past two decades, a variety of prestigious theoretical methodologies have been developed to facilitate the design and analysis of LDPC codes. Among all existing techniques, DE [5], [6], EXIT function [9], [10], and AWD [172], [173] have attracted growing interests in the coding theory community because of their high efficiency and accuracy. In particular, DE and EXIT algorithms are very useful in calculating the iterative decoding threshold and predicting the asymptotic error performance in the low SNR region. The AWD is extremely powerful in estimating the minimum (Hamming) distance and predicting the asymptotic error performance in the high-SNR region. In the previous literature, it has been shown that LDPC codes having capacity-approaching decoding thresholds are normally subject to undesirable minimum distances [68], [101]. This simply means that it is extremely difficult for an LDPC code to achieve excellent error performance in both low and high-SNR regions.

To the best of our knowledge, the DE and EXIT algorithms are related to both the types of code and channel, while the AWD is only related to the type of code. Earlier works have only investigated the DE and EXIT algorithms over memoryless channels, such as AWGN channels [5], [6], [9], [10]. With an increasing demand for designing LDPC codes over MR channels, greater research effort has been dedicated to formulating new DE [69], [70] and EXIT algorithms [55], [71], [107] under the conditions of OD-ISI and TD-ISI. These theoretical advancements have dramatically eased the code construction and decoding design for LDPC-based codes in MR channels.

In the following, we will review the principles of the above three techniques for binary LDPC codes over OD-ISI channels. Note that these techniques are also applicable to LDPC-code variants and TD-ISI scenarios after minor modifications.

A. Density Evolution

As a typical asymptotic analysis tool for LDPC codes, DE has been first proposed over AWGN channels [5], [6] and then extended to MR channels [70]. The basic idea of this technique is to trace the evolution of the LLR distribution in the iterative decoder so as to determine the decoding threshold of an LDPC code. Based on the joint coding-and-channel factor graph of a serial concatenated coding scheme over MR channels, one can define five types of probability density functions (PDFs) as below.

- $f_n(\xi)$ denotes the PDF of Gaussian noise;
- $f_{\mathrm{cv}}(\xi)$ denotes the average PDF of the LLR passing from a CN to a VN;
- $f_{\mathrm{vc}}(\xi)$ denotes the average PDF of the LLR passing from a VN to a CN;
- $f_{\mathrm{I,v}}(\xi)$ denotes the average PDF of the LLR passing from the BCJR detector to a VN;
- $f_{\mathrm{v,I}}(\xi)$ denotes the average PDF of the LLR passing from a VN to the BCJR detector.

Here, the LLR message passing from the BCJR detector to a VN is viewed as the initial LLR for the BP decoder. Given a degree-distribution pair $(\lambda(x), \rho(x))$, DE can be used to evaluate the decoding threshold $(E_b/N_0)_{\mathrm{th}}$, i.e., the minimum SNR for which the LDPC code can be decoded with an arbitrarily small error probability as the codeword length approaches infinity.[12] The block diagram of the DE algorithm over an MR channel is shown in Fig. 7. As seen, there exist two sub-decoders, i.e., BCJR detector and BP decoder, in an LDPC-coded MR system. In the DE algorithm, one should update $f_{\mathrm{I,v}}(\xi)$ and $f_{\mathrm{v,I}}(\xi)$ once during each turbo iteration, and subsequently update $f_{\mathrm{vc}}(\xi)$ and $f_{\mathrm{cv}}(\xi)$ T_{BP} $(T_{\mathrm{BP}} \geq 1)$ times, where T_{BP} is the maximum number of BP iterations in each turbo iteration. Assuming that t_{TU} is the number of turbo iterations performed, and t_{BP} is the number of BP iterations performed in the current turbo iteration, then the total number of DE iterations performed equals $t = t_{\mathrm{TU}} T_{\mathrm{BP}} + t_{\mathrm{BP}}$. The DE algorithm is summarized as ***Algorithm 2***, in which the total number of DE iterations is shown as the superscript.

Remark:

- Monte-Carlo simulation should be performed to estimate the PDF $f^t_{\mathrm{I,v}}(\xi)$ since there is no closed-form expression for it. To ensure the accuracy and ergodicity of the DE algorithm, the codeword length should be set to a sufficiently large positive integer.

[12] Alternatively, the decoding threshold can be defined as the maximum noise standard deviation for which the LDPC codes can be decoded with an arbitrarily small error probability. It is denoted by $\sigma_{n,\mathrm{th}} = \sqrt{E_s/(2R(E_b/N_0)_{\mathrm{th}})}$, where the average energy per transmitted symbol E_s is always set to be 1. In order to distinguish $\sigma_{n,\mathrm{th}}$ from $(E_b/N_0)_{\mathrm{th}}$, the former metric is called *noise decoding threshold* while the latter metric is called *SNR decoding threshold*. For the sake of conciseness, we directly adopt $(E_b/N_0)_{\mathrm{th}}$ as the decoding threshold in this treatise.

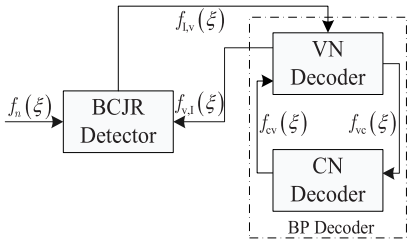

Fig. 7. Block diagram of the DE algorithm over an MR channel.

Algorithm 2: Density Evolution

(1) **Initialization:** Initialize $t = t_{\mathrm{BP}} = 1, f^0_{\mathrm{I,v}}(\xi) = f^0_{\mathrm{cv}}(\xi) = \delta(\xi)$, and $f_n(\xi) = (1/\sqrt{2\pi\sigma_n^2})e^{-(\xi/(2\sigma_n^2))}$, where $\delta(\cdot)$ is the Dirac function.

(2) **Evolving VN-to-CN density:** Calculate the PDF $f^t_{\mathrm{vc}}(\xi)$ by

$$f^t_{\mathrm{vc}}(\xi) = f^{t-1}_{\mathrm{I,v}}(\xi) \otimes \left[\sum_{d_{v_j}=1}^{d_{\mathrm{v,max}}} \lambda_{d_{v_j}} \left(\bigotimes_{\mu=1}^{d_{v_j}-1} f^{t-1}_{\mathrm{cv}}(\xi) \right) \right],$$

where $\otimes$ is the convolution operation, $\bigotimes_{\mu=1}^{d_{v_j}-1}$ is the convolution of $d_{v_j}-1$ PDFs, $d_{\mathrm{v,max}}$ is the maximum VN degree.

(3) **Evolving CN-to-VN density:** Calculate the PDF $f^t_{\mathrm{cv}}(\xi)$ by

$$f^t_{\mathrm{cv}}(\xi) = \sum_{d_{c_i}=1}^{d_{\mathrm{c,max}}} \rho_{d_{c_i}} \Psi_c^{d_{c_i}-1}(f^t_{\mathrm{vc}}(\xi)),$$

where $\Psi_c^{d_{c_i}-1}(\cdot)$ represents the density-evolving processor of a degree-d_{c_i} CN, which is utilized to evolve the density $f^t_{\mathrm{vc}}(\xi)$ through the corresponding CN.

(4) **Evolving VN-to-BCJR-detector and BCJR-detector-to VN densities:** If $t = \mu T_{\mathrm{BP}}$ $(\mu = 1, 2, \ldots)$, calculate the PDF $f^t_{\mathrm{v,I}}(\xi)$ by

$$f^t_{\mathrm{v,I}}(\xi) = \sum_{d_{v_j}=1}^{d_{\mathrm{v,max}}} \frac{\lambda_{d_{v_j}}}{\left(d_{v_j} \int_0^1 \lambda(x)\,\mathrm{d}x\right)} \left(\bigotimes_{\mu=1}^{d_{v_j}} f^t_{\mathrm{cv}}(\xi) \right).$$

Afterwards, measure the PDF $f^t_{\mathrm{I,v}}(\xi)$ using $f^t_{\mathrm{I,v}}(\xi) = \Psi_{\mathrm{I}}(f^t_{\mathrm{v,I}}(\xi), f_n(\xi))$, where $\Psi_{\mathrm{I}}(\cdot)$ represents the density-evolving processor of the channel trellis, which is utilized to evolve the density $f^t_{\mathrm{I,v}}(\xi)$ through the joint coding-and-channel factor graph in [70].

(5) **Finalization:** Compute the average error probability by $\bar{P}^t_{\mathrm{e}} = \int_{-\infty}^{0} f^{t+1}_{\mathrm{vc}}(\xi)\,\mathrm{d}x$, where $f^{t+1}_{\mathrm{vc}}(\xi)$ is the updated VN-to-CN PDF based on the results in Steps (2) and (5).

Repeat Steps (2) $\sim$ (5) until $\bar{P}^t_{\mathrm{e}} \to 0$ or t reaches the maximum number of iterations, i.e., $t = T_{\mathrm{BP}}T_{\mathrm{TU}}$, where T_{TU} is the maximum number of turbo iterations.

- It can be easily observed that the log-BP decoding algorithm and DE algorithm obey similar updating rules. However, the LLR is assumed as the updating metric in the former case while the PDF is assumed as the updating metric in the latter case.

B. EXIT Algorithms

In earlier years of the development of LDPC-coded MR systems, most research related to coding analysis and design only relies on DE. Following the milestone work of [9], MI-based EXIT chart has been invoked to characterize the flow of extrinsic information through two SISO decoders [10], [11]. As a complementary methodology of DE, the exchange characteristics of extrinsic information between two component decoders can be visualized by a decoding tunnel of an EXIT chart. More importantly, the EXIT algorithm can not only calculate the decoding threshold and optimize the code construction with comparable accuracy as DE, but also possess extra advantages such as lower computational complexity and being easier to visualize and program. Thanks to its simplicity and accuracy, the EXIT chart has gained considerable attention and has been extensively used in the design of LDPC-coded MR systems [37], [55], [71], [93].

With the aid of EXIT algorithms, it is very convenient to trace the convergence behavior of LDPC-coded MR systems and design capacity-approaching codes. Broadly speaking, there are two types of EXIT algorithms, namely IL EXIT algorithm [37], [55], [71] and FL EXIT algorithm [41], [91], [95], [96]. The IL algorithm belongs to the category of asymptotically analytical tools, while the FL EXIT algorithm belongs to the category of Monte-Carlo analytical tools. Here, we first concisely portray the main idea of the IL EXIT algorithm and then spend more attention on the FL EXIT algorithm because the updating rule of the former is very similar to that of DE algorithm.

In order to elaborate the two types of EXIT algorithms, we should define two classes of MIs for turbo decoder and BP decoder, respectively, based on the LLRs defined in Section III-A3.

(i) Turbo decoder:

- $I_{\mathrm{A,IO}}$ denotes the *a-priori* MI between the coded bits $\{v_j\}$ and the input *a-priori* LLRs $\{L_{\mathrm{A,IO}}\}$;
- $I_{\mathrm{A,OI}}$ denotes the *a-priori* MI between the coded bits $\{v_j\}$ and the input *a-priori* LLRs $\{L_{\mathrm{A,OI}}\}$;
- $I_{\mathrm{E,IO}}$ denotes the *extrinsic* MI between the coded bits $\{v_j\}$ and the output *extrinsic* LLRs $\{L_{\mathrm{E,IO}}\}$;
- $I_{\mathrm{E,OI}}$ denotes the *extrinsic* MI between the coded bits $\{v_j\}$ and the output *extrinsic* LLRs $\{L_{\mathrm{E,OI}}\}$.

(ii) BP decoder:

- I_{Av} denotes the *a-priori* MI between the coded bits $\{v_j\}$ and the input *a-priori* LLRs $\{L_{\mathrm{Av}}(i,j)\}$;
- I_{Ac} denotes the *a-priori* MI between the coded bits $\{v_j\}$ and the input *a-priori* LLRs $\{L_{\mathrm{Ac}}(i,j)\}$;
- I_{Ev} denotes the *extrinsic* MI between the coded bits $\{v_j\}$ and the output *extrinsic* LLRs $\{L_{\mathrm{Ev}}(i,j)\}$;
- I_{Ec} denotes the *extrinsic* MI between the coded bits $\{v_j\}$ and the output *extrinsic* LLRs $\{L_{\mathrm{Ec}}(i,j)\}$.

Similar to the turbo decoding and BP decoding algorithms, we also have $I_{\mathrm{A,OI}} = I_{\mathrm{E,IO}}$ and $I_{\mathrm{A,IO}} = I_{\mathrm{E,OI}}$ in each global

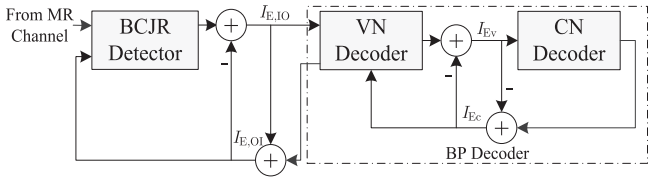

Fig. 8. Block diagram of the IL EXIT algorithm over an MR channel.

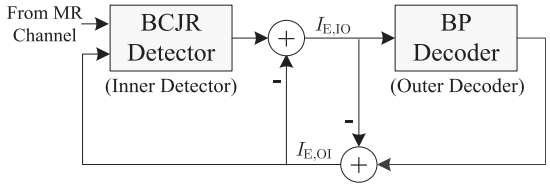

Fig. 9. Block diagram of the FL EXIT algorithm over an MR channel.

iteration (i.e., turbo iteration) and $I_{Ac} = I_{Ev}$ and $I_{Av} = I_{Ec}$ in each local iteration (i.e., BP iteration).

1) IL EXIT Algorithm: As an asymptotically theoretical analysis method, the IL EXIT algorithm provides an efficient way to predict the performance and guide the design of LDPC-like codes.[13] The block diagram of the IL EXIT algorithm over an MR channel is shown in Fig. 8. The IL EXIT chart, which can visualize the asymptotic decoding trajectory of an iterative decoder, is composed of two component EXIT curves. In the IL EXIT chart, one curve is used to depict the relationship between I_{Ev} and I_{Av}, while the other curve is used to depict the relationship between I_{Ec} and I_{Ac}. These two relationships can be mathematically expressed by $I_{Ev} = I_{VND}(I_{Av}, I_{E,IO})$ and $I_{Ec} = I_{CND}(I_{Ac})$, where the functions $I_{VND}(\cdot)$ and $I_{CND}(\cdot)$ are defined in [55, eq. (11)] and [55, eq. (7)], respectively. The BP decoder is said to converge successfully if the two component EXIT curves do not touch or cross each other except at the value of unity. In this algorithm, the initialized parameter $I_{E,IO}$ is output from the BCJR detector, which is related to the type of channel. When executing the EXIT algorithm, one should first estimate the value of this parameter through Monte-Carlo simulations for a given E_b/N_0 and a given $I_{E,OI}$. Here, we omit the derivation of the EXIT algorithm, the details of which are available in [55], [71], and [93].

2) FL EXIT Algorithm: One important assumption for both DE and EXIT algorithms is that the codeword length approaches infinity. For the scenario of short or moderate codeword length, these analytical tools can no longer work so well because the typicality and ergodicity properties do not hold. To overcome this shortcoming of DE and EXIT algorithms and to make a more accurate prediction, some FL analytical tools have been proposed. Of particular interest are the FL EXIT analyses, which not only inherit the desirable superiorities of IL EXIT chart but also are very effective for FL LDPC codewords [41], [91], [95], [96]. Although the previous FL EXIT algorithms have been proposed for designing and analyzing convolutional codes and protograph codes, they are readily applicable to LDPC codes and their variants after minor modifications. After the modifications, such FL EXIT algorithms can be utilized to design and analyze the related codes in transmission environments with ISI.

Unlike IL EXIT charts, the FL EXIT chart consists of two EXIT bands rather than two EXIT curves. Each EXIT band includes an expected EXIT curve, an upper-bound curve and a lower-bound curve. Particularly, the upper-bound curve and the lower-bound curve are used to ensure that all individual EXIT curves of the FL codewords lie within the band with a high probability (e.g., 99%), while the expected EXIT curve is used to represent the central line of the EXIT band. Typically, all the individual EXIT curves included in the EXIT band should be uniformly distributed on the two sides of the central line. As illustrated in [41] and [91], the FL EXIT algorithm stands out as a convenient analytical technique to anticipate the convergence performance of turbo-like receivers that involve two SISO decoders. In such scenarios, one can say that the iterative decoder will converge successfully with a high probability if the EXIT band corresponding to the inner detector and the EXIT band corresponding to the outer decoder do not touch each other until $(I_{A,IO}, I_{E,\,OI}) = (1, 1)$. Furthermore, the region between the two expected EXIT curves is referred to as the *decoding tunnel*. For a given E_b/N_0 and a given codeword length, the code having a larger decoding tunnel should enable relatively better convergence and error performance.

The block diagram of the FL EXIT algorithm over an MR channel is shown in Fig. 9. As observed, the two major performance metrics in FL EXIT algorithms are $I_{E,IO}$ and $I_{E,OI}$. It is worth noting that the derivation procedures of these two metrics in an FL EXIT algorithm are different from those in its IL counterpart. In the former scenario, the BP decoder is treated as an entire decoder and works together with the BCJR detector in a FL manner. Thus, one should exploit Monte-Carlo simulation to evaluate the extrinsic MIs $I_{E,IO}$ and $I_{E,OI}$ because no closed-form formula is available. On the other hand, in the IL EXIT algorithm, the BP decoder is partitioned into two sub-decoders (i.e., VN decoder and CN decoder), in which MIs are exchanged based on the IL codeword assumption. Thus, the extrinsic MI passing from BP decoder to BCJR detector can be calculated by a closed-form expression [10], [93].

Since both BCJR detector and BP decoder can only measure the LLR rather than the MI, one should first formulate the relationship between the a-priori/extrinsic MI and its corresponding a-priori/extrinsic LLR before implementing the FL algorithm. The extrinsic MI output from inner detector/outer decoder can be measured, based on the actual PDF of its corresponding LLRs, using

$$I_{E,\theta} = \frac{1}{2} \sum_{\mu \in \{+1,-1\}} \int_{-\infty}^{\infty} f_{E,\theta}(\xi | X = \mu) \times \log_2 \frac{2 f_{E,\theta}(\xi | X = \mu)}{f_{E,\theta}(\xi | X = +1) + f_{E,\theta}(\xi | X = -1)} \, d\xi \quad (7)$$

where $f_{E,\theta}(\xi | X = \mu)$ is the conditional PDF of the output extrinsic LLRs $\{L_{E,\theta}(j)\}$ given $X = (-1)^{v_j} = \mu \in \{+1, -1\}$, and $\theta \in \{\text{IO, OI}\}$. Furthermore, given the a-priori MI $I_{A,\theta}$ of each component decoder, the standard derivation of the

[13] We may use "EXIT chart/algorithm" instead of "IL EXIT chart/algorithm" in the remainder of this paper for brevity.

Algorithm 3 : FL EXIT Algorithm for Calculating the Extrinsic MI Output From the Inner Detector

(1) For a fixed E_b/N_0, randomly generate a sequence of information bits $\{s_j\}$ and a channel realization. These information bits are encoded by an LDPC code $\{v_j\}$ and then modulated into bipolar symbols $\{x_j = (-1)^{v_j}\}$. Based on the MR-channel output, the channel initial LLRs $\{L_{\rm ch}(j)\}$ can be promptly calculated.

(2) For a given a-priori MI $I_{\rm A,IO} \in [0, 1]$, the standard deviation $\sigma_{\rm A,IO}$ of the a-priori LLRs $\{L_{\rm A,IO}(j)\}$ can be evaluated using [91, eq. (4)]. With the employment of $\sigma_{\rm A,IO}$, one can further generate a Gaussian-distributed LLR sequence $\{L_{\rm A,IO}(j)\}$ utilizing (8).

(3) The sequences $\{L_{\rm ch}(j)\}$ and $\{L_{\rm A,IO}(j)\}$ are passed through the inner detector in order to yield the extrinsic LLR sequence $\{L_{\rm E,IO}(j)\}$. The relationship among these three parameters can be written as $L_{\rm E,IO}(j) = \mathcal{F}_{\rm inner}(L_{\rm ch}(j), L_{\rm A,IO}(j))$, where $\mathcal{F}_{\rm inner}(\cdot)$ is used to describe the behavior of the LLR-message processor of inner detector.

(4) Based on $\{L_{\rm E,IO}(j)\}$, the conditional PDF $f_{\rm E,IO}(\xi|X = \mu)$ can be estimated using Monte-Carlo histogram, where $\mu \in \{+1, -1\}$. Subsequently, the extrinsic MI can be measured utilizing (7).

(5) Repeat Steps (1) $\sim$ (4) without changing $I_{\rm A,IO}$ to obtain a sufficient set of $I_{\rm E,IO}$ values. Then, the mean and variance of $I_{\rm E,IO}$, i.e., $\mathbb{E}[I_{\rm E,IO}]$ and $\mathrm{var}[I_{\rm E,IO}]$, can be calculated, respectively.

(6) Execute Steps (1) $\sim$ (5) for different values of $I_{\rm A,IO} \in [0, 1]$ to obtain the EXIT band of the inner detector. In particular, the EXIT band includes three EXIT curves, i.e., the expected EXIT curve $(I_{\rm A,IO}, \mathbb{E}[I_{\rm E,IO}])$, the upper-bound curve $(I_{\rm A,IO}, \mathbb{E}[I_{\rm E,IO}] + 3\sqrt{\mathrm{var}[I_{\rm E,IO}]})$ and the lower-bound curve $(I_{\rm A,IO}, \mathbb{E}[I_{\rm E,IO}] - 3\sqrt{\mathrm{var}[I_{\rm E,IO}]})$.

input a-priori LLRs can be evaluated as $\theta_{\rm A,\theta} = J^{-1}(I_{\rm A,\theta})$, where the $J(\cdot)$ function and its inverse function are available in [10]. Utilizing $\theta_{\rm A,\theta}$, the a-priori LLR of a VN v_j for the inner detector/outer decoder can be computed by

$$L_{\rm A,\theta}(j) = \left(\sigma^2_{\rm A,\theta}/2\right)x_j + n_{{\rm L},j}, \tag{8}$$

where $n_{{\rm L},j} \sim \mathcal{N}(0, \sigma^2_{\rm A,\theta})$ is a Gaussian-distributed random variable. Based on the above knowledge, the FL EXIT algorithm for calculating the extrinsic MI output from the inner detector is presented as ***Algorithm 3***.

Likewise, one can calculate the extrinsic MI output from the outer decoder in a similar way as above. The relationship between a-priori LLR $I_{\rm A,\,OI}(j)$ and its corresponding extrinsic LLR $I_{\rm E,\,OI}(j)$ can be written as $L_{\rm E,OI}(j) = \mathcal{F}_{\rm outer}(L_{\rm A,\,OI}(j))$ where $\mathcal{F}_{\rm outer}(\cdot)$ is used to describe the behavior of the LLR-message processor of the outer decoder. In the EXIT band of the outer decoder, the expected EXIT curve, the upper-bound curve and the lower-bound curve of the EXIT band are denoted by $(I_{\rm A,\,OI}, \mathbb{E}[I_{\rm E,\,OI}])$, $(I_{\rm A,\,OI}, \mathbb{E}[I_{\rm E,\,OI}] + 3\sqrt{\mathrm{var}[I_{\rm E,\,OI}]})$ and $(I_{\rm A,\,OI}, \mathbb{E}[I_{\rm E,\,OI}] - 3\sqrt{\mathrm{var}[I_{\rm E,\,OI}]})$, respectively.

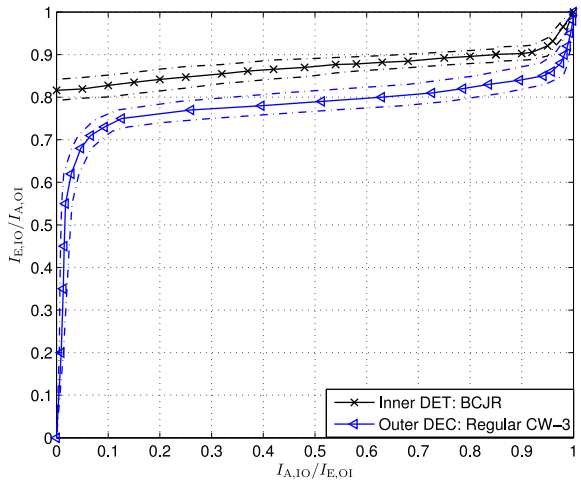

Fig. 10. FL EXIT chart of the regular CW-3 LDPC code over a dicode channel. The expected EXIT curves are denoted by the solid lines, the upper-bound curves and lower-bound curves are denoted by the dashed lines. The parameters used are $R = 4/5$, $K = 4096$, $T_{\rm BP} = 15$, and $E_b/N_0 = 4.0$ dB.

Remark: The EXIT band of the inner detector is determined by the channel realization while the EXIT band of the outer decoder is determined by the type of code.

Example 2: Based on a rate-4/5 regular column-weight-3 (CW-3) LDPC code [53], we plot the FL EXIT chart over a dicode channel in Fig. 10, where $K = 4096$, $T_{\rm BP} = 15$ and $E_b/N_0 = 4.0$ dB. Referring to this figure, the regular CW-3 LDPC code possesses an open decoding tunnel (i.e., there is no intersection between the two EXIT bands of BCJR detector and BP decoder for $I_{\rm A,IO}/I_{\rm E,OI} \in (0, 1)$), indicating that the turbo decoder can successfully converge at $E_b/N_0 = 4.0$ dB. It is expected that a larger decoding tunnel will be obtained as E_b/N_0 increases.

C. AWD Analysis

DE and EXIT algorithms are particularly useful in designing LDPC-based codes with capacity-approaching decoding thresholds. However, the decoding threshold is good for analyzing the error performance in the low-SNR region, but is no longer valid in the high-SNR region. The LDPC codes optimized by DE/EXIT-based algorithms possess desirable performance in the low-SNR region but are likely subject to an error floor, i.e., an abrupt decrease in the slope of the bit-error-rate (BER) curve, in the high-SNR region [5], [6], [9], [10], [173]. Instead of the decoding threshold, the minimum distance along with its distribution should be used to indicate the error performance of LDPC codes in the high-SNR region [172]–[175]. Furthermore, the decoding threshold under the maximum likelihood (ML) decoding algorithm can be derived exploiting the distance distribution, which provides excellent estimates on the gap between the sub-optimal BP decoding and the optimal ML decoding. As a result, the asymptotic distance distribution (or weight distribution) of LDPC-based code ensembles has attracted increasing attention and has been intensely investigated [84], [101], [172]. It has been proved in the above related works that the LDPC-based code ensembles that have minimum distance growing linearly

with codeword length (i.e., linear-minimum-distance property) exhibit relatively better error performance and lower error floors in the high-SNR region with respect to their counterparts that do not show such a property.

Consider an LDPC-based code with N VNs and K information bits, and a code rate $R = K/N$. Let δ be the normalized weight, $\omega = \delta N$ be the Hamming weight (or distance) and $\mathcal{A}_\omega$ be the ensemble weight enumerator for this code. The normalized logarithmic AWD function of the code ensemble can be defined as $r(\delta) = \lim_{N\to\infty} \sup(\ln(\mathcal{A}_\omega)/N)$, where $\sup(\cdot)$ is the supremum operation. The expression of the ensemble weight enumerator varies for different types of ensembles. For example, the weight enumerators for the LDPC code ensemble and protograph code ensemble are derived in [173] and [175], respectively. Besides deriving the ML decoding threshold, AWD function can also be used to determine whether the linear-minimum-distance property holds. In fact, the AWD function $r(\delta)$ begins with zero (i.e., $r(0) = 0$) and may go to zero again. Suppose that the second zero crossing of $r(\delta)$ exists, i.e., $\exists\, \delta_{\min} > 0, r(\delta_{\min}) = 0$. If $r(\delta) \leq 0$ for all $0 < \delta < \delta_{\min}$, then $\delta_{\min}$ is called the *typical minimum distance ratio (TMDR)*. In this case, we have $\Pr(0 < \omega < N\delta_{\min}) \leq \sum_{0<\delta<\delta_{\min}} e^{Nr(\delta)}$, meaning that the ensemble weight is asymptotically larger than $N\delta_{\min}$ as N approaches infinity. Thus, the distance of any code extracting from this ensemble should satisfy $\Pr(d \geq N\delta_{\min}) \geq 1 - \varsigma$ for any $\varsigma > 0$. In other words, with a high probability all the codes belonging to this ensemble have minimum distances increasing linearly with codeword length, i.e., $d_{\min} = N\delta_{\min}$.

For the LDPC-based code ensembles that possess TMDRs, the ensemble with a larger TMDR should asymptotically outperform its counterparts with lower TMDRs in the high-SNR region. Especially, SC code ensemble should asymptotically outperform its LDPC code ensemble in the high-SNR region even if they possess the same TMDR. It is because the minimum distance of an LDPC code can be significantly increased via spatial coupling [101], [170]. As an extreme case of LDPC-based codes, the AWD function of the ensemble of rate-R random codes is $r(\delta) = (R-1)\ln 2 + H(\delta)$, where $H(\delta) = -\delta\ln\delta - (1-\delta)\ln(1-\delta)$ is the entropy function [175]. This AWD curve is referred to as the *Gilbert-Varshamov bound* and serves as the fundamental upper-limit on the AWD curves for all binary LDPC-based code ensembles.

Example 3: Utilizing the AWD analysis, we calculate the TMDRs of the rate-1/2 AR3A code, AR4JA code, $(3, 6)$-regular LDPC code and $(3, 6)$-regular tail-biting SC code, and show the corresponding results in Fig. 11.[14] As a benchmark, we also include the Gilbert-Varshamov bound in this figure. Referring to this figure, the AR4JA code, regular LDPC code and its SC counterpart have TMDRs, and thus benefit from the linear-minimum-distance property. Nevertheless, the AR3A code does not have the TMDR and may suffer from an error-floor behavior. Moreover, the regular LDPC code and the SC code provide the TMDRs closest to the Gilbert-Varshamov bound, and thus should achieve the best error performance in the high-SNR region over both OD-ISI and TD-ISI channels. This phenomenon agrees well with the statement in [53], [79], and [91], which have illustrated that the regular CW-3 code can offer very desirable error performance in MR channels. It should also be noted that the SC code may outperform the regular CW-3 code in the high-SNR region because of a larger minimum distance [170].

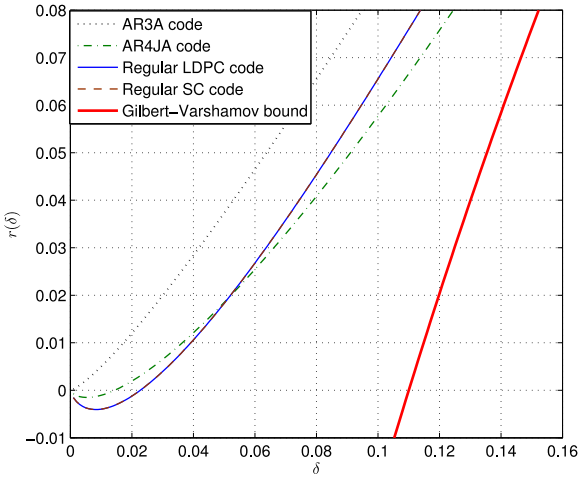

Fig. 11. AWD curves of the rate-1/2 AR3A code, AR4JA code, $(3, 6)$-regular LDPC codes, $(3, 6)$-regular SC, and Gilbert-Varshamov bound. The parameters used for $(3, 6)$-regular SC are $\omega_c = 2$ and $L_c = 5$.

In summary, the LDPC-based codes that have both capacity-approaching decoding thresholds and Gilbert-Varshamov-bound-approaching TMDRs stand out as best candidates for MR systems. However, it is very difficult to achieve both goals for one code. For this reason, some researchers have resorted to designing LDPC-based codes that have both capacity-approaching decoding thresholds and linear-minimum-distance property (i.e., $d_{\min} = N\delta_{\min}$) over MR channels [91], [93].

Remark:

- The decoding threshold is dependent on both the type of code and the type of channel.
- The minimum distance is dependent on the type of code but is independent of the type of channel.

V. Design of LDPC Codes for MR Systems

In this section, we present an overview of selected contributions on the code construction and decoder design of binary LDPC codes over MR channels from the rich literature.

A. Code Construction

1) Design of LDPC Codes Over OD-ISI Channels: In the existing references, DE and EXIT algorithms are two major techniques for designing LDPC codes. In addition, several graph-based design techniques have also been investigated.

(1) DE-based Design: Varnica and Kavcic [57] and Kavcic *et al.* [70] have optimized the degree-distribution pairs

[14] Accumulate-repeat-3-accumulate (AR3A) code and accumulate-repeat-by- 4-jagged-accumulate (AR4JA) code are two classical types of protograph codes. They can be viewed as the precoded RA codes, and thus are able to realize linear encoding complexity and fast decoding [84], [91], [176]. Additionally, in this figure, the coupling width and coupling length for the $(3, 6)$-regular tail-biting SC code are assumed to be $\omega_c = 2$ and $L_c = 5$, respectively.

of LDPC codes for OD-ISI channels by utilizing a DE-based method. Specifically, in order to find a good LDPC code with a given code rate R, a hill-climbing optimization scheme has been introduced in [57]. To begin with, one should fix the target error probability P_{e} and the maximum number of iterations $T_{\max}$.[15] Afterwards, one can initialize the degree-distribution pair $(\lambda_0(x), \rho_0(x))$ of an LDPC code which can achieve P_{e} after $T_{\max}$ DE iterations (see *Algorithm 2*) conditioned on a decoding threshold $(E_b/N_0)_{\mathrm{th}} = (E_b/N_0)_{\mathrm{th},0}$. Based on the above parameter setting, one makes minor change to the VN-degree distribution, i.e., $\lambda_0(x) \rightarrow \lambda_0'(x)$, and checks whether $(\lambda_0'(x), \rho_0(x))$ can achieve $P_{\mathrm{e}} - \varsigma$ (ς is an arbitrarily small positive value) with a smaller threshold (i.e., $(E_b/N_0)'_{\mathrm{th},0} < (E_b/N_0)_{\mathrm{th},0}$). If so, one sets $(\lambda_0(x), \rho_0(x)) = (\lambda_0'(x), \rho_0(x))$ and $(E_b/N_0)_{\mathrm{th}} = (E_b/N_0)'_{\mathrm{th},0}$; otherwise keeps $(\lambda_0(x), \rho_0(x))$ unchanged. The optimized VN-degree distribution $\lambda_{\mathrm{opt}}(x)$ can be found via repeating the above step with a sufficient number of times, which guarantees the smallest threshold $(E_b/N_0)_{\mathrm{th,min}}$. Once $\lambda_{\mathrm{opt}}(x)$ is acquired, the best CN-degree distribution $\rho_{\mathrm{opt}}(x)$ can also be derived using a method analogous to that for optimizing VN-degree distribution. The detailed DE-based degree-distribution pair optimization algorithm for LDPC codes is available in [57].

Unfortunately, the computational complexity for the optimization algorithm is extremely high if no constraint is imposed on the polynomial expressions of $\lambda(x)$ and $\rho(x)$. To accelerate the optimization procedure, one can appropriately limit the search space by either fixing the CN-degree distribution $\rho(x)$ or assuming that $\rho(x)$ has only a few nonzero terms. It has been recognized in various articles [6], [55], [57] that the CN-degree distribution of a well-performing LDPC code contains only a few nonzero terms.

Example 4: Consider a given rate-7/10 LDPC code with degree-distribution pair $(\lambda_0(x), \rho_0(x))$. For the sake of minimizing the decoding thresholds $(E_b/N_0)_{\mathrm{th}}$ over dicode and EPR4 channels, two capacity-approaching LDPC codes have been constructed by exploiting the DE-based computer-search method. The degree-distribution pairs, decoding thresholds, and capacity gaps of the two optimized LDPC codes are shown in Table IV [57].[16] Referring to this table, the decoding threshold of the optimized OD-A LDPC code is 2.166 dB over a dicode channel while that of the optimized OD-B LDPC code is 2.595 dB over a EPR4 channel, both of which have gaps within 0.15 dB to their corresponding capacity limits. Experimental results have shown that both optimized LDPC codes of length 10^6 are about 0.2 dB away from the capacity limits at a BER of 10^{-6}, which reasonably match with the theoretical analyses.

(2) EXIT-based Design: Along with the DE-based design advancement, EXIT-based techniques have also been extensively developed to optimize LDPC codes [71], [132], [177], [178] for MR systems. In recent years, the EXIT algorithm has attracted more attention and has become a more favorable tool for LDPC-code design because it not only requires much less computational complexity relative to the DE algorithm, but also provides accurate result for threshold calculation.

TABLE IV
DEGREE-DISTRIBUTION PAIRS, DECODING THRESHOLDS $(E_b/N_0)_{\mathrm{TH}}$ (dB) AND CAPACITY GAPS Δ (dB) OF THE TWO OPTIMIZED LDPC CODES WITH A CODE RATE $R = 7/10$ OVER DICODE AND EPR4 CHANNELS, RESPECTIVELY

OD-A Code for Dicode Channel			OD-B Code for EPR4 Channel		
d_{v_j}/d_{c_i}	$\lambda_{d_{v_j}}$	$\rho_{d_{c_i}}$	d_{v_j}/d_{c_i}	$\lambda_{d_{v_j}}$	$\rho_{d_{c_i}}$
2	0.2032	0.0004	2	0.2022	0
3	0.2298	0.0002	3	0.2244	0
5	0.1397	0	4	0	0
6	0.0077	0	6	0.0417	0
15	0	0.6252	10	0	0.1934
16	0	0.3588	11	0.0048	0.1023
30	0	0.0154	12	0.0007	0
47	0.1271	0	14	0	0.0658
48	0.2925	0	23	0	0.3138
N.A.			24	0	0.3247
			42	0.1576	0
			43	0.3157	0
			50	0.0260	0
$(E_b/N_0)_{\mathrm{th}}$	2.166		$(E_b/N_0)_{\mathrm{th}}$	2.595	
$C_{\mathrm{i.u.d}}$	2.029		$C_{\mathrm{i.u.d}}$	2.445	
Δ	0.137		Δ	0.150	

In accordance with [9]–[11], an LDPC code can successfully converge under BP decoding if there is an open decoding tunnel in the IL EXIT chart comprising of a VN-decoder MI curve $I_{\mathrm{Ev}} = I_{\mathrm{VND}}(I_{\mathrm{Av}}, I_{\mathrm{E,IO}})$ and a CN-decoder MI curve $I_{\mathrm{Ac}} = I_{\mathrm{CND}}^{-1}(I_{\mathrm{Ec}}) = I_{\mathrm{CND}}^{-1}(I_{\mathrm{Av}})$, where $I_{\mathrm{CND}}^{-1}(\cdot)$ is the inverse function of $I_{\mathrm{Ec}} = I_{\mathrm{CND}}(I_{\mathrm{Ac}})$.[17] To guarantee a successful convergence, I_{Ev} should be larger than I_{Ac} for all $I_{\mathrm{Av}} \in (0, 1)$. In other words, $I_{\mathrm{Ev}} \geq I_{\mathrm{Ac}} + \varsigma$ should be satisfied for all $I_{\mathrm{Av}} \in (0, 1)$, where ς is an arbitrarily small positive value. In particular, for a given degree-distribution pair, the decoding tunnel will become wider as E_b/N_0 increases, indicating that fewer iterations are required for achieving convergence by the decoder. It has been shown theoretically [10] that matching the two component MI curves can optimize the degree-distribution pair of LDPC codes and approach the capacity of memoryless channels. This statement is also true for memory channels, such as ISI channels [71], [132], [178] and slow fading channels [26]. To have more insight, we briefly present the optimization method for VN-degree distribution of LDPC codes over MR channels. The optimization for CN-degree distribution or joint optimization for the degree-distribution pair can be carried out in a similar manner.

The EXIT-chart-based optimization procedure can be started with a rate-R LDPC code with the degree-distribution pair $(\lambda_0(x), \rho_0(x))$. The decoding threshold of this LDPC code is defined as $(E_b/N_0)_{\mathrm{th}} = (E_b/N_0)_{\mathrm{th},0}$. Now, one can slightly change $\lambda_0(x)$ to $\lambda_0'(x)$ while fixing $\rho_0(x)$, and check whether the new degree-distribution pair can satisfy the condition $I_{\mathrm{Ev}} \geq$

[15]The target error probability should be set to a sufficiently small value, e.g., $P_{\mathrm{e}} = 10^{-5}$.

[16]The gap to capacity is defined as the difference between the decoding threshold (i.e., $(E_b/N_0)_{\mathrm{th}}$) and the capacity SNR limit (i.e., $C_{\mathrm{i.i.d.}}$). Also, it should be noted that the SNR is defined as $E_b/N_0 = \sqrt{1/(2R\sigma_n^2)}$ in this paper as in most other existing references, while it is defined as $E_s/N_0 = 1/\sigma_n^2$ in [57]. More precisely, E_b/N_0 corresponds to the bit SNR while E_s/N_0 corresponds to the symbol SNR.

[17]In the IL EXIT chart, the decoding tunnel is defined as the region between the two component EXIT curves (i.e., I_{Ev} and I_{Ac}).

$I_{\mathrm{Ac}} + \varsigma, \forall I_{\mathrm{Ac}} \in (0, 1)$ with a lower decoding threshold (i.e., $(E_b/N_0)'_{\mathrm{th},0} < (E_b/N_0)_{\mathrm{th},0}$). If the above condition holds, one sets $\lambda_0(x) = \lambda'_0(x)$ and $(E_b/N_0)_{\mathrm{th},0} = (E_b/N_0)'_{\mathrm{th},0}$, otherwise keeps $\lambda_0(x)$ unchanged. Repeatedly executing the above step with a sufficiently number of times yields the optimized VN-degree distribution $\lambda_{\mathrm{opt}}(x)$. As compared with the DE-based optimization method, the convergence of MIs is viewed as the design criterion in the EXIT-chart-based method.

Given a target code rate R in MR channels, the "curve-fitting" technique [71], [132], [177] can be exploited to find a VN-decoder MI curve that not only can lie above a given CN-decoder MI curve but also can achieve the smallest decoding threshold. This means that the LDPC code designed with this technique requires the minimum E_b/N_0 to realize reliable communication in such scenarios. We then conclude that the corresponding degree-distribution pair can provide the best fit for the characteristic of MR channels.

The first attempt to utilize the above EXIT-chart-based method for LDPC-code design in ISI scenarios is the work of [71] and [177]. Referring to that work, the authors have considered a binary LDPC code combined with Gray-mapped QPSK modulation in OD-ISI channels.[18] According to the specific modulation scheme and channel environment, a modified channel detector, which comprises a QPSK demapper and a BCJR detector, has been proposed at the receiver terminal. In the underlying decoding framework, a semi-random-walk-based algorithm has been further developed to optimize the degree-distribution pair of rate-1/2 LDPC code for an OD-ISI channel with an impulse response $\mathbf{\Lambda}(D) = 1 + 2D + 3D^2 + 2D^4 + D^5$. As observed from [71], the optimized LDPC code accomplishes a performance gain of about 1.1 dB relative to the AWGN-optimized LDPC code over the given OD-ISI channel.

In addition to the work [71], a modified EXIT-chart-based approach has been proposed in [132] and [178] to design degree-distribution pairs of LDPC codes over OD-ISI channels. In such works, the IL EXIT algorithm is implemented in a very similar fashion to that for the FL EXIT algorithm (see *Algorithm 3*). Specifically, the design principle is to match the EXIT curve of the LDPC decoder (outer decoder) with the EXIT curve of the channel detector (inner detector) to find the best degree-distribution pair. The authors have adopted an infinite-codeword-length assumption and have derived a simplified expression of the extrinsic MI for the outer decoder, denoted by $I_{\mathrm{E,OI}} = \Phi_{\mathrm{DEC}}(I_{\mathrm{E,IO}})$, based on the symmetric Gaussian approximation. On the contrary, the extrinsic MI for the inner detector, denoted by $I_{\mathrm{E,IO}} = \Phi_{\mathrm{DET}}(I_{\mathrm{E,OI}}, \mathbf{\Lambda}(D), \sigma_n^2)$, should be computed using (7), in which the PDF of extrinsic LLRs is obtained via Monte-Carlo simulations. For a given E_b/N_0 and a given LDPC code, the EXIT curves for the inner detector $I_{\mathrm{E,IO}}$ and outer decoder $I_{\mathrm{E,OI}}$ can be plotted in the same figure to establish an EXIT chart, in which the former is plotted in the standard way but the latter is plotted on the transposed axes. The decoding threshold can be estimated via changing the value of E_b/N_0 until the two EXIT curves touch each other. Afterwards, the optimized degree-distribution pair that determines the lowest decoding threshold can be found by exploiting the computer-search method.

Nonetheless, most of the designed LDPC codes in [57], [70], [71], [132], [177], and [178] have code rates smaller than 4/5, which may not be able to fully satisfy the high-rate requirement for practical MR applications. Consequently, some researchers have delved into high-rate LDPC codes in the context of OD-ISI channels.

(3) Graph-based Design: Here, we offer a design example of high-rate LDPC codes by modifying the structures of Tanner graphs based on the characteristics of a particular PR channel, but not exploiting the DE and EXIT algorithms.

As mentioned in [41], the joint precoder-and-channel-code design is a viable alternative to the sole code design for improving the convergence and error performance of channel-coded MR systems. Although precoding often cannot bring performance improvement for LDPC-coded MR systems, Legg and Uchoa-Filho [54] have demonstrated that some particular types of LDPC codes, such as the RA-like codes, can attain an enhanced error-correction capability by making use of the precoding structures.

It is apparent that the parity bits output from the accumulator in an RA code resemble those output from the precoder $g(D) = 1/(1+D)$. Motivated by the above inherent precoding property, a type of LDPC codes, called *graph-matched LDPC codes*, has been constructed by modifying the structure of conventional RA codes in [54]. Distinguished from RA codes, in a graph-matched LDPC code, the j-th parity bit is directly generated by its corresponding CN rather than accumulating two adjacent CNs. According to the impulse response of a particular OD-ISI channel, both the original information bits and parity bits should be precoded so as to generate the real codeword that is suitable for transmission.

To be specific, given an information sequence of length K, all the information bits are first repeated q times to attain an expanded bit sequence of length Kq. After processed by an interleaver, every μq bits are grouped to generate a parity bit via the direct connection of a CN. Aiming at alleviating the interference coming from an OD-ISI channel, both the original information bits and parity bits are further precoded by $1/\mathbf{\Lambda}(D)$ and thus the output bits of the precoder constitute the graph-matched LDPC code, where $\mathbf{\Lambda}(D)$ is the impulse response of the OD-ISI channel. In this sense, the code rate of graph-matched LDPC code equals $R = K/(K + (Kq)/(\mu q)) = \mu/(\mu + 1)$. According to the proposed encoding scheme, the initial LLR and the modified Tanner graph for BP iterative decoding can be easily derived. Subsequently, one can recover the original information bits by executing the BP decoding algorithm. Similar to RA codes, graph-matched LDPC codes can also realize linear encoding and linear decoding.

Consider a rate-8/9 graph-matched LDPC code with $K = 3641, q = 3,$ and $\mu = 24$ over a PR4 channel. It has been indicated in [54] that this graph-matched LDPC code not only achieves similar error performance as the optimized LDPC code and SPC/TP code, but also requires much lower implementation complexity. The aforementioned advantages make

[18] QPSK modulation is not applicable to practical MR environments. However, the EXIT-chart-based LDPC-code design principles proposed in [71] and [177] are still useful for LDPC-coded MR systems with bipolar baseband modulations.

TABLE V
VN-DEGREE DISTRIBUTIONS OF TWO OPTIMIZED LDPC CODES WITH A CODE RATE $R = 8/9$ OVER TD-ISI CHANNELS WITH RECORDING DENSITIES OF $1\,\mathrm{Tb/in^2}$ AND $4\,\mathrm{Tb/in^2}$, RESPECTIVELY. THE CN DEGREE OF BOTH CODES IS SET TO BE 27

Code Type \ d_{v_j}	2	3	9	10
TD-A code for $1\,\mathrm{TB/in^2}$	0.0676	0.6250	0.0763	0.2312
TD-B code for $4\,\mathrm{TB/in^2}$	0.1445	0.8146	0.0378	0.0031

the graph-matched coding scheme extremely attractive for MR systems.

Remark: Legg and Uchoa-Filho [54] have only focused on the encoding design of LDPC codes over ODMR channels under the BP decoding but have not considered the effect of turbo detection.

2) Design of LDPC Codes Over TD-ISI Channels: TD-ISI channels involve another type of interference in addition to ISI, namely ITI, which may impose significant effect on the design results. In such type of channels, LDPC-code design has been predominantly investigated by utilizing EXIT algorithms [37], [55].

Kong *et al.* [55] have first estimated the SIRs of TD-ISI channels with different recording densities. Then, they have considered LDPC codes with a code rate $R = 8/9$ and a fixed CN degree, and have optimized the VN-degree distribution over TD-ISI channels with recording densities of $1\,\mathrm{Tb/in^2}$ and $4\,\mathrm{Tb/in^2}$, respectively, by fitting the MI curve for VND with the MI curve for CND in the EXIT chart. Assuming that all CN degrees are set to be 27, the VN-degree distributions for two optimized LDPC codes, referred to as *TD-A LDPC code* and *TD-B LDPC code*, are presented in Table V. Simulation results have illustrated that both optimized LDPC codes can obtain remarkable gains as compared to the AWGN-optimized LDPC code over TD-ISI channels. Moreover, at a BER of 10^{-5}, the TD-B LDPC code of length 13824 is only 0.33 dB away from the capacity of a TD-ISI channel with a recording density of $4\,\mathrm{Tb/in^2}$, and thus appears to be an excellent candidate for UHD MR systems.

Note that although a modified DE algorithm has been introduced to analyze the decoding threshold of LDPC codes over TD-ISI channels in [69], no previous work has studied the DE-based LDPC-code design in such scenarios till now.

3) Design of QC-LDPC Codes Over MR Channels: Apart from RA-like codes, QC-LDPC codes are also very promising for data-storage applications because they can dramatically reduce the complexity of conventional LDPC codes without deteriorating their error performance. In the past decade, different types of QC-LDPC codes that enable excellent error performance in MR systems have been proposed [81], [82], [167], [179]. In particular, Zhong *et al.* [81], [82], Liu *et al.* [167], and Kong *et al.* [179] have carried out their designs over OD-ISI channels and TD-ISI channels.

According to Section III-A2, QC-LDPC codes can be constructed based on circulant permutation matrices and are capable of realizing linear encoding with the aid of simple shift registers. Furthermore, the QC structure can significantly facilitate the development of hardware-friendly decoders. For example, the feasibility of FPGA-based implementation of QC-LDPC codes over MR channels has been extensively discussed in [82]. Aiming at increasing the decoding throughput, the authors have conceived a new decoding hardware architecture in addition to the encoding design. It has been demonstrated that the proposed QC-LDPC codes and their decoder can achieve superior error performance and desirable throughput in the FPGA-based simulation platform.

Unfortunately, thus far, no related work has studied LDPC codes with linear-minimum-distance property over MR channels.

B. Decoder Design

In parallel with the development of code-construction technique in MR systems, a variety of detection/decoding algorithms have also been proposed in order to improve the overall performance or reduce the implementation complexity of such systems.

1) OD-ISI Channels: In the error-performance aspect, a state-based parallel MP detector has been introduced to circumvent the high-delay issue of BCJR algorithm [30]. Furthermore, the state-based MP detector can perform as well as the BCJR detector with acceptable iterations over OD-ISI channels. Due to the unified decoding mechanisms, the proposed MP detection algorithm can be seamlessly combined with the LDPC-based MP decoding algorithm to form a joint MP decoding algorithm for LDPC-coded MR systems.

Inspired by this work, Pfister and Siegel [63], Radhakrishnan and Vasic [74], Qin *et al.* [127], and Zhao *et al.* [153] have conceived several efficient joint detection-and-decoding algorithms for LDPC codes over OD-ISI channels, which can outperform the combination of BCJR detector and BP decoder at the cost of increasing computational complexity. For example, in [74], a modified Tanner graph that describes the relationship between the noiseless channel output symbols (i.e., $\{y'_j\}$) and CNs has been developed in contrast to the conventional Tanner graph for LDPC codes. Meanwhile, based on the constraints imposed by the channel trellis, a channel graph that describes the relationship between the channel states (referred to as the *channel nodes*) and $\{y'_j\}$ can be plotted. Hence, one can build a modified factor graph which represents the relationship among the channel nodes, channel output symbols and CNs. In order to substantially exploit both channel and code information, the conventional MP decoder has been improved, which produces the a-posteriori messages of channel output symbols rather than channel input symbols (i.e., $\{x_j\}$) [74]. Through such a manner, a joint MP detection-and-decoding algorithm can be formulated by taking into consideration both the symbol-based MP detection algorithm and the symbol-based MP decoding algorithm. Based on the a-posteriori messages of $\{y'_j\}$, one can easily derive the a-posteriori messages of $\{x_j\}$, which are used to retrieve the original information bits. As shown in [74], the joint MP detection-and-decoding algorithm is remarkably superior to the conventional turbo (i.e., joint BCJR-and-BP) decoding algorithm at the expense of relatively higher computation complexity.

With an aim to addressing the error-floor problem existing in LDPC codes, the bit-pinning, trellis-pruning techniques as well as the generalized LDPC decoder previously proposed for AWGN channels [180] have been extended to OD-ISI channels [51]. In [51], a modified importance sampling technique has been first proposed to estimate the error-floor behavior and to find the dominant trapping sets of an LDPC code. The dominant trapping sets are of great importance to determine the error performance in the high-SNR region. After that, the bit-pinning and trellis-pruning techniques have been utilized to pin certain bits in such trapping sets prior to transmitting the codeword.[19] As a further insight, a generalized LDPC decoder has been designed to connect the dominant trapping sets so as to prevent the decoding process from being trapped in these trapping sets. Analytical and simulated results in [51] have shown that the three proposed techniques can significantly lower the error floor of LDPC codes in OD-ISI channels, especially in PR1 and EPR4 channels.

In addition to the above-reported contributions, the works in [75] and [155] have considered the complexity problems of existing detection/decoding algorithms for OD-ISI channels and have developed several low-complexity detection and decoding algorithms. On the one hand, Qin and Teh [155] have conceived a reduced-state SISO detector that can significantly lower the complexity of BCJR detector with a slight performance degradation. On the other hand, Qin *et al.* [75] have further proposed an efficient method to reduce the computational complexity of BP decoding algorithm. To compensate the performance degradation arising from the simplified computation, an attenuation factor has also been introduced in [75] when calculating the LLRs output from the CN decoder. As compared with the conventional BP decoding algorithm, the reduced-complexity BP decoding algorithm benefits from much lower computational complexity with a negligible performance loss.

2) TD-ISI Channels: In recent years, the channel detection algorithms, LDPC decoding algorithms as well as the joint detection-and-decoding algorithms have also been discussed for LDPC-coded TDMR systems [52], [60], [77]–[80], [142], [152], [156], [181].

Although the symbol-based BCJR detector can provide optimal performance over TD-ISI channels, the high computational complexity is a challenging problem for its hardware implementation. Hence, several sub-optimal detection algorithms, e.g., iterative row-column soft decision feedback algorithm (IRCSDF) [181], have been developed so as to reduce the complexity of BCJR detector without sacrificing much performance. Unlike the BCJR detector, the IRCSDF detector consists of two component detectors, namely *row detector and column detector*, which can exchange their corresponding extrinsic soft information iteratively. After performing a sufficient number of iterations, the two types of extrinsic information are combined and passed to the LDPC decoder for further processing. In the IRCSDF detection algorithm, the row/column detector utilizes a modified BCJR algorithm to detect the equivalent horizontal/vertical data strips, which are mapped from the readback data array. Unfortunately, the complexity of the IRCSDF algorithm is still exponentially increasing with the size of the TD CIR matrix.

To reduce the complexity of the IRCSDF detection algorithm, the original TD-ISI channel is reduced to an OD-ISI channel based on Gaussian approximation (GA). Consequently, a GA-IRCSDFA-based BCJR detector has been proposed to detect the channel input signal more efficiently [79], in which each component TD-BCJR detector can be replaced by an OD-BCJR detector. To elaborate a little further, we consider the component row detector and rewrite the channel output (4) as $y_{l,j} = \sum_{\tau=1}^{\kappa_\tau} h_{1,\tau} x_{l-1,j-\tau} + \sum_{\mu=2}^{\kappa_\mu} \sum_{\tau=1}^{\kappa_t} h_{\mu,\tau} x_{l-\mu,j-\tau} + n_{l,j} = \sum_{\tau=1}^{\kappa_\tau} h_{1,\tau} x_{l-1,j-\tau} + n_{\mathrm{R},l,j}$, where $n_{\mathrm{R},l,j} = \sum_{\mu=2}^{\kappa_\mu} \sum_{\tau=1}^{\kappa_\tau} h_{\mu,\tau} x_{l-\mu,j-\tau} + n_{l,j}$. As observed, the first term on the right-hand side of $y_{l,j}$ is the summation of down-track interference, while the second term is the equivalent noise for the row detector. Specifically, the equivalent noise $n_{\mathrm{R},l,j}$ is the summation of $(\kappa_\mu - 1)\kappa_\tau + 1$ independent random variables. Although the exact PDF of $n_{\mathrm{R},l,j}$ is difficult to be derived, it can be approximately characterized by a Gaussian distribution based on the central-limit theorem. Hence, $n_{\mathrm{R},l,j}$ is considered as a modified Gaussian noise, whose PDF can be computed by evaluating the mean and variance of its $(\kappa_\mu - 1)\kappa_\tau + 1$ component random variables. The column detector can be processed utilizing a similar method. According to the above discussions, the GA-IRCSDF-based BCJR detector has much lower complexity in comparison with the symbol-based BCJR detector and IRCSDF-based detector. The detailed complexity comparison among these three detectors is available in [79].

Example 5: Assume that a rate-7/8 regular CW-3 LDPC code of length 4800 is transmitted over a TD-ISI channel with a recording density of $4\,\mathrm{Tb/in^2}$ and the maximum number of the BP iterations is $T_{\mathrm{BP}} = 30$. We adopt the FL PEXIT algorithm to derive the extrinsic MIs of the symbol-based BCJR detector and GA-IRCSDFA-based BCJR detector at $E_b/N_0 = 4.4$ dB, and plot their corresponding EXIT curves in Fig. 12.[20] Referring to this figure, the symbol-based BCJR detector achieves a slight gain over the GA-IRCSDFA-based BCJR detector for a given a-priori MI, which leads to a larger decoding tunnel. Although the GA-IRCSDFA-based BCJR detector is inferior to the symbol-based BCJR detector in terms of convergence speed, the former is superior to the latter in terms of implementation complexity.

As a further study, Fig. 13 presents the BER curves of the two different detectors over a TD-ISI channel, where the maximum number of turbo iterations is assumed to be $T_{\mathrm{TU}} = 10$. It can be seen that the symbol-based BCJR detector achieves a gain of about 0.3 dB compared with the GA-IRCSDFA-based BCJR detector at a BER of 10^{-6}, which agrees well with

[19] A *trapping set* is a subset of VNs in the Tanner graph that cannot converge correctly under the BP iterative decoder. Precisely speaking, an $(n_{\mathrm{T}}, m_{\mathrm{T}})$ trapping set is a subset of n_{T} VNs, which induces a subgraph with m_{T} CNs having an odd number of edges connecting to the n_{T} VNs. The bit-pinning and trellis-pruning techniques are proposed for the BP decoder and BCJR detector, respectively, to eliminate such detrimental sets.

[20] For conciseness, we ignore the upper-bound curve and lower-bound curve of the EXIT band in this figure.

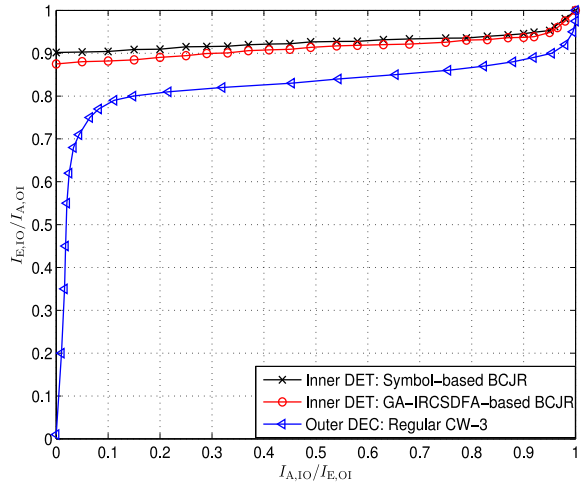

Fig. 12. Expected FL PEXIT curves of the symbol-based BCJR detector and GA-IRCSDFA-based BCJR detector over a TD-ISI channel with a recording density of $4\,\mathrm{Tb/in^2}$, where the regular CW-3 LDPC code is adopted as the channel code. The parameters used are $R = 7/8, N = 4800, T_{\mathrm{BP}} = 30$ and $E_b/N_0 = 4.4$ dB.

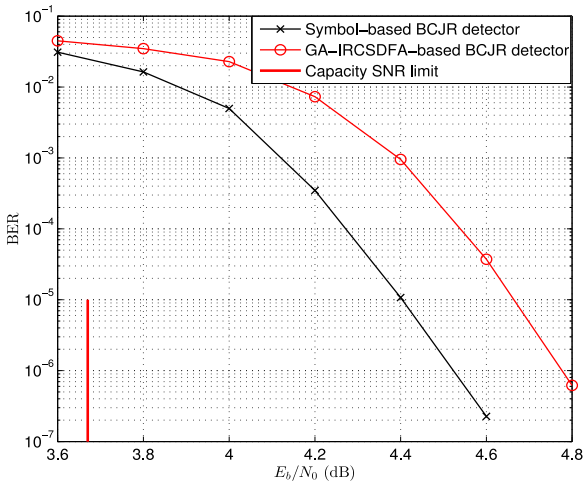

Fig. 13. BER curves of the symbol-based BCJR detector and GA-IRCSDFA BCJR detector over a TD-ISI channel with a recording density of $4\,\mathrm{Tb/in^2}$, where the regular CW-3 LDPC code is adopted as the channel code. The parameters used are $R = 7/8,\ N = 4800, T_{\mathrm{TU}} = 10$ and $T_{\mathrm{BP}} = 30$.

the FL PEXIT-chart analysis. In summary, the GA-IRCSDFA-based BCJR detector strikes a good tradeoff between error performance and implementation complexity, and therefore stands out as a superb candidate for use in practical MR systems.

From the perspective of decoding algorithm, a linear-programming decoding framework has been conceived for LDPC codes over TD-ISI channels [52]. The linear-programming decoding algorithm can serve as an alternative to the BP decoding algorithm because the former produces better performance than the latter in the high-SNR region. Furthermore, two enhanced min-sum decoding algorithms have been proposed in [80], which not only can achieve better performance than the conventional min-sum algorithm, but also can retain the low-computational-complexity property.

As in OD-ISI channels, there also exist some relevant works investigating the joint detection-and-decoding algorithms for LDPC-coded TDMR systems [77], [78], [142], [152]. Of particular interest is the work of [77], in which the authors have not only proposed an efficient joint MP decoding algorithm but also developed a modified EXIT chart to validate the fast convergence speed and excellent error performance of the proposed algorithm. Here, we do not present the details of the corresponding algorithms in [77] because they are not the major focus of this paper.

VI. Design of LDPC-Code Variants for MR Systems

Thanks to their desirable properties, LDPC codes have been thoroughly investigated in the context of MR channels. In the wake of the remarkable success of LDPC-coded MR systems, a myriad of LDPC-code variants have been proposed in such environments, all of which are superior to the conventional LDPC codes in certain aspects. In this section, we cover the development of the design of several representative variants of LDPC codes over MR channels.

A. Design of Protograph Codes

Among all the variants of LDPC codes, protograph codes have received growing interests due to their simple structures and desirable error performance. In the past five years, the performance of protograph codes has been comprehensively investigated over OD-ISI and TD-ISI channels [68], [83], [91]–[96]. Different from the research of conventional LDPC codes, most research on the protograph-code design for MR systems has considered not only the decoding threshold but also the linear-minimum-distance property. Indeed, the design of protograph codes is very sensitive to degree-2 VNs. Although degree-2 VNs can help lowering the decoding threshold, too many degree-2 VNs may deteriorate the linear-minimum-distance property. Therefore, degree-2 VNs should be carefully incorporated into the protograph in order to obtain the smallest decoding threshold while retaining TMDR. To this end, Abu-Surra *et al.* [176] have proposed a certain class of protograph codes with degree-2 VNs, which can ensure the existence of TMDR.

In OD-ISI channels, Fang *et al.* [91] and Yang *et al.* [92] have utilized the FL PEXIT algorithm to design punctured protograph codes, while Van Nguyen *et al.* [93], [94] have utilized the IL PEXIT algorithm to design non-punctured protograph codes. All of these codes possess fast convergence speed without losing the linear-minimum-distance property, and thus are very promising candidates for MR systems. Since we have already introduced the research progress in the design and analysis of protograph codes over OD-ISI channels in [68], we turn our attention to the recent achievements related to designing such codes over TD-ISI channels [83], [95], [96].

Inspired by the superiorities of protograph codes in OD-ISI channels, this type of codes have been applied to TD-ISI channels. Yet, Chen *et al.* [95] and Fang *et al.* [96] have found that both OD-ISI-optimized LDPC codes and protograph codes are no longer suitable for TD-ISI channels, and

hence have developed a computer-search-based methodology to design good-performing protograph codes in such scenarios.

To beginning with, one can first adopt a rate-1/2 non-punctured protograph code of size 3×6, which includes one degree-2 VN and one degree-4 VN.[21] Then, the base matrix can be initialized with

$$\mathbf{B} = \begin{pmatrix} 1 & 1 & b_{1,3} & b_{1,4} & b_{1,5} & b_{1,6} \\ 1 & 2 & b_{2,3} & b_{2,4} & b_{2,5} & b_{2,6} \\ 0 & 1 & b_{3,3} & b_{3,4} & b_{3,5} & b_{3,6} \end{pmatrix}, \tag{9}$$

where the (i, j)-th element $b_{i,j}$ is a non-negative integer. To guarantee the linear-minimum-distance property, one should limit the fraction of degree-2 VNs and impose a constraint on such VNs. Based on the principles proposed in [176], we assume that the maximum number of degree-2 VNs is 2 (i.e., the first and the last VNs) and that no cycle exists in the sub-graph induced by these two degree-2 VNs as well as their associated CNs and edges. Also, we set $b_{i,j} \in \{0, 1, 2, 3\}$ to keep the low-complexity property of protograph codes. Under the above constraints, the optimization objective is to minimize the decoding tunnel by changing the elements in the base matrix. In particular, the area of the decoding tunnel can be evaluated by exploiting the FL PEXIT algorithm and be visualized in the FL PEXIT chart. In consequence, the optimization problem is to resolve the function $\min_{\{b_{i,j}\}} \mathcal{D}_{\mathrm{P}}$, where $\mathcal{D}_{\mathrm{P}}$ is the decoding tunnel of the protograph code. One can promptly obtain the optimized base matrix via a simple search, i.e., [96]

$$\mathbf{B}_{\mathrm{M}} = \begin{pmatrix} 1 & 1 & 0 & 2 & 0 & 0 \\ 1 & 2 & 1 & 1 & 3 & 1 \\ 0 & 1 & 2 & 0 & 0 & 1 \end{pmatrix}. \tag{10}$$

Here, we refer to the rate-1/2 optimized protograph code as the *mother protograph code* C_{M}. Aiming at realizing higher code rates, an RC virtual sub-codeword $\mathcal{V}_{\mathrm{E}}$ has been designed to concatenate with the rate-1/2 protograph code so as to constitute an overall RC optimized protograph (RCOP) code $C = (C_{\mathrm{M}}, \mathcal{V}_{\mathrm{E}})$. The protograph of a rate-$(n+1)/(n+2)$ RCOP code is presented in Fig. 14 where $n = 0, 1, \ldots$. As can be seen, all the component VNs in $\mathcal{V}_{\mathrm{E}}$ have a degree of 3. Moreover, the RC virtual sub-codeword $\mathcal{V}_{\mathrm{E}}$ and the mother protograph code C_{M} share the same CNs.

Example 6: Fig. 15 depicts the expected FL EXIT curves of three rate-7/8 codes, i.e., the RCOP code, the protograph code optimized for OD-ISI channels (referred to as *OD-ISI protograph code*) [94] and the good-performing regular CW-3 LDPC code [53], [79], over a TD-ISI channel where the symbol-based BCJR detector is adopted as the channel decoder. One can observe that the RCOP code offers a larger decoding tunnel as compared with the regular CW-3 code and OD-ISI protograph code. Accordingly, the RCOP code should obtain an additional gain over the other two codes in terms of decoding threshold and error performance.

To further validate the code design and analytical result, we compare the BER performance of the three codes over a TD-ISI channel in Fig. 16. As shown in this figure, at $E_b/N_0 = 4.6$ dB, the RCOP code achieves a BER of 3×10^{-8}, while the regular CW-3 code and OD-ISI protograph code merely accomplish BERs of 2×10^{-7} and 4×10^{-6}, respectively. Furthermore, a larger BER performance gain can be obtained by the RCOP code as E_b/N_0 increases.

[21] We assume that this protograph code does not include any degree-1 VN.

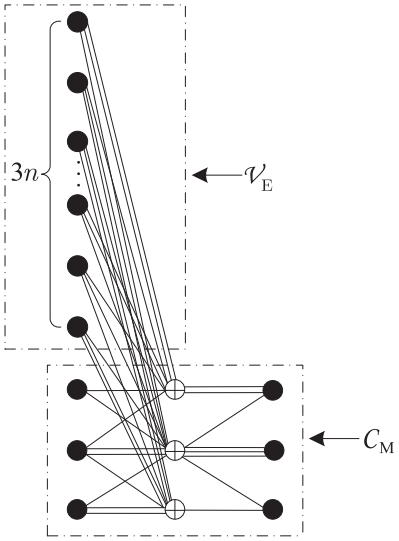

Fig. 14. Protograph of a rate-$(n+1)/(n+2)$ RCOP code.

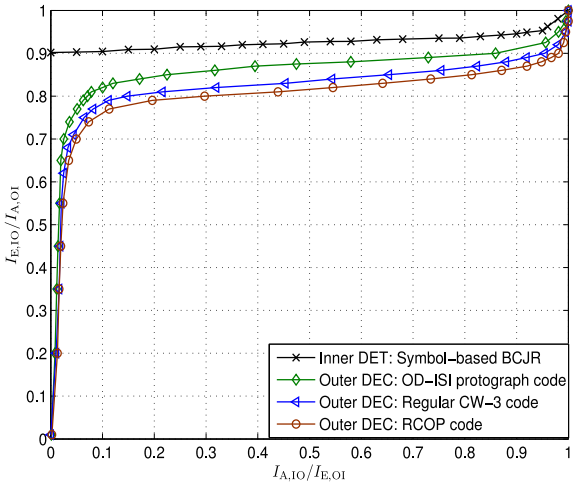

Fig. 15. Expected FL EXIT curves of the RCOP code, OD-ISI protograph code and regular CW-3 LDPC code over a TD-ISI channel with a recording density of 4 Tb/in^2. The parameters used are $R = 7/8, N = 4800, T_{\mathrm{BP}} = 30$ and $E_b/N_0 = 4.4$ dB, where T_{BP} denotes the maximum number of BP iterations.

To get more implementation benefits, a modified PEG algorithm has been developed by Kong *et al.* [83] and large-girth QC-protograph codes have been constructed. It has been suggested that the proposed QC-protograph code can perform very close to the optimized irregular LDPC codes over TD-ISI channels. Thanks to the low-complexity encoder and decoder structures, the QC-protograph codes can serve as an excellent alternative to the conventional LDPC codes for MR applications.

To the best of our knowledge, all the previous protograph-code-related works have restricted their attention to the code-construction aspect and have never mentioned the decoding algorithm.

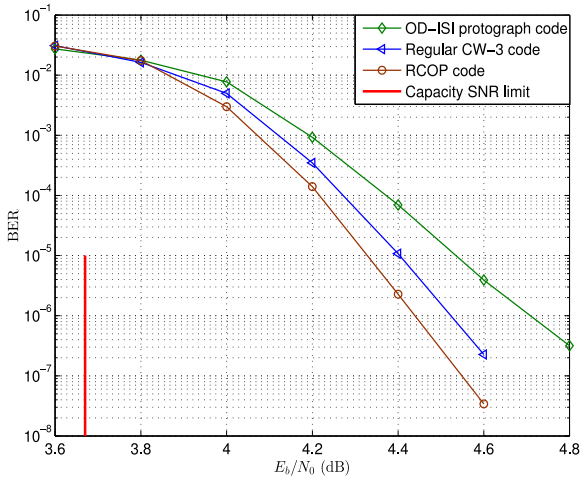

Fig. 16. BER curves of the RCOP code, OD-ISI protograph code and regular CW-3 LDPC code over a TD-ISI channel with a recording density of 4 Tb/in^2. The parameters used are $R = 7/8$, $N = 4800$, $T_{\mathrm{TU}} = 10$ and $T_{\mathrm{BP}} = 30$, where T_{TU} denotes the maximum number of turbo iterations.

B. Design of RA Codes

As mentioned in Section III-B2, RA codes are a simple variant of LDPC codes that can achieve desirable error performance with relatively lower encoding and decoding complexity. The graph-matched LDPC codes introduced in Section V-A1 can be considered as a design paradigm of RA-like codes in ODMR systems.

On the other hand, the irregular LDPC codes (i.e., the TD-A and TD-B codes in Table V) optimized for TDMR systems are unstructured and thus require high encoding and decoding complexity [55]. To solve this problem, Mehrnoush *et al.* [37] have conducted an insightful study on IRA codes in such scenarios. Unlike [55], a more practical channel model, namely *Voronoi model*, has been considered in [37]. This channel model not only includes TD-ISI, but also takes into account the overwrite effect occurring in the UHD MR systems.[22] In this channel model, two EXIT-chart methods, i.e., theory-based method and simulation-based method, have been conceived to optimize the VN degree distribution of IRA codes for the MR system with one turbo iteration (i.e., global iteration). In what follows, we briefly review these two methods.

Due to the overwrite effect in the TD-ISI channel, the extrinsic LLRs output from the VN decoder no longer follow a symmetric Gaussian distribution, and thus the closed-form MI expression proposed in [55] is not applicable. For this reason, in the simulation-based EXIT-chart design method, the authors have employed Monte-Carlo simulation to attain the extrinsic LLRs output from the degree-d_{v_j} VN decoder and has estimated the PDF of these LLRs. Based on the given PDF, the extrinsic MI $I_{\mathrm{Ev}}(d_{v_j})$ can be calculated utilizing (7). The simulated EXIT curve for a VN decoder can be easily obtained by $I_{\mathrm{Ev}} = \sum_{j=2}^{d_{\mathrm{v,max}}} I_{\mathrm{Ev}}(d_{v_j})$. Likewise, one can get the simulated EXIT curve for a CN decoder through a similar method. By fitting the EXIT curve of the VN decoder with that of the CN decoder, the optimized degree distribution of VNs can be obtained.

As can be observed from the extrinsic LLR histograms output from a VN decoder, the PDF shape of these LLRs can be well characterized by a two-component Gaussian mixture model [37]. Moreover, the extrinsic LLRs output from a CN decoder can be approximately described by a symmetric Gaussian distribution. Thus, in the theory-based EXIT-chart design method, the PDF of the LLR sequence $\{L_{\mathrm{Ev}}(i,j)\}$ is evaluated based on the feature of two component Gaussian distributions. Then, one can substitute the resultant PDF into (7) to yield the EXIT curve for a VN decoder. On the other hand, the EXIT curve for a CN decoder can be generated utilizing [55, eq. (7)]. After formulating the two theoretical EXIT curves, one can immediately optimize the degree distribution of VNs by exploiting a curve-fitting technique. Especially, a linear-programming-based optimization method has been proposed to fit the two component EXIT curves.

As illustrated in [37], the IRA codes optimized by the theory-based method and simulation-based method outperform the AWGN-optimized IRA code in a Voronoi TDMR channel. Moreover, the theory-based optimized IRA code performs similarly as or better than the simulation-based optimized counterpart. It is worth noting that the simulation-based code-design method has also been extended to a turbo-equalization framework with multiple global iterations in the same paper.

To ensure the good performance of IRA-coded TDMR systems, a new turbo detector based on a BCJR-aided row-column detector and an IRA decoder has been conceived in [50]. Simulation results have suggested that this turbo detector significantly outperforms the counterpart proposed in [182].

C. Design of SC Codes

SC codes are an appealing type of structured LDPC codes that can easily accomplish excellent error performance in both low and high-SNR regions. Despite their rich literature, SC codes have been predominantly investigated in the context of binary erasure and AWGN channels. One notable contribution related to SC-code design for MR systems is the work of [99]. Referring to this work, Esfahanizadeh *et al.* have provided the first comprehensive study on the design of FL non-protograph-based SC codes over OD-ISI channels. Particularly, they have dedicated special attention to designing non-binary circulant-based SC codes rather than binary SC codes for MR systems.

In [99], the major design objective is to lower the error floor of non-binary SC codes while preserving their original structure. Unlike the IL case, the FL LDPC-based codes used in practical MR systems cannot avoid (small) cycles, which may result in trapping sets. The *absorbing sets (ASs)* are a special case of trapping sets [31], [32], [99], in which the number of neighboring even-degree CNs is strictly larger than that of the neighboring odd-degree CNs (see Fig. 17). If the number of odd-degree CNs m_{T} is smaller than a certain threshold, the $(n_{\mathrm{T}}, m_{\mathrm{T}})$ AS is called a *balanced AS (BAS)* [99]. It has been proved by a variety of research articles that the BASs are

[22] In TDMR systems, the number of coded bits is always larger than the number of magnetic grains. In this case, some bits may be overwritten on the surrounding grains rather than any of the given grains. This phenomenon is called *overwrite effect* [37].

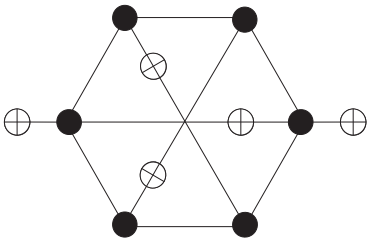

Fig. 17. Structure of a (6, 2) AS, which includes 6 VNs, 3 even-degree CNs and 2 odd-degree CNs.

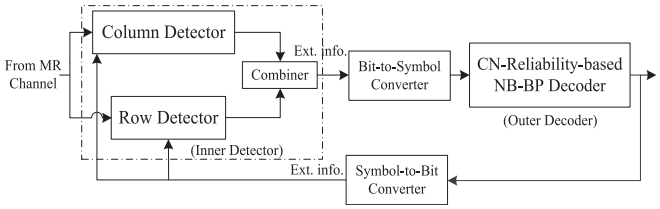

Fig. 18. Block diagram of the joint detection-and-decoding algorithm for non-binary LDPC codes over a TD-ISI channel.

the primary detrimental factor causing the error-floor behavior in MR environments. Through spatial coupling, some conditions for the existence of BASs reduce such that the SC codes always possess relatively fewer BASs with respect to their uncoupled counterparts. Furthermore, the number of BASs in a non-binary SC code is dependent on both the edge weight and cutting vector.

For this reason, a two-step optimization approach has been proposed to eliminate the BASs from the Tanner graph of a non-binary circulant-based SC code over OD-ISI channels. The optimization approach is outlined as below [99].

(1) Given a non-binary circulant-based LDPC code and a coupling length L_c, select a type of cutting vector $\Xi = (\varepsilon_1, \varepsilon_2, \ldots, \varepsilon_{d_v})$ which leads to the minimum number of BASs.[23]
(2) Appropriately change the edge weights of the non-binary Tanner graph, which can thoroughly eliminate the remaining dominant BASs.

According to the above-mentioned optimization approach, two efficient algorithms have been introduced so as to find the optimal cutting vector and edge-weight distribution for non-binary SC codes, respectively. As demonstrated in [99], the optimized SC codes possess a noticeable performance gain over their uncoupled counterparts as well as the unoptimized SC codes. More importantly, no error floor is observed for the optimized SC codes at a word error rate (WER) of 10^{-10}.

D. Design of Non-Binary LDPC-Based Codes

Non-binary LDPC-based codes represent another prevailing research direction for channel-coded MR systems. Apart from the non-binary SC codes mentioned in Section VI-C, other non-binary LDPC-based codes, such as non-binary LDPC codes and non-binary protograph codes, have also attracted significant amount of attention in both coding and MR communities.

1) Non-Binary LDPC Codes: The design of non-binary LDPC codes for MR channels has been studied in [31], [106], and [110]. Hareedy *et al.* [31], [110] have conducted an in-depth investigation on the error-floor problem of non-binary LDPC codes over MR channels. As in non-binary SC codes, BASs are also considered as the dominant error type that leads to the error floor of non-binary LDPC codes. Hence, the design algorithm adopted in [31] and [110] is very similar to that in [99]. In particular, an edge-weight distribution optimization algorithm has been invoked for the corresponding Tanner graph of non-binary LDPC codes so as to break as many BASs as possible in MR scenarios. As a further advancement, a novel prediction technique that combines both analyses and biased simulations to accurately estimate the error-floor level of non-binary LDPC codes has been proposed in [31]. Especially, the proposed prediction technique can overcome the time-consuming weakness of conventional Monte-Carlo simulations. With an aim to enhancing the burst-error-correction capability of non-binary LDPC codes in MR systems, another design methodology has also been conceived in [106].

Besides the code-construction aspect, a myriad of detection and decoding algorithms have been proposed to match the characteristics of different non-binary LDPC codes in the context of MR channels [48], [60], [109], [115], [127], [153], [161]. Here, we provide a brief introduction of the joint detection-and-decoding algorithm proposed in [109], which can achieve outstanding error performance with relatively low complexity.

Fig. 18 depicts the block diagram of the joint detection-and-decoding algorithm, which can be utilized to decode non-binary LDPC codes over TD-ISI channels. Referring to this figure, the inner detector and the outer decoder are implemented by the GA-IRCSDFA-based detector and the CN-reliability-based non-binary BP decoder [183], respectively. The extrinsic message is updated between the inner detector (i.e., GA-IRCSDFA-based BCJR detector) and the outer decoder (i.e., CN-reliability-based non-binary BP decoder) for the sake of boosting the overall error performance. Since the GA-IRCSDFA-based detector has already been introduced in Section V-B2, we only summarize the principles of CN-reliability-based non-binary BP decoder here.

Distinguished from the standard BP decoding algorithm, the CN-reliability-based BP decoding algorithm only allows a fraction of the CNs and VNs to exchange extrinsic messages with their neighboring nodes in each iteration. In the proposed decoding algorithm, the reliability of a CN is measured by the checksum and probability mass function of its associated q-ary symbols. At the end of each iteration, the CN will be labeled as unreliable if (i) its checksum is non-zero or (ii) the checksum is zero but its probability mass function is smaller than a predefined threshold. In the next iteration, only the unreliable CNs and their associated VNs are allowed to further update their extrinsic messages, while the reliable CNs and their associated VNs are forbidden to do so. In fact, most

[23]Here, ε_μ is the μ-th element of Ξ ($0 \leq \varepsilon_\mu \leq d_c$); and d_v and d_c are, respectively, the VN and CN degrees of the circulant-based LDPC code.

VNs can converge to a sufficiently reliable status (i.e., can achieve sufficiently large LLRs) after a few iterations under the BP decoding algorithm. Thereby, the computational complexity of the decoding algorithm can be substantially reduced by skipping the message propagation for high-reliability VNs at the cost of slight degradation in error performance.

Since the performance metric used in the CN-reliability-based BP decoding algorithm is the symbol-based extrinsic message while the performance metric used in the GA-IRCSDFA-based BCJR detector is the bit-based extrinsic message, a bit-to-symbol converter and a symbol-to-bit converter should be exploited to realize conversion between these two metrics (see Fig. 18).

2) Non-Binary Protograph Codes: Like other non-binary counterparts, non-binary protograph codes may also exhibit good error performance over MR channels. To date, there have been two major works studying the design and analysis of non-binary protograph codes over MR channels [73], [107].

Concretely speaking, the IL PEXIT algorithm for OD-ISI channels has been extended to the non-binary domain in [107]. This algorithm can be utilized to calculate the decoding threshold of non-binary protograph code and to predict their error performance in the low-SNR region over OD-ISI channels. It has been shown in [107] that the decoding threshold of a $(2, 4)$-regular protograph code dramatically decreases with the GF size (i.e., q) while the decoding threshold of a $(3, 6)$-regular protograph code increases slowly with q. However, no code-design result has been presented in the paper.

In the context of TD-ISI channels, a PEXIT-AWD-aided optimization method has been proposed by Chen *et al.* [73] to design protographs that can achieve good performance in both low-SNR region and high-SNR region over small GF sizes (i.e., $4 \leq q \leq 32$). It has been proved in [104] and [107] that the non-binary protograph codes having a large fraction of degree-2 VNs may improve the decoding threshold but degrade the linear-minimum-distance property simultaneously. Based on the above principle, two optimized non-binary protograph codes, namely *NP1 code and NP2 code*, have been formulated to strike a good balance between the error performance in the low-SNR region and high-SNR region [73]. In the non-binary code design, it has been assumed that the edge weights in the protographs are randomly selected from the set $\mathcal{D}_q = \{0, 1, \ldots, q-1\}$. Moreover, the number of degree-2 VNs has been carefully chosen. The structures of the non-binary NP1 code and non-binary NP2 code are presented in Fig. 19. As seen from this figure, the code rates of the NP1 code and NP2 code equal $R_{\mathrm{NP1}} = 8/9$ and $R_{\mathrm{NP2}} = (n+1)/(n+2)$, respectively, where $n = 0, 1, \ldots$. Especially, when $n = 7$, the code rate of NP2 code also becomes $R_{\mathrm{NP2}} = 8/9$.

With the help of non-binary PEXIT analysis, one can easily find that both the rate-8/9 NP1 and NP2 codes possess the lowest decoding thresholds, i.e., 3.95 dB and 3.9 dB, when $q = 16$. Additionally, exploiting the non-binary AWD analysis, one can find that the AWD curves of both NP1 and NP2 codes can converge to the Gilbert-Varshamov bound as the normalized weight δ becomes larger [73]. In particular, the NP1 code has a TDMR closer to the Gilbert-Varshamov bound as compared with the NP2 code. Thus, it can be conjectured that both NP1 and NP2 have good error-floor performance. Moreover, the NP1 code may have an even lower BER in the high-SNR region relative to the NP2 code. To have more insight, the BER simulation of the NP1 and NP2 codes over GF(16) is given as below.

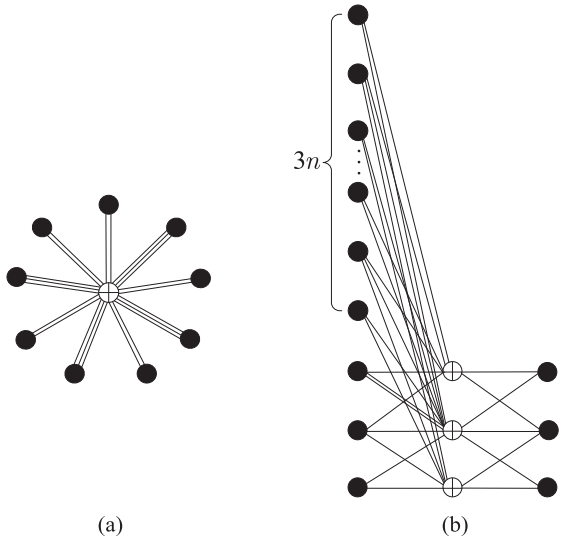

Fig. 19. Protographs of (a) a rate-8/9 non-binary NP1 code and (b) a rate-$(n+1)/(n+2)$ non-binary NP2 code.

Example 7: Considering a TD-ISI channel with a recording density of 4 Tb/in^2, Fig. 20 presents the BER curves of the rate-8/9 non-binary (i) NP1 code, (ii) NP2 code, and (iii) LDPC code proposed in [48] over GF(16). For comparison, the BER curves of the binary RCOP code in [96] and the optimized TD-B LDPC code in [55] are also included in this figure.[24] We observe that both the NP1 code and NP2 code perform better than the non-binary LDPC code and the two binary counterparts. Between the two optimized non-binary protograph codes, the NP1 code outperforms the NP2 code by about one order of magnitude at $E_b/N_0 = 4.65$ dB, which is highly consistent with the AWD analysis. Moreover, at a BER of 10^{-6}, the NP1 code has a gap of only 0.6 dB to the capacity limit. Accordingly, the NP1 code exhibits attractive benefits from the performance and complexity perspectives, and thus should be a great choice for UHD MR systems.

Despite the on-going surge of interest in non-binary-protograph-coded MR systems, the improvement of their decoding algorithms remains to be explored.

VII. Concluding Remarks and Future Research Directions

A. Concluding Remarks

In this treatise, we have presented a comprehensive literature review on LDPC codes and their valuable variants applied in modern MR systems. We have summarized the most representative design and analysis methodologies related to these LDPC-based codes in the associated references. In particular, we have limited our elaborations to the code construction and

[24]Note that the structures of the binary RCOP code and TD-B LDPC code can be obtained in Fig. 14 and Table V, respectively.

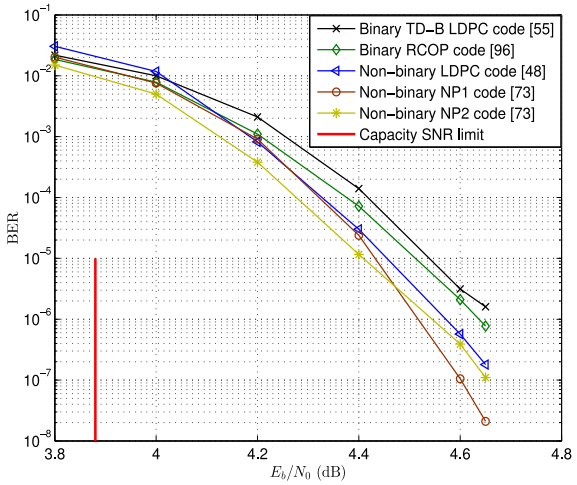

Fig. 20. BER curves of the non-binary NP1 code, NP2 code, and LDPC code over GF(16), as well as the binary optimized protograph code and optimized TB-2 LDPC code over a TD-ISI channel with a recording density of 4 $\mathrm{Tb/in^2}$. The parameters used are $R = 8/9$, $N = 4608$ bits, $T_{\mathrm{TU}} = 10$, and $T_{\mathrm{BP}} = 30$.

decoder design in the context of OD-ISI and TD-ISI transmission scenarios. In order to reveal the latest development trends in LDPC-coded MR systems, we have selected more than one hundred technical papers that were published in recent ten years.

In Section II, we have commenced the discourse by outlining the basic working mechanism of LDPC-coded MR systems, including the transmitter and receiver architectures. Then, we have highlighted the channel models, the concept of SIR as well as the major anti-ISI techniques for LDPC-coded MR systems. Following these preliminary foundations, a compact historical overview of the contributions pertaining to LDPC-code design for MR systems has been provided.

In Section III, we have introduced the fundamental knowledge of LDPC codes and their variants that are suitable for MR applications. In Section III-A, we have summarized the representation methods, general code-construction techniques and decoding algorithms of LDPC codes over MR channels. In Section III-B, we have proceeded to providing a brief review on the protograph codes, RA codes, SC codes as well as the non-binary LDPC-based codes, which have been proved to show excellent error performance in MR environments. It is worth noting that the Tanner-graph-based BP decoding algorithm is valid for all the LDPC-based codes.

In Section IV, we have offered a general discussion on the three classical theoretical-analysis methodologies for LDPC-coded MR systems, which not only can be utilized to predict the error performance of LDPC-based codes over MR channels, but also can be employed to guide the optimization of their code structures and detection/decoding schemes. To be specific, the DE algorithm, EXIT algorithm and AWD analysis have been summarized in Sections IV-A, IV-B, and IV-C, respectively. Especially, the DE and EXIT algorithms can calculate the decoding threshold of a code and estimate its error performance in the low-SNR region, while the AWD analysis can assert whether a code preserves the linear-minimum-distance property and predict its performance in the high-SNR region.

In Section V, we have presented various contributions of LDPC-code design for MR systems that have been put forward in the literature. In Section V-A, we have given a concise portrayal of the research works concerning the code construction of LDPC codes and their QC counterparts over both OD-ISI and TD-ISI channels. We have noted that most existing works regarding the code design rely on the DE and EXIT algorithms and only a few works rely on the modification of Tanner graphs. In Section V-B, we have taken a quick glance at the majority of the detection and decoding algorithms in such transmission scenarios. In this subsection, we have enumerated several design paradigms for the detection algorithms, decoding algorithms as well as the joint detection-and-decoding algorithms. Of particular interest is the GA-IRCSDFA-based BCJR detector which achieves a good tradeoff between performance and complexity.

In Section VI, we have turned our attention to the current research progress of meritorious variants of LDPC codes that fit well with the low-BER requirement of MR systems. More specifically, the state-of-the-art protograph coding schemes that possess both capacity-approaching decoding thresholds and linear-minimum-distance property have been reviewed in Section VI-A. The optimization approaches for RA codes over MR channels have been summarized in Section VI-B. Moreover, the design methodologies for FL non-binary SC codes that possess good error-floor performance have been presented in Section VI-C. In the end, the employment of non-binary LDPC codes and protograph codes in MR systems has been extensively discussed in Section VI-D. In this subsection, we have dedicated special attention to the low-complexity joint detection-and-decoding algorithm design for non-binary LDPC codes because the implementation complexity is a major concern for such type of codes. Besides that, we have introduced a PEXIT-AWD-aided optimization approach for non-binary protograph codes in the context of MR channels.

To summarize, as a classical type of near-capacity ECCs, LDPC codes have demonstrated their superiority for use in MR systems. In the past five years, more attempts have been concentrated on the application and design of protograph codes, SC codes and their non-binary counterparts in such scenarios, which have created new opportunities for modern channel-coded MR-system research.

B. Future Research Directions

Thanks to the distinguished advantages of LDPC codes, they have been widely accepted as a strongly feasible solution for the MR industry. Beyond any doubt, LDPC codes and their variants have great potential to be included in some MR-related standards in the future. However, in order to perfectly meet the requirements of UHD MR systems and other promising storage devices, much more attention should be paid to this research area. Indeed, there are numerous challenging problems and open issues related to LDPC-coded MR systems needing to be addressed, some of which are listed as follows.

1) As mentioned in Section V, the asymptotic performance of LDPC codes has been intensely analyzed by means of DE and EXIT algorithms, and a variety of LDPC codes

that possess capacity-approaching decoding thresholds have been constructed. Nonetheless, no prior study has yet been devoted to evaluating the TMDRs of LDPC codes in such scenarios. With an aim to achieving excellent performance in both low-SNR region and high-SNR region, it is necessary to modify the conventional AWD analysis approach in order to design LDPC codes that not only possess good decoding thresholds over MR channels but also enable the linear-minimum-distance property.

2) Although SC codes have been successfully applied in OD-ISI channels, their performance in TD-ISI channels has not been fully investigated. As a type of emerging ECCs, SC codes are able to attain decoding thresholds approaching Shannon limit and minimum distances growing linearly with codeword length. These advantages make such codes highly desirable for data storage systems that require extremely low BERs. Therefore, developing excellent SC-code design methodologies to approach the capacity of TDMR systems will be more appreciated because such TDMR systems can support much higher data-storage density as compared with the ODMR systems.
3) According to Section VI, the design of protograph codes and SC codes over MR systems has been well studied, while the decoding schemes of such types of codes have been scarcely discussed in the open literature. Besides a sophisticated code structure, good decoding algorithms are also very crucial for reducing the performance gap to the capacity of MR channels. So, it makes sense to conceive improved decoding schemes which can provide better fits for protograph codes and SC codes in MR environments.
4) We also anticipate that another important research issue is to further explore other excellent LDPC-code variants or ECCs that are more suitable for use in MR systems. As can be observed in Section VI, a couple of variants based on LDPC code have been introduced to both ODMR and TDMR systems. Unfortunately, there still exists a nontrivial gap (e.g., 0.6 dB) between these codes and their corresponding capacities in FL settings. Recently, polar codes have also been invoked to achieve the capacity of MR channels and have exhibited very desirable performance comparable to LDPC codes [184]. In order to obtain more desirable FL error performance in MR channels, a strong focus on devising more efficient LDPC-like code architectures or other meritorious code architectures is certainly to be expected.
5) Till now, most research activities in the existing literature have been endeavored to the theoretical and algorithmic advancement of LDPC-coded MR systems. As far as we know, only a few references, e.g., [82] and [185], have paid attention to the hardware implementation of their designs. In fact, the hardware feasibility of LDPC encoding and decoding frameworks is of great importance to formulate a complete channel-coding technical solution for the MR industry. Due to the aforementioned reason, the hardware implementation of LDPC-coded MR systems is a very challenging and meaningful task, and definitely deserves a future line.
6) In recent years, NAND flash memory has appeared to be a very appealing data-storage system because it can offer more superb performance than the existing MR systems in terms of access speed and power consumption [39]. LDPC codes have been considered as a competitive alternative to conventional algebraic codes, e.g., Bose-Chaudhuri-Hocquenghem (BCH) codes, for the next-generation NAND flash memory [32], [186]. Nevertheless, the design of LDPC codes and their variants for NAND flash memory is still in its infancy, and thus there are a range of related issues awaiting investigation.

REFERENCES

[1] R. G. Gallager, *Low-Density Parity-Check Codes*. Cambridge, MA, USA: MIT Press, 1963.

[2] C. Berrou, A. Glavieux, and P. Thitimajshima, "Near Shannon limit error-correcting coding and decoding: Turbo-codes," in *Proc. IEEE Int. Conf. Commun. (ICC)*, vol. 2. Geneva, Switzerland, May 1993, pp. 1064–1070.

[3] D. J. C. MacKay and R. M. Neal, "Good codes based on very sparse matrices," in *Proc. 5th IMA Conf. Cryptography Coding*, vol. 1025. Cirencester, U.K., Oct. 1995, pp. 100–111.

[4] D. J. C. MacKay, "Good error-correcting codes based on very sparse matrices," *IEEE Trans. Inf. Theory*, vol. 45, no. 2, pp. 399–431, Mar. 1999.

[5] T. Richardson and R. Urbanke, "The capacity of low-density parity-check codes under message-passing decoding," *IEEE Trans. Inf. Theory*, vol. 47, no. 2, pp. 599–618, Feb. 2001.

[6] T. J. Richardson, M. A. Shokrollahi, and R. L. Urbanke, "Design of capacity-approaching irregular low-density parity-check codes," *IEEE Trans. Inf. Theory*, vol. 47, no. 2, pp. 619–637, Feb. 2001.

[7] T. J. Richardson and R. L. Urbanke, "The renaissance of Gallager's low-density parity-check codes," *IEEE Commun. Mag.*, vol. 41, no. 8, pp. 126–131, Aug. 2003.

[8] T. J. Richardson and R. L. Urbanke, "Efficient encoding of low-density parity-check codes," *IEEE Trans. Inf. Theory*, vol. 47, no. 2, pp. 638–656, Feb. 2001.

[9] S. ten Brink, "Convergence behavior of iteratively decoded parallel concatenated codes," *IEEE Trans. Commun.*, vol. 49, no. 10, pp. 1727–1737, Oct. 2001.

[10] S. ten Brink, G. Kramer, and A. Ashikhmin, "Design of low-density parity-check codes for modulation and detection," *IEEE Trans. Commun.*, vol. 52, no. 4, pp. 670–678, Apr. 2004.

[11] A. Ashikhmin, G. Kramer, and S. ten Brink, "Extrinsic information transfer functions: Model and erasure channel properties," *IEEE Trans. Inf. Theory*, vol. 50, no. 11, pp. 2657–2673, Nov. 2004.

[12] M. Franceschini, G. Ferrari, and R. Raheli, "Does the performance of LDPC codes depend on the channel?" *IEEE Trans. Commun.*, vol. 54, no. 12, pp. 2129–2132, Dec. 2006.

[13] F. Peng, W. E. Ryan, and R. D. Wesel, "Surrogate-channel design of universal LDPC codes," *IEEE Commun. Lett.*, vol. 10, no. 6, pp. 480–482, Jun. 2006.

[14] X.-Y. Hu, E. Eleftheriou, and D.-M. Arnold, "Regular and irregular progressive edge-growth tanner graphs," *IEEE Trans. Inf. Theory*, vol. 51, no. 1, pp. 386–398, Jan. 2005.

[15] X. Zheng, F. C. M. Lau, and C. K. Tse, "Constructing short-length irregular LDPC codes with low error floor," *IEEE Trans. Commun.*, vol. 58, no. 10, pp. 2823–2834, Oct. 2010.

[16] N. Bonello, S. Chen, and L. Hanzo, "Low-density parity-check codes and their rateless relatives," *IEEE Commun. Surveys Tuts.*, vol. 13, no. 1, pp. 3–26, 1st Quart., 2011.

[17] J. M. F. Moura, J. Lu, and H. Zhang, "Structured low-density parity-check codes," *IEEE Signal Process. Mag.*, vol. 21, no. 1, pp. 42–55, Jan. 2004.

[18] G. Liva *et al.*, "Design of LDPC codes: A survey and new results," *J. Commun. Softw. Syst.*, vol. 2, no. 3, pp. 191–211, Sep. 2006.

[19] K.-J. Kim, J.-H. Chung, and K. Yang, "Bounds on the size of parity-check matrices for quasi-cyclic low-density parity-check codes," *IEEE Trans. Inf. Theory*, vol. 59, no. 11, pp. 7288–7298, Nov. 2013.

[20] A. Tasdighi, A. H. Banihashemi, and M.-R. Sadeghi, "Efficient search of girth-optimal QC-LDPC codes," *IEEE Trans. Inf. Theory*, vol. 62, no. 4, pp. 1552–1564, Apr. 2016.

[21] F. Steiner, G. Böcherer, and G. Liva, "Protograph-based LDPC code design for shaped bit-metric decoding," *IEEE J. Sel. Areas Commun.*, vol. 34, no. 2, pp. 397–407, Feb. 2016.

[22] X. Mu, C. Shen, and B. Bai, "A combined algebraic- and graph-based method for constructing structured RC-LDPC codes," *IEEE Commun. Lett.*, vol. 20, no. 7, pp. 1273–1276, Jul. 2016.

[23] R. M. Tanner, "A recursive approach to low complexity codes," *IEEE Trans. Inf. Theory*, vol. 27, no. 5, pp. 533–547, Sep. 1981.

[24] K. S. Andrews *et al.*, "The development of turbo and LDPC codes for deep-space applications," *Proc. IEEE*, vol. 95, no. 11, pp. 2142–2156, Nov. 2007.

[25] G. P. Calzolari, M. Chiani, F. Chiaraluce, R. Garello, and E. Paolini, "Channel coding for future space missions: New requirements and trends," *Proc. IEEE*, vol. 95, no. 11, pp. 2157–2170, Nov. 2007.

[26] A. G. D. Uchoa, C. T. Healy, and R. C. de Lamare, "Iterative detection and decoding algorithms for MIMO systems in block-fading channels using LDPC codes," *IEEE Trans. Veh. Technol.*, vol. 65, no. 4, pp. 2735–2741, Apr. 2016.

[27] I. B. Djordjevic, "On the irregular nonbinary QC-LDPC-coded hybrid multidimensional OSCD-modulation enabling beyond 100 Tb/s optical transport," *J. Lightw. Technol.*, vol. 31, no. 16, pp. 2669–2675, Aug. 15, 2013.

[28] A. Rafati, H. Lou, and C. Xiao, "Soft-decision feedback turbo equalization for LDPC-coded MIMO underwater acoustic communications," *IEEE J. Ocean. Eng.*, vol. 39, no. 1, pp. 90–99, Jan. 2014.

[29] H. Song and B. V. K. V. Kumar, "Low-density parity check codes for partial response channels," *IEEE Signal Process. Mag.*, vol. 21, no. 1, pp. 56–66, Jan. 2004.

[30] B. M. Kurkoski, P. H. Siegel, and J. K. Wolf, "Joint message-passing decoding of LDPC codes and partial-response channels," *IEEE Trans. Inf. Theory*, vol. 48, no. 6, pp. 1410–1422, Jun. 2002.

[31] A. Hareedy, B. Amiri, R. Galbraith, and L. Dolecek, "Non-binary LDPC codes for magnetic recording channels: Error floor analysis and optimized code design," *IEEE Trans. Commun.*, vol. 64, no. 8, pp. 3194–3207, Aug. 2016.

[32] A. Hareedy, C. Lanka, and L. Dolecek, "A general non-binary LDPC code optimization framework suitable for dense flash memory and magnetic storage," *IEEE J. Sel. Areas Commun.*, vol. 34, no. 9, pp. 2402–2415, Sep. 2016.

[33] S. Tanakamaru, Y. Yanagihara, and K. Takeuchi, "Error-prediction LDPC and error-recovery schemes for highly reliable solid-state drives (SSDs)," *IEEE J. Solid-State Circuits*, vol. 48, no. 11, pp. 2920–2933, Nov. 2013.

[34] A. Dholakia, E. Eleftheriou, T. Mittelholzer, and M. P. C. Fossorier, "Capacity-approaching codes: Can they be applied to the magnetic recording channel?" *IEEE Commun. Mag.*, vol. 42, no. 2, pp. 122–130, Feb. 2004.

[35] S. Karakulak, P. H. Siegel, J. K. Wolf, and H. N. Bertram, "A new read channel model for patterned media storage," *IEEE Trans. Magn.*, vol. 44, no. 1, pp. 193–197, Jan. 2008.

[36] Y. L. Guan *et al.*, "Coding and signal processing for ultra-high density magnetic recording channels," in *Proc. Int. Conf. Comput. Netw. Commun. (ICNC)*, Honolulu, HI, USA, Feb. 2014, pp. 194–199.

[37] M. Mehrnoush, B. J. Belzer, K. Sivakumar, and R. Wood, "EXIT chart-based IRA code design for TDMR turbo-equalization system," *IEEE Trans. Commun.*, vol. 65, no. 4, pp. 1762–1774, Apr. 2017.

[38] C. Vogler, C. Abert, F. Bruckner, D. Suess, and D. Praetorius, "Heat-assisted magnetic recording of bit-patterned media beyond 10 $\mathrm{Tb/in^2}$," *Appl. Phys. Lett.*, vol. 108, no. 10, pp. 1–5, Feb. 2016.

[39] Y. Cai, S. Ghose, E. F. Haratsch, Y. Luo, and O. Mutlu, "Error characterization, mitigation, and recovery in flash-memory-based solid-state drives," *Proc. IEEE*, vol. 105, no. 9, pp. 1666–1704, Sep. 2017.

[40] D. Raphaeli and Y. Zarai, "Combined turbo equalization and turbo decoding," *IEEE Commun. Lett.*, vol. 2, no. 4, pp. 107–109, Apr. 1998.

[41] P. Tan and J. Li, "Finite-length extrinsic information transfer (EXIT) analysis for coded and precoded ISI channels," *IEEE Trans. Magn.*, vol. 44, no. 5, pp. 648–655, May 2008.

[42] K. R. Narayanan, "Effect of precoding on the convergence of turbo equalization for partial response channels," *IEEE J. Sel. Areas Commun.*, vol. 19, no. 4, pp. 686–698, Apr. 2001.

[43] J. Moon and F. R. Rad, "Turbo equalization via constrained-delay APP estimation with decision feedback," *IEEE Trans. Commun.*, vol. 53, no. 12, pp. 2102–2113, Dec. 2005.

[44] B. Lu, G. Yue, and X. Wang, "Performance analysis and design optimization of LDPC-coded MIMO OFDM systems," *IEEE Trans. Signal Process.*, vol. 52, no. 2, pp. 348–361, Feb. 2004.

[45] A. Rafati, H. Lou, and C. Xiao, "Low-complexity soft-decision feedback turbo equalization for MIMO systems with multilevel modulations," *IEEE Trans. Veh. Technol.*, vol. 60, no. 7, pp. 3218–3227, Sep. 2011.

[46] Y. Lyu, L. Wang, G. Cai, and G. Chen, "Iterative receiver for *M*-ary DCSK systems," *IEEE Trans. Commun.*, vol. 63, no. 11, pp. 3929–3936, Nov. 2015.

[47] L. Bahl, J. Cocke, F. Jelinek, and J. Raviv, "Optimal decoding of linear codes for minimizing symbol error rate," *IEEE Trans. Inf. Theory*, vol. 20, no. 2, pp. 284–287, Mar. 1974.

[48] S. Jeon and B. V. K. V. Kumar, "Binary SOVA and nonbinary LDPC codes for turbo equalization in magnetic recording channels," *IEEE Trans. Magn.*, vol. 46, no. 6, pp. 2248–2251, Jun. 2010.

[49] W. E. Ryan, "Performance of high rate turbo codes on a PR4-equalized magnetic recording channel," in *Proc. IEEE Int. Conf. Commun. (ICC)*, vol. 2. Atlanta, GA, USA, Jun. 1998, pp. 947–951.

[50] M. Mehrnoush, B. J. Belzer, K. Sivakumar, and R. Wood, "Turbo equalization for two dimensional magnetic recording using Voronoi model averaged statistics," *IEEE J. Sel. Areas Commun.*, vol. 34, no. 9, pp. 2439–2449, Sep. 2016.

[51] Y. Han and W. E. Ryan, "Low-floor detection/decoding of LDPC-coded partial response channels," *IEEE J. Sel. Areas Commun.*, vol. 28, no. 2, pp. 252–260, Feb. 2010.

[52] A. R. Krishnan, R. Radhakrishnan, and B. Vasic, "LDPC decoding strategies for two-dimensional magnetic recording," in *Proc. IEEE Glob. Telecommun. Conf. (GLOBECOM)*, Honolulu, HI, USA, Nov. 2009, pp. 1–5.

[53] J. Li, K. R. Narayanan, E. Kurtas, and C. N. Georghiades, "On the performance of high-rate TPC/SPC codes and LDPC codes over partial response channels," *IEEE Trans. Commun.*, vol. 50, no. 5, pp. 723–734, May 2002.

[54] A. P. Legg and B. F. Uchoa-Filho, "Graph-matched LDPC codes for partial-response channels," in *Proc. IEEE Int. Conf. Commun. (ICC)*, Beijing, China, May 2008, pp. 2066–2070.

[55] L. Kong *et al.*, "EXIT-chart-based LDPC code design for 2D ISI channels," *IEEE Trans. Magn.*, vol. 49, no. 6, pp. 2823–2826, Jun. 2013.

[56] W. Tan and J. R. Cruz, "Performance evaluation of low-density parity-check codes on partial-response channels using density evolution," *IEEE Trans. Commun.*, vol. 52, no. 8, pp. 1253–1256, Aug. 2004.

[57] N. Varnica and A. Kavcic, "Optimized low-density parity-check codes for partial response channels," *IEEE Commun. Lett.*, vol. 7, no. 4, pp. 168–170, Apr. 2003.

[58] X. Liu, C. Shi, M. Teng, and X. Ma, "Error correction coding with LDPC codes for patterned media storage," *IEEE Trans. Magn.*, vol. 45, no. 10, pp. 3745–3748, Oct. 2009.

[59] K. Cai *et al.*, "Modeling, detection, and LDPC codes for bit-patterned media recording," in *Proc. IEEE GLOBECOM Workshops (GC Wkshps)*, Miami, FL, USA, Dec. 2010, pp. 1910–1914.

[60] G. Han, Y. L. Guan, K. Cai, and K. S. Chan, "Asymmetric iterative multi-track detection for 2-D non-binary LDPC-coded magnetic recording," *IEEE Trans. Magn.*, vol. 49, no. 10, pp. 5215–5221, Oct. 2013.

[61] H. D. Pfister, J. B. Soriaga, and P. H. Siegel, "On the achievable information rates of finite state ISI channels," in *Proc. IEEE Glob. Commun. Conf. (GLOBECOM)*, vol. 5. San Antonio, TX, USA, Nov. 2001, pp. 2992–2996.

[62] H. D. Pfister, "On the capacity of finite state channels and the analysis of convolutional accumulate-*m* codes," Ph.D. dissertation, Dept. Elect. Eng., Univ. California, at San Diego, San Diego, CA, USA, Mar. 2003.

[63] H. D. Pfister and P. H. Siegel, "Joint iterative decoding of LDPC codes for channels with memory and erasure noise," *IEEE J. Sel. Areas Commun.*, vol. 26, no. 2, pp. 320–337, Feb. 2008.

[64] J. Chen and P. H. Siegel, "On the symmetric information rate of two-dimensional finite-state ISI channels," *IEEE Trans. Inf. Theory*, vol. 52, no. 1, pp. 227–236, Jan. 2006.

[65] S. Nabavi, S. Jeon, and B. V. K. V. Kumar, "An analytical approach for performance evaluation of bit-patterned media channels," *IEEE J. Sel. Areas Commun.*, vol. 28, no. 2, pp. 135–142, Feb. 2010.

[66] O. Shental *et al.*, "Discrete-input two-dimensional Gaussian channels with memory: Estimation and information rates via graphical models and statistical mechanics," *IEEE Trans. Inf. Theory*, vol. 54, no. 4, pp. 1500–1513, Apr. 2008.

[67] A. Kavcic, X. Huang, B. Vasic, W. Ryan, and M. F. Erden, "Channel modeling and capacity bounds for two-dimensional magnetic recording," *IEEE Trans. Magn.*, vol. 46, no. 3, pp. 812–818, Mar. 2010.

[68] Y. Fang, G. Bi, Y. L. Guan, and F. C. M. Lau, "A survey on protograph LDPC codes and their applications," *IEEE Commun. Surveys Tuts.*, vol. 17, no. 4, pp. 1989–2016, 4th Quart., 2015.

[69] J. Yao, K. C. Teh, and K. H. Li, "Performance analysis of low-density parity-check codes over 2D interference channels via density evolution," *CoRR*, vol. abs/1701.03840, pp. 1–28, Jan. 2017. [Online]. Available: http://arxiv.org/abs/1701.03840

[70] A. Kavcic, X. Ma, and M. Mitzenmacher, "Binary intersymbol interference channels: Gallager codes, density evolution, and code performance bounds," *IEEE Trans. Inf. Theory*, vol. 49, no. 7, pp. 1636–1652, Jul. 2003.

[71] M. Franceschini, G. Ferrari, and R. Raheli, "EXIT chart-based design of LDPC codes for inter-symbol interference channels," in *Proc. IST Mobile Wireless Commun.*, Jun. 2005, pp. 1–5.

[72] Y. Chen, P. Njeim, T. Cheng, B. J. Belzer, and K. Sivakumar, "Iterative soft decision feedback zig-zag equalizer for 2D intersymbol interference channels," *IEEE J. Sel. Areas Commun.*, vol. 28, no. 2, pp. 167–180, Feb. 2010.

[73] P. Chen, K. Cai, L. Kong, Z. Chen, and M. Zhang, "Non-binary protograph-based LDPC codes for 2D ISI magnetic recording channels," *IEEE Trans. Magn.*, vol. 53, no. 11, pp. 1–5, Nov. 2017.

[74] R. Radhakrishnan and B. Vasic, "Joint message-passing symbol-decoding of LDPC coded signals over partial-response channels," in *Proc. IEEE Int. Conf. Commun. (ICC)*, Dresden, Germany, Jun. 2009, pp. 1–5.

[75] Z. Qin, K. Cai, and S. Zhang, "Reduced-complexity decoding of high-rate LDPC codes over partial-response channels," in *Proc. IEEE Int. Conf. Commun. Syst.*, Singapore, Nov. 2010, pp. 777–781.

[76] A. Risso, "Layered LDPC decoding over GF(q) for magnetic recording channel," *IEEE Trans. Magn.*, vol. 45, no. 10, pp. 3683–3686, Oct. 2009.

[77] J. Yao, K. C. Teh, and K. H. Li, "Joint message-passing decoding of LDPC codes and 2-D ISI channels," *IEEE Trans. Magn.*, vol. 49, no. 2, pp. 675–681, Feb. 2013.

[78] J. Yao, K. C. Teh, and K. H. Li, "Joint iterative detection/decoding scheme for discrete two-dimensional interference channels," *IEEE Trans. Commun.*, vol. 60, no. 12, pp. 3548–3555, Dec. 2012.

[79] J. Zheng, X. Ma, Y. L. Guan, K. Cai, and K. S. Chan, "Low-complexity iterative row-column soft decision feedback algorithm for 2-D inter-symbol interference channel detection with Gaussian approximation," *IEEE Trans. Magn.*, vol. 49, no. 8, pp. 4768–4773, Aug. 2013.

[80] L. Kong, Y. Jiang, G. Han, F. C. M. Lau, and Y. L. Guan, "Improved min-sum decoding for 2-D intersymbol interference channels," *IEEE Trans. Magn.*, vol. 50, no. 11, pp. 1–4, Nov. 2014.

[81] H. Zhong, T. Zhang, and E. F. Haratsch, "High-rate quasi-cyclic LDPC codes for magnetic recording channel with low error floor," in *Proc. IEEE Int. Symp. Circuits Syst. (ISCAS)*, May 2006, p. 4.

[82] H. Zhong, T. Zhong, and E. F. Haratsch, "Quasi-cyclic LDPC codes for the magnetic recording channel: Code design and VLSI implementation," *IEEE Trans. Magn.*, vol. 43, no. 3, pp. 1118–1123, Mar. 2007.

[83] L. Kong, L. He, P. Chen, G. Han, and Y. Fang, "Protograph-based quasi-cyclic LDPC coding for ultrahigh density magnetic recording channels," *IEEE Trans. Magn.*, vol. 51, no. 11, pp. 1–4, Nov. 2015.

[84] D. Divsalar, S. Dolinar, C. R. Jones, and K. Andrews, "Capacity-approaching protograph codes," *IEEE J. Sel. Areas Commun.*, vol. 27, no. 6, pp. 876–888, Aug. 2009.

[85] T. V. Nguyen, A. Nosratinia, and D. Divsalar, "Bilayer protograph codes for half-duplex relay channels," *IEEE Trans. Wireless Commun.*, vol. 12, no. 5, pp. 1969–1977, May 2013.

[86] Y. Fang, Y. L. Guan, G. Bi, L. Wang, and F. C. M. Lau, "Rate-compatible root-protograph LDPC codes for quasi-static fading relay channels," *IEEE Trans. Veh. Technol.*, vol. 65, no. 4, pp. 2741–2747, Apr. 2016.

[87] T. V. Nguyen, "Design of capacity-approaching protograph-based LDPC coding systems," Ph.D. dissertation, Dept. Elect. Eng., Univ. Texas at Dallas, Dallas, TX, USA, Dec. 2012.

[88] Y. Fang, G. Bi, and Y. L. Guan, "Design and analysis of root-protograph LDPC codes for non-ergodic block-fading channels," *IEEE Trans. Wireless Commun.*, vol. 14, no. 2, pp. 738–749, Feb. 2015.

[89] M. Karimi and A. H. Banihashemi, "On the girth of quasi-cyclic protograph LDPC codes," *IEEE Trans. Inf. Theory*, vol. 59, no. 7, pp. 4542–4552, Jul. 2013.

[90] A. K. Pradhan, A. Thangaraj, and A. Subramanian, "Construction of near-capacity protograph LDPC code sequences with block-error thresholds," *IEEE Trans. Commun.*, vol. 64, no. 1, pp. 27–37, Jan. 2016.

[91] Y. Fang, P. Chen, L. Wang, and F. C. M. Lau, "Design of protograph LDPC codes for partial response channels," *IEEE Trans. Commun.*, vol. 60, no. 10, pp. 2809–2819, Oct. 2012.

[92] S. Yang, L. Wang, Y. Fang, and P. Chen, "Performance of improved AR3A code over EPR4 channel," in *Proc. Int. Conf. Comput. Res. Develop. (ICCRD)*, vol. 2. Shanghai, China, Mar. 2011, pp. 60–64.

[93] T. Van Nguyen, A. Nosratinia, and D. Divsalar, "Protograph-based LDPC codes for partial response channels," in *Proc. IEEE Int. Conf. Commun. (ICC)*, Ottawa, ON, Canada, Jun. 2012, pp. 2166–2170.

[94] T. Van Nguyen, A. Nosratinia, and D. Divsalar, "Rate-compatible protograph-based LDPC codes for inter-symbol interference channels," *IEEE Commun. Lett.*, vol. 17, no. 8, pp. 1632–1635, Aug. 2013.

[95] P. Chen, L. Kong, Y. Fang, and L. Wang, "The design of protograph LDPC codes for 2-D magnetic recording channels," *IEEE Trans. Magn.*, vol. 51, no. 11, pp. 1–4, Nov. 2015.

[96] Y. Fang *et al.*, "Finite-length extrinsic information transfer analysis and design of protograph low-density parity-check codes for ultra-high-density magnetic recording channels," *IET Commun.*, vol. 10, no. 11, pp. 1303–1311, Jul. 2016.

[97] S. Kudekar, T. Richardson, and R. L. Urbanke, "Spatially coupled ensembles universally achieve capacity under belief propagation," *IEEE Trans. Inf. Theory*, vol. 59, no. 12, pp. 7761–7813, Dec. 2013.

[98] S. Kudekar, T. J. Richardson, and R. L. Urbanke, "Threshold saturation via spatial coupling: Why convolutional LDPC ensembles perform so well over the BEC," *IEEE Trans. Inf. Theory*, vol. 57, no. 2, pp. 803–834, Feb. 2011.

[99] H. Esfahanizadeh, A. Hareedy, and L. Dolecek, "Spatially coupled codes optimized for magnetic recording applications," *IEEE Trans. Magn.*, vol. 53, no. 2, pp. 1–11, Feb. 2017.

[100] H. Esfahanizadeh, A. Hareedy, and L. Dolecek, "Spatially coupled LDPC codes optimized for 1-D magnetic recording channels," in *Proc. IEEE Asilomar Conf. Signals Syst. Comput.*, Nov. 2016, pp. 1–5.

[101] D. G. M. Mitchell, M. Lentmaier, and D. J. Costello, "Spatially coupled LDPC codes constructed from protographs," *IEEE Trans. Inf. Theory*, vol. 61, no. 9, pp. 4866–4889, Sep. 2015.

[102] M. C. Davey and D. MacKay, "Low-density parity check codes over GF(q)," *IEEE Commun. Lett.*, vol. 2, no. 6, pp. 165–167, Jun. 1998.

[103] J. Huang, L. Liu, W. Zhou, and S. Zhou, "Large-girth nonbinary QC-LDPC codes of various lengths," *IEEE Trans. Commun.*, vol. 58, no. 12, pp. 3436–3447, Dec. 2010.

[104] L. Dolecek, D. Divsalar, Y. Sun, and B. Amiri, "Non-binary protograph-based LDPC codes: Enumerators, analysis, and designs," *IEEE Trans. Inf. Theory*, vol. 60, no. 7, pp. 3913–3941, Jul. 2014.

[105] L. Wei, T. Koike-Akino, D. G. M. Mitchell, T. E. Fuja, and D. J. Costello, "Threshold analysis of non-binary spatially-coupled LDPC codes with windowed decoding," in *Proc. IEEE Int. Symp. Inf. Theory (ISIT)*, Honolulu, HI, USA, Jun. 2014, pp. 881–885.

[106] A. Marinoni, P. Savazzi, and S. Valle, "Efficient design of non-binary LDPC codes for magnetic recording channels, robust to error bursts," in *Proc. Int. Symp. Turbo Codes Related Topics*, Lausanne, Switzerland, Sep. 2008, pp. 288–293.

[107] W. Phakphisut, P. Supnithi, and N. Puttarak, "EXIT chart analysis of nonbinary protograph LDPC codes for partial response channels," *IEEE Trans. Magn.*, vol. 50, no. 11, pp. 1–4, Nov. 2014.

[108] H. Song and J. R. Cruz, "Reduced-complexity decoding of Q-ary LDPC codes for magnetic recording," *IEEE Trans. Magn.*, vol. 39, no. 2, pp. 1081–1087, Mar. 2003.

[109] G. Han, M. Wang, Y. Fang, and L. Kong, "Joint low-complexity detection and reliability-based BP decoding for non-binary LDPC coded TDMR channels," in *Proc. IEEE Magn. Conf. (INTERMAG)*, Beijing, China, May 2015, p. 1.

[110] A. Hareedy, B. Amiri, S. Zhao, R. Galbraith, and L. Dolecek, "Non-binary LDPC code optimization for partial-response channels," in *Proc. IEEE Glob. Commun. Conf. (GLOBECOM)*, San Diego, CA, USA, Dec. 2015, pp. 1–6.

[111] T. Mittelholzer and E. Eleftheriou, "Channel precoding and low-density parity-check codes for magnetic recording," in *Proc. IEEE Int. Symp. Inf. Theory (ISIT)*, Yokohama, Japan, Jun./Jul. 2003, p. 47.

[112] A. Bhatia, S. Yang, and P. H. Siegel, "Precoding mapping optimization for magnetic recording channels," *IEEE Trans. Magn.*, vol. 50, no. 11, pp. 1–4, Nov. 2014.

[113] B. Vasic and E. Kurtas, *Coding and Signal Processing for Magnetic Recording Systems*. New York, NY, USA: CRC Press, 2004.

[114] Z. Qin, K. Cai, and K. S. Chan, "Iterative reduced-complexity graph-based detection for LDPC coded 2D recording channels," *IEEE Trans. Magn.*, vol. 49, no. 6, pp. 2598–2602, Jun. 2013.

[115] M. Fujii, "Iterative multi-track ITI canceller for nonbinary-LDPC-coded two-dimensional magnetic recording," *IEICE Trans. Electron.*, vol. E95-C, no. 1, pp. 163–171, Jan. 2012.

[116] G. Han, Y. L. Guan, K. Cai, K. S. Chan, and L. Kong, "Embedded marker code for channels corrupted by insertions, deletions, and AWGN," *IEEE Trans. Magn.*, vol. 49, no. 6, pp. 2535–2538, Jun. 2013.

[117] J. Li and K. R. Narayanan, "Rate-compatible low density parity check codes for capacity-approaching ARQ schemes in packet data communications," in *Proc. Int. Conf. Commun. Internet Inf. Technol. (CIIT)*, Nov. 2002, pp. 201–206.

[118] H. Pishro-Nik and F. Fekri, "Results on punctured low-density parity-check codes and improved iterative decoding techniques," *IEEE Trans. Inf. Theory*, vol. 53, no. 2, pp. 599–614, Feb. 2007.

[119] J. Li, E. Kurtas, K. R. Narayanan, and C. N. Georghiades, "Iterative decoding of turbo product codes over PR-equalized Lorentzian channels with colored noise," in *Proc. IEEE Glob. Telecommun. Conf. (GLOBECOM)*, vol. 5. San Antonio, TX, USA, Dec. 2001, pp. 2972–2976.

[120] Z. Wu, "Channel modeling, signal processing and coding for perpendicular magnetic recording," Ph.D. dissertation, Dept. Elect. Eng., Univ. California, at San Diego, San Diego, CA, USA, Sep. 2009.

[121] E. M. Kurtas and B. Vasic, *Advanced Error Control Techniques for Data Storage Systems*. New York, NY, USA: CRC Press, 2005.

[122] T. V. Souvignier, M. Oberg, P. H. Siegel, R. E. Swanson, and J. K. Wolf, "Turbo decoding for partial response channels," *IEEE Trans. Commun.*, vol. 48, no. 8, pp. 1297–1308, Aug. 2000.

[123] A. R. Krishnan, R. Radhakrishnan, and B. Vasic, "Read channel modeling for detection in two-dimensional magnetic recording systems," *IEEE Trans. Magn.*, vol. 45, no. 10, pp. 3679–3682, Oct. 2009.

[124] K. S. Chan *et al.*, "Channel models and detectors for two-dimensional magnetic recording," *IEEE Trans. Magn.*, vol. 46, no. 3, pp. 804–811, Mar. 2010.

[125] S. S. Tehrani, P. H. Siegel, S. Mannor, and W. J. Gross, "Joint stochastic decoding of LDPC codes and partial-response channels," in *Proc. IEEE Workshop Signal Process. Syst.*, Québec City, QC, Canada, Oct. 2012, pp. 13–18.

[126] J. B. Soriaga, P. H. Siegel, J. K. Wolf, and M. Marrow, "On achievable rates of multistage decoding on two-dimensional ISI channels," in *Proc. Int. Symp. Inf. Theory (ISIT)*, Adelaide, SA, Australia, Sep. 2005, pp. 1348–1352.

[127] Z. Qin, K. Cai, and S. Zhang, "Iterative symbol-level detection and decoding for nonbinary LDPC coded 2D intersymbol interference channels," in *Proc. IEEE Int. Conf. Commun. (ICC)*, London, U.K., Jun. 2015, pp. 407–411.

[128] J. Caroselli and J. K. Wolf, "Applications of a new simulation model for media noise limited magnetic recording channels," *IEEE Trans. Magn.*, vol. 32, no. 5, pp. 3917–3919, Sep. 1996.

[129] R. Wood, "The feasibility of magnetic recording at 1 terabit per square inch," *IEEE Trans. Magn.*, vol. 36, no. 1, pp. 36–42, Jan. 2000.

[130] W. Chang and J. R. Cruz, "Inter-track interference mitigation for bit-patterned magnetic recording," *IEEE Trans. Magn.*, vol. 46, no. 11, pp. 3899–3908, Nov. 2010.

[131] C. Douillard *et al.*, "Iterative correction of intersymbol interference: Turbo-equalization," *Eur. Trans. Telecommun.*, vol. 6, no. 5, pp. 507–511, Sep./Oct. 1995.

[132] D. N. Doan and K. R. Narayanan, "Design of good low-rate coding schemes for ISI channels based on spectral shaping," *IEEE Trans. Wireless Commun.*, vol. 4, no. 5, pp. 2309–2317, Sep. 2005.

[133] M. H. Kryder *et al.*, "Heat assisted magnetic recording," *Proc. IEEE*, vol. 96, no. 11, pp. 1810–1835, Nov. 2008.

[134] J.-G. Zhu, X. Zhu, and Y. Tang, "Microwave assisted magnetic recording," *IEEE Trans. Magn.*, vol. 44, no. 1, pp. 125–131, Jan. 2008.

[135] C. S. Modlin, K. D. Fisher, and J. M. Cioffi, "Analysis of and detector comparisons using the microtrack model of magnetic recording," *IEEE Trans. Magn.*, vol. 34, no. 1, pp. 63–68, Jan. 1998.

[136] Y. Ng, K. Cai, B. V. K. V. Kumar, S. Zhang, and T. C. Chong, "Modeling and two-dimensional equalization for bit-patterned media channels with media noise," *IEEE Trans. Magn.*, vol. 45, no. 10, pp. 3535–3538, Oct. 2009.

[137] S. M. Khatami and B. Vasić, "Detection for two-dimensional magnetic recording systems," in *Proc. Int. Conf. Conf. Comput. Netw. Commun. (ICNC)*, San Diego, CA, USA, Jan. 2013, pp. 535–539.

[138] M. Bahrami *et al.*, "Investigation into harmful patterns over multitrack shingled magnetic detection using the Voronoi model," *IEEE Trans. Magn.*, vol. 51, no. 12, pp. 1–7, Dec. 2015.

[139] M. C. Davey and D. J. C. Mackay, "Reliable communication over channels with insertions, deletions, and substitutions," *IEEE Trans. Inf. Theory*, vol. 47, no. 2, pp. 687–698, Feb. 2001.

[140] M. Khatami and B. Vasié, "Constrained coding and detection for TDMR using generalized belief propagation," in *Proc. IEEE Int. Conf. Commun. (ICC)*, Sydney, NSW, Australia, Jun. 2014, pp. 3889–3895.

[141] H. Saito, "Multi-track joint decoding schemes using two-dimensional run-length limited codes for bit-patterned media magnetic recording," *IEICE Trans. Fundam. Electron. Commun. Comput. Sci.*, vol. E99-A, no. 12, pp. 2248–2255, Dec. 2016.

[142] T. Wu, M. A. Armand, and J. R. Cruz, "Detection-decoding on BPMR channels with written-in error correction and ITI mitigation," *IEEE Trans. Magn.*, vol. 50, no. 1, pp. 1–11, Jan. 2014.

[143] G. Han, Y. L. Guan, K. Cai, K. S. Chan, and L. Kong, "Coding and detection for channels with written-in errors and inter-symbol interference," *IEEE Trans. Magn.*, vol. 50, no. 10, pp. 1–6, Oct. 2014.

[144] W. Hirt, "Capacity and information rates of discrete-time channels with memory," Ph.D. dissertation, Swiss Federal Inst. Technol., Zürich, Switzerland, Dec. 1988.

[145] S. Shamai, L. H. Ozarow, and A. D. Wyner, "Information rates for a discrete-time Gaussian channel with intersymbol interference and stationary inputs," *IEEE Trans. Inf. Theory*, vol. 37, no. 6, pp. 1527–1539, Nov. 1991.

[146] W. E. Ryan, "Concatenated codes for class IV partial response channels," *IEEE Trans. Commun.*, vol. 49, no. 3, pp. 445–454, Mar. 2001.

[147] B. M. Kurkoski, K. Yamaguchi, and K. Kobayashi, "Turbo equalization with single-parity check codes and unequal error protection codes," *IEEE Trans. Magn.*, vol. 42, no. 10, pp. 2579–2581, Oct. 2006.

[148] B. M. Kurkoski and K. Yamaguchi, "Turbo equalization as a postprocessor for partial-response channels," in *Proc. IEEE Int. Magn. Conf. (INTERMAG)*, San Diego, CA, USA, May 2006, p. 303.

[149] J. Hagenauer and P. Hoeher, "A Viterbi algorithm with soft-decision outputs and its applications," in *Proc. Glob. Telecommun. Conf. (GLOBECOM)*, vol. 3. Dallas, TX, USA, Nov. 1989, pp. 1680–1686.

[150] S. Lin and D. J. Costello, *Error Control Coding: Fundamentals and Applications*, 2nd Ed. Upper Saddle River, NJ, USA: Prentice-Hall, 2004.

[151] Q. Huang, Q. Xiao, L. Quan, Z. Wang, and S. Wang, "Trimming soft-input soft-output Viterbi algorithms," *IEEE Trans. Commun.*, vol. 64, no. 7, pp. 2952–2960, Jul. 2016.

[152] S. S. Shafiee, C. K. Sann, and G. Y. Liang, "Novel joint detection and decoding schemes for TDMR channels," *IEEE Trans. Magn.*, vol. 51, no. 4, pp. 1–6, Apr. 2015.

[153] S. Zhao, Z. Lu, X. Ma, and B. Bai, "Joint detection/decoding algorithms for non-binary low-density parity-check codes over inter-symbol interference channels," *IET Commun.*, vol. 7, no. 14, pp. 1522–1531, Sep. 2013.

[154] B. M. Kurkoski, "Towards efficient detection of two-dimensional inter-symbol interference channels," *IEICE Trans. Fundam.*, vol. E91-A, no. 10, pp. 2696–2703, Oct. 2008.

[155] Z. Qin and K. C. Teh, "Iterative reduced-state decoding for coded partial-response channels," *IEEE Trans. Magn.*, vol. 41, no. 11, pp. 4335–4337, Nov. 2005.

[156] J. Yao, K. C. Teh, and K. H. Li, "Reduced-state Bahl–Cocke–Jalinek–Raviv detector for patterned media storage," *IEEE Trans. Magn.*, vol. 46, no. 12, pp. 4108–4110, Dec. 2010.

[157] J. B. Anderson, A. Prlja, and F. Rusek, "New reduced state space BCJR algorithms for the ISI channel," in *Proc. IEEE Int. Symp. Inf. Theory (ISIT)*, Seoul, South Korea, Jun. 2009, pp. 889–893.

[158] W. E. Ryan and S. Lin, *Channel Codes: Classical and Modern*. New York, NY, USA: Cambridge Univ. Press, 2009.

[159] R. Suzutou *et al.*, "Performance evaluation of TDMR R/W channel with head skew by LDPC coding and iterative decoding system," *IEEE Trans. Magn.*, vol. 51, no. 11, pp. 1–4, Nov. 2015.

[160] A. Marinoni and P. Savazzi, "Efficient receivers for q-ary LDPC coded signals over partial response channels," in *Proc. IEEE Int. Conf. Commun.*, May 2010, pp. 1–6.

[161] Z. Qin, K. Cai, and Y. Ng, "Iterative detection and decoding for non-binary LDPC coded partial-response channels with written-in errors," *IET Commun.*, vol. 10, no. 4, pp. 399–406, Mar. 2016.

[162] J. L. Fan, E. Kurtas, A. Friedmann, and S. W. McLaughlin, "LDPC codes for magnetic recording," in *Proc. 36th Allerton Conf.*, Monticello, IL, USA, Sep. 1999, pp. 1314–1323.
[163] H. Song, R. M. Todd, and J. R. Cruz, "Low density parity check codes for magnetic recording channels," *IEEE Trans. Magn.*, vol. 36, no. 5, pp. 2183–2186, Sep. 2000.
[164] D. J. C. MacKay and R. M. Neal, "Near Shannon limit performance of low density parity check codes," *Electron. Lett.*, vol. 33, no. 6, pp. 457–458, Mar. 1997.
[165] W. M. Tam, F. C. M. Lau, and C. K. Tse, "A class of QC-LDPC codes with low encoding complexity and good error performance," *IEEE Commun. Lett.*, vol. 14, no. 2, pp. 169–171, Feb. 2010.
[166] D. G. M. Mitchell, R. Smarandache, and D. J. Costello, "Quasi-cyclic LDPC codes based on pre-lifted protographs," *IEEE Trans. Inf. Theory*, vol. 60, no. 10, pp. 5856–5874, Oct. 2014.
[167] X. Liu, W. Zhang, and Z. Fan, "Construction of quasi-cyclic LDPC codes and the performance on the PR4-equalized MRC channel," *IEEE Trans. Magn.*, vol. 45, no. 10, pp. 3699–3702, Oct. 2009.
[168] A. Abbasfar, D. Divsalar, and K. Yao, "Accumulate-repeat-accumulate codes," *IEEE Trans. Commun.*, vol. 55, no. 4, pp. 692–702, Apr. 2007.
[169] H. Jin, A. Khandekar, and R. McEliece, "Irregular repeat-accumulate codes," in *Proc. Int. Symp. Turbo Codes*, Brest, France, Sep. 2000, pp. 1–8.
[170] D. G. M. Mitchell, A. E. Pusane, and D. J. Costello, "Minimum distance and trapping set analysis of protograph-based LDPC convolutional codes," *IEEE Trans. Inf. Theory*, vol. 59, no. 1, pp. 254–281, Jan. 2013.
[171] A. E. Pusane, R. Smarandache, P. O. Vontobel, and D. J. Costello, "Deriving good LDPC convolutional codes from LDPC block codes," *IEEE Trans. Inf. Theory*, vol. 57, no. 2, pp. 835–857, Feb. 2011.
[172] D. Burshtein and G. Miller, "Asymptotic enumeration methods for analyzing LDPC codes," *IEEE Trans. Inf. Theory*, vol. 50, no. 6, pp. 1115–1131, Jun. 2004.
[173] S. Litsyn and V. Shevelev, "Distance distributions in ensembles of irregular low-density parity-check codes," *IEEE Trans. Inf. Theory*, vol. 49, no. 12, pp. 3140–3159, Dec. 2003.
[174] A. Orlitsky, K. Viswanathan, and J. Zhang, "Stopping set distribution of LDPC code ensembles," *IEEE Trans. Inf. Theory*, vol. 51, no. 3, pp. 929–953, Mar. 2005.
[175] S. Abu-Surra, D. Divsalar, and W. E. Ryan, "Enumerators for protograph-based ensembles of LDPC and generalized LDPC codes," *IEEE Trans. Inf. Theory*, vol. 57, no. 2, pp. 858–886, Feb. 2011.
[176] S. Abu-Surra, D. Divsalar, and W. E. Ryan, "On the existence of typical minimum distance for protograph-based LDPC codes," in *Proc. IEEE Inf. Theory Appl. Workshop (ITA)*, San Diego, CA, USA, Jan. 2010, pp. 1–7.
[177] M. Franceschini, G. Ferrari, and R. Raheli, *LDPC Coded Modulations*. Berlin, Germany: Springer-Verlag, 2009.
[178] K. R. Narayanan, D. N. Doan, and R. V. Tamma, "Design and analysis of LDPC codes for turbo equalization with optimal and suboptimal soft output equalizers," in *Proc. Allerton Conf. Commun. Control Comput.*, Oct. 2002, pp. 737–746.
[179] L. Kong, K. Cai, P. Chen, and B. Fan, "A detector-aware LDPC code optimization for ultra-high density magnetic recording channels," *IEEE Trans. Magn.*, vol. 53, no. 11, pp. 11–14, Nov. 2017.
[180] Y. Han and W. E. Ryan, "Low-floor decoders for LDPC codes," *IEEE Trans. Commun.*, vol. 57, no. 6, pp. 1663–1673, Jun. 2009.
[181] T. Cheng, B. J. Belzer, and K. Sivakumar, "Row-column soft-decision feedback algorithm for two-dimensional intersymbol interference," *IEEE Signal Process. Lett.*, vol. 14, no. 7, pp. 433–436, Jul. 2007.
[182] E. Hwang, R. Negi, and B. V. K. V. Kumar, "Signal processing for near 10 Tbit/in^2 density in two-dimensional magnetic recording (TDMR)," *IEEE Trans. Magn.*, vol. 46, no. 6, pp. 1813–1816, Jun. 2010.
[183] G. Han, Y. L. Guan, and X. Huang, "Check node reliability-based scheduling for BP decoding of non-binary LDPC codes," *IEEE Trans. Commun.*, vol. 61, no. 3, pp. 877–885, Mar. 2013.
[184] A. Bhatia *et al.*, "Polar codes for magnetic recording channels," in *Proc. IEEE Inf. Theory Workshop (ITW)*, Apr. 2015, pp. 1–5.
[185] H. Zhong, T. Zhang, and E. F. Haratsch, "VLSI design of high-rate quasi-cyclic LDPC codes for magnetic recording channel," in *Proc. IEEE Custom Integrated Circuits Conf.*, San Jose, CA, USA, Sep. 2006, pp. 325–328.
[186] K.-C. Ho, C.-L. Chen, and H.-C. Chang, "A 520k (18900, 17010) array dispersion LDPC decoder architectures for NAND flash memory," *IEEE Trans. Very Large Scale Integr. (VLSI) Syst.*, vol. 24, no. 4, pp. 1293–1304, Apr. 2016.

Yi Fang (M'15) received the B.Sc. degree in electronic engineering from East China Jiaotong University, China, in 2008, and the Ph.D. degree in communication engineering from Xiamen University, China, in 2013. In 2012, he was a Research Assistant in electronic and information engineering from Hong Kong Polytechnic University, Hong Kong, for two months. From 2012 to 2013, he was a Visiting Scholar in electronic and electrical engineering from University College London, U.K. From 2014 to 2015, he was a Research Fellow with the School of Electrical and Electronic Engineering, Nanyang Technological University, Singapore. He is currently an Associate Professor with the School of Information Engineering, Guangdong University of Technology, China. His research interests include information and coding theory, LDPC/protograph codes, spread-spectrum modulation, and cooperative communications. He is an Associate Editor of IEEE ACCESS.

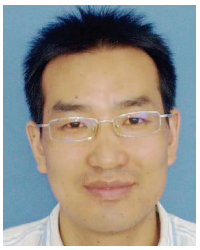

Guojun Han (M'12–SM'14) received the Ph.D. degree from Sun Yat-sen University, Guangzhou, China, and the M.E. degree in electronic engineering from the South China University of Technology, Guangzhou. From 2011 to 2013, he was a Research Fellow with the School of Electrical and Electronic Engineering, Nanyang Technological University, Singapore. From 2013 to 2014, he was a Research Associate with the Department of Electrical and Electronic Engineering, Hong Kong University of Science and Technology. He is currently a Full Professor and the Vice Dean with the School of Information Engineering, Guangdong University of Technology. His research interests include wireless communications, and coding and signal processing for data storage.

Guofa Cai (M'17) received the B.Sc. degree in communication engineering from Jimei University, Xiamen, China, in 2007, the M.Sc. degree in circuits and systems from Fuzhou University, Fuzhou, China, in 2012, and the Ph.D. degree in communication engineering from Xiamen University, Xiamen, China, in 2015. In 2017, he was a Research Fellow with the School of Electrical and Electronic Engineering, Nanyang Technological University, Singapore, for eight months. He is currently an Associate Professor with the School of Information Engineering, Guangdong University of Technology, China. His primary research interests include information theory and coding, chaotic communications, and UWB communications.

Francis C. M. Lau (M'93–SM'03) received the B.Eng. degree (Hons.) in electrical and electronic engineering and the Ph.D. degree from King's College London, University of London, U.K. He is a Professor and the Associate Head with the Department of Electronic and Information Engineering, Hong Kong Polytechnic University, Hong Kong. He is also a fellow of IET.

He has co-authored the book entitled *Chaos-Based Digital Communication Systems* (Heidelberg: Springer-Verlag, 2003) and *Digital Communications with Chaos: Multiple Access Techniques and Performance Evaluation* (Oxford: Elsevier, 2007). He is also a co-holder of five U.S. patents. He has published over 280 papers. His main research interests include channel coding, cooperative networks, wireless sensor networks, chaos-based digital communications, applications of complex-network theories, and wireless communications. He was the Chair of Technical Committee on Nonlinear Circuits and Systems, IEEE Circuits and Systems Society in 2012-13. He served as an Associate Editor for the IEEE TRANSACTIONS ON CIRCUITS AND SYSTEMS—II: EXPRESS BRIEFS from 2004 to 2005 and the IEEE TRANSACTIONS ON CIRCUITS AND SYSTEMS—I: REGULAR PAPERS from 2006 to 2007, and *IEEE Circuits and Systems Magazine* from 2012 to 2015. He has been a Guest Associate Editor of the *International Journal and Bifurcation and Chaos* since 2010 and an Associate Editor of the IEEE TRANSACTIONS ON CIRCUITS AND SYSTEMS—II: EXPRESS BRIEFS since 2016.

Pingping Chen (M'15) received the Ph.D. degree in electronic engineering, Xiamen University, China, in 2013. In 2012, he was a Research Assistant in electronic and information engineering with Hong Kong Polytechnic University, Hong Kong, for four months. From 2013 to 2015, he was a Post-Doctoral Fellow with the Institute of Network Coding, Chinese University of Hong Kong, Hong Kong. He is currently a Full Professor with Fuzhou University, China. His primary research interests include channel coding, joint source and channel coding, network coding, and UWB communications.

Yong Liang Guan (M'99–SM'17) received the B.Eng. degree (with First Class Hons.) from the National University of Singapore and the Ph.D. degree from the Imperial College of London, U.K. He is a tenured Associate Professor with the School of Electrical and Electronic Engineering, Nanyang Technological University, Singapore. His research interests broadly include coding and signal processing for communication and storage systems. His homepage is http://www3.ntu.edu.sg/home/eylguan/index.htm.